The isotope geochemistry of zinc and copper

Frédéric Moynier[1,2], Derek Vance[3], Toshiyuki Fujii[4], Paul Savage[5]

[1]Institut de Physique du Globe de Paris, Université Paris Diderot, Université Sorbonne Paris Cité, CNRS UMR 7154, 1 rue Jussieu, 75238 Paris Cedex 05

[2]Institut Universitaire de France, Paris, France

[3]ETH Zürich, Institute for Geochemistry and Petrology, Department of Earth Sciences, Clausiusstrasse 25, 8092 Zürich, Switzerland.

[4]Research Reactor Institute, Kyoto University, 2-1010 Asashiro Nishi, Kumatori, Sennan, Osaka 590-0494, Japan

[5]Department of Earth and Environmental Sciences, University of St Andrews, Irvine Building, Fife KY16 9AL, United Kingdom

Corresponding author: *moynier@ipgp.fr*

INTRODUCTION

Copper, a native metal found in ores, is the principal metal in bronze and brass. It is a reddish metal with a density of 8920 kg m^{-3}. All of copper's compounds tend to be brightly colored: for example, copper in hemocyanin imparts a blue color to blood of mollusks and crustaceans. Copper has three oxidation states, with electronic configurations of Cu^0([Ar]3d^{10}4s^1), Cu$^+$([Ar]3d^{10}), and Cu^{2+}([Ar]3d^9). Cu^0 does not react with aqueous hydrochloric or sulfuric acids, but is soluble in concentrated nitric acid due to its lesser tendency to be oxidized. Cu(I) exists as the colorless cuprous ion, Cu^{+}. Cu(II) is found as the sky-blue cupric ion, Cu^{2+}. The Cu^{+} ion is unstable, and tends to disproportionate to Cu^{0} and Cu^{2+}. Nevertheless, Cu(I) forms compounds such as Cu_2O. Cu(I) bonds more readily to carbon than Cu(II), hence Cu(I) has an extensive chemistry with organic compounds.

In aqueous solutions, Cu^{2+} ion occurs as an aquacomplex. There is no clearly predominant structure among the four-, five-, and six- fold coordinated Cu(II) species (Chaboy et al. 2006). Hydrated Cu(II) ion has been represented as the hexaaqua complex $Cu(H_2O)_6^{2+}$, which shows the Jahn-Teller distortion effect (Sherman 2001; Bersuker 2006), whereby the two Cu-O distances of the vertical axial bond ($Cu\text{-}O_{ax}$) are longer than four Cu-O distances in the equatorial plane ($Cu\text{-}O_{eq}$). The Jahn-Teller effect lowers the symmetry of $Cu(H_2O)_6^{2+}$ from octahedral T_h to D_{2h}. The sixfold coordination of hydrated Cu(II) species is questioned by a finding of fivefold coordination (Pasquarello et al. 2001; Chaboy et al. 2006; Little et al. 2014b; Sherman et al. 2015). The bond distance related to $Cu(H_2O)_6^{2+}$ is considered to reflect a rapid switch between the square pyramid and trigonal bipyramid configurations (Pasquarello et al. 2001; de Almeida et al. 2009). The fivefold coordination is supported by computational (Amira et al. 2005) and spectroscopic (Benfatto et al. 2002) studies.

In aqueous media at elevated temperatures, Cu(I) is thermodynamically more stable than Cu(II). The structures of Cu(I) species are thought to be due to the splitting of degenerate $4p_{x,y,z}$ orbitals by a ligand field (Kau et al. 1987). Cu(I) complexes possess simple linear structures (Fulton et al. 2004) due to $4p_z$ and $4p_{x,y}$ orbitals. The splitting of $4p_{x,y}$ orbital and/or the formation of degenerate $4p_{y,z}$ orbitals give the Cu(I) species threefold coordination structures (T-shaped or trigonal planar coordination). For the fourfold tetrahedral coordination (T_d) structure, the $p_{x,y,z}$ orbitals may be close to degenerate.

Zinc is an element of Group 2B, the last column of the *d* block. Zinc is not a transition metal by definition because it has a *d* subshell that is only partially occupied. Zinc has two oxidation states, with electronic configurations of Zn^0([Ar]$3d^{10}4s^2$) and Zn^{2+}([Ar]$3d^{10}$), where Zn(II) has $3d^{10}$ with two electrons per orbital. Zinc is sometimes included with the transition metals because its properties are more similar to these than to the post-transition metals, whose properties are determined by partially filled *p* subshells. Fresh zinc has a shiny metallic luster, but it tarnishes easily. It is hard and brittle, becomes malleable with increasing temperature, and melts at 419.53°C. Metallic zinc is easily oxidized and hence it is used as a reducing agent. Reduction of acids like HCl to H_2 by Zn^0 is well known.

In compounds or complex ions, Zn is present only as Zn(II). Hydrated Zn^{2+} is generally thought to be present as the octahedral $Zn(H_2O)_6^{2+}$, this being the most stable structure (Mhin et al. 1992). Besides the marked preference for sixfold coordination, Zn(II) can easily be fourfold or fivefold coordinated. The coordination number is attributable to a balance between bonding energies and repulsions among the ligands.

Zinc and Cu are both moderately volatile elements, with 50% condensation temperatures (T_c) of 726K and 1037K, respectively (Lodders 2003). It was long thought that Zn behaved as a lithophile element during planetary (and especially, Earth's) differentiation, hence there is negligible Zn in Earth's core (e.g. McDonough 2003). This assumption was used to place broad bounds on the amount of S (which has a similar T_c to Zn) in Earth's core (around 1.7wt% Dreibus and Palme 1996). However, more recent work indicates that Zn behaves as a moderately siderophile element, with potentially ~30% of terrestrial Zn stored in Earth's core (Siebert et al. 2011), significantly affecting the conclusions of Dreibus and Palme (1996). Zinc is the most abundant lithophile element with a T_c<750K, 100 times more abundant than the second-most abundant (Br, Tc=546K). Its high abundance relative to other moderately volatile elements (due to the relatively high binding energies per nucleon of its isotopes) makes Zn a good tracer of volatility in rocks and a major application of its isotopes has been related to understanding volatility processes.

Copper is a siderophile and highly chalcophile element (Siebert et al. 2011), with ~2/3 of the terrestrial Cu thought to be stored in Earth's core (Palme and O'Neill 2003). Copper is also moderately volatile, but is the most refractory of the chalcophile elements, meaning that Cu may be a good tracer of the role of sulphides during differentiation and igneous processes.

Zn is comprised of five natural stable isotopes, ^{64}Zn (49.2%), ^{66}Zn (27.8%), ^{67}Zn (4.0%), ^{68}Zn (18.4%) and ^{70}Zn (0.6%) and Cu of two stable isotopes, ^{63}Cu (69.2%), and ^{65}Cu (30.8%) (Shields et al. 1964). Due to their relatively high first ionization potentials (9.4 eV for Zn and 7.7 eV for Cu), the measurement of Zn and Cu isotope ratios by Thermal-Ionization Mass-Spectrometry (TIMS) is very difficult. This explains the very limited amount of Zn and Cu isotopic data produced before the advent of Multiple-Collector Inductively-Coupled-Plasma Mass-Spectrometry (MC-ICP-MS). In addition, since Cu has only two stable isotopes it is not possible to use a double spike technique to correct for instrumental bias on TIMS. Since the first commercialized MC-ICP-MS in the late 90s and the first 'high precision' Zn and Cu isotope ratio measurements (Maréchal et al. 1999), more than 500 papers have been published (source: ISI Web of Science) on various geochemical topics associated with Zn and Cu isotopes (e.g. oceanography, cosmochemistry, environmental sciences, medical sciences). With the exception of medical sciences, for which there is a dedicated chapter in this volume, here we review these varied applications and discuss the potential of these isotope systems for future studies.

METHODS

Measurement of Zn and Cu isotope ratio was originally made using TIMS (Shields et al. 1964; Shields et al. 1965; Rosman 1972). As for any element with only two isotopes, it was not possible to properly assess the instrumental isotopic fractionation for Cu and the analytical uncertainty was therefore poor (no better than 2 ‰/amu; Shields et al. 1964; Shields et al. 1965). With five stable isotopes, for Zn it is possible to correct for instrumental bias and TIMS was originally used with double spike methods to measure Zn isotopic compositions. The earliest measurements, on the older generation of TIMS were associated with analytical precisions of around 1 ‰/amu (Rosman 1972; Loss et al. 1990), but modern generation TIMS can reach precisions of 0.1-0.2 ‰/amu (Ghidan and Loss 2011).

The vast majority of recent Cu and Zn isotopic data have been acquired by MC-ICP-MS, either by standard-sample bracketing (e.g. Maréchal et al. 1999; Mason et al.

2004ab; Weiss et al. 2005; Bermin et al. 2006; Viers et al. 2007; Balistrieri et al. 2008; Peel et al. 2008; Vance et al. 2008; Savage et al. 2015a, b; Sossi et al. 2015) or by the double spike method (e.g. Bermin et al. 2006; Arnold et al. 2010b; Conway and John 2015) for Zn. The pioneering work of Maréchal et al. (1999) showed that instrumental mass bias could be corrected by a combination of elemental doping (Cu for Zn, and Zn for Cu) and standard bracketing, so that it was possible to obtain isotope ratios of both Cu and Zn with precisions better than 0.1 ‰/amu on the VG Elemental Plasma 54 MC-ICP-MS. Subsequent studies by Zhu et al. (2000; 2002) and Archer and Vance (2002; 2004) have further tested this approach and together with Maréchal et al. (1999) provided the ground work for modern Zn and Cu isotopic studies. An alternative method using Ni doping (instead of Zn) for Cu isotope analyses has also been used (Larner et al. 2011).

More recently, double spike Zn isotopic measurements by MC-ICP-MS have also been employed, providing consistent results with those obtained by standard bracketing techniques. An advantage of the double spike technique is that it provides high precision absolute elemental abundances together with the isotope ratios. The fact that the double spike approach also accounts for mass discrimination during chemical separation means that it has been a key methodology for the analysis of Zn in difficult matrixes such as seawater (e.g. Bermin et al. 2006; Arnold et al. 2010b; Zhao et al. 2014; Conway and John 2015; Vance et al. In review). Using a similar approach, the absolute abundance of Zn isotopes were determined by analyzing synthetic isotope mixtures (Tanimizu et al. 2002; Ponzevera et al. 2006).

The precision of Zn and Cu isotopic measurements depends on the quality of the chemical extraction (purity, low blank compared to the amount of Zn and Cu present in the samples, high/quantitative yields) and on the correction of the instrumental bias. The high purity of the final Zn fraction is needed to remove both isobaric interferences and non-isobaric interference that are the cause of so-called 'matrix effects' (see Chaussidon et al. 20XX, this volume). As Zn and Cu isotopes can be fractionated during ion-exchange chromatography (Maréchal and Albarède, 2002) the chemical procedure requires quantitative yields, unless a double-spike is added pre-column chemistry.

The chemical purification of Cu and Zn is generally made by ion-exchange chromatography in 6-10N HCl medium on either macro-porous resin such as AG-MP1 or on regular bead resin such as AG1-X8 (e.g. Maréchal et al. 1999; Archer and Vance 2004; Borrok et al. 2007; Conway and John 2015; Sossi et al. 2015). In order to obtain a very pure elution of Cu, many workers (e.g. Savage et al. 2015b; Vance et al., 2016) repeat the whole procedure. For Zn purification, an alternative method takes advantage of the strong complexation of Zn with bromide, which allows for the use of more dilute acids (HBr/HNO_3 media) on micro-columns (0.1 µl) of anion-exchange resin (AG1-X8; Luck et al. 2005; Moynier et al. 2006; Moynier and Le Borgne 2015).

When analyzing Zn by MC-ICPMS, the potential nickel interference on mass 64 is normally monitored and corrected for by analyzing the intensity of the ^{62}Ni beam. Typically, ^{70}Zn is not measured (or at least, not reported) due to the low abundance of this isotope, and the potential for overwhelming interference from ^{70}Ge. In most instances, it is not necessary to measure ^{70}Zn (even when using the double-spike method), as terrestrial isotope variations are all mass-dependent. However, the introduction of higher resistance amplifiers attached to Faraday detectors should allow the more accurate measurement of ^{70}Zn in, for example, studies involving mass-independent Zn isotope variations. However, so far the results have been inconclusive (Moynier et al. 2009a; Savage et al. 2014). For Cu, neither masses 63 and 65 have direct elemental interferences, although there is evidence that the formation of $^{23}Na^{40}Ar+$ and $^{25}Mg^{40}Ar+$ in the plasma can create anomalous isotope ratios (Archer and Vance 2004; Larner et al. 2011; Savage et al. 2015b), so that careful monitoring to ensure complete removal of both Na and Mg from each sample aliquot is necessary to ensure accurate data.

The correction of instrumental mass bias by elemental doping (Cu for Zn and Zn for Cu, or Ni for Cu) has been extensively discussed in Maréchal et al. (1999) and further by Larner et al. (2011). The principle is that the instrumental bias can be expressed with an exponential law, for example for the $^{66}Zn/^{64}Zn$ and $^{65}Cu/^{63}Cu$ ratios:

$$\left(\frac{^{66}Zn}{^{64}Zn}\right)_{Measured} = \left(\frac{^{66}Zn}{^{64}Zn}\right)_{True} \times \left(\frac{M_{66}}{M_{64}}\right)^{f_{Zn}} \qquad (1)$$

$$\left(\frac{^{65}Cu}{^{63}Cu}\right)_{Measured} = \left(\frac{^{65}Cu}{^{63}Cu}\right)_{True} \times \left(\frac{M_{65}}{M_{63}}\right)^{f_{Cu}} \qquad (2)$$

where M_{63}, M_{64}, M_{65}, M_{66} are the atomic masses of ^{64}Zn, ^{65}Cu, ^{66}Zn, ^{68}Zn, respectively. f_{Zn} and f_{Cu} are mass-independent fractionation factors that depend on the element. Taking the example of Zn measurements, the elemental doping method consists of adding an identical Cu elemental standard to all aliquots to be analysed, which can then be used to determine the f_{Zn}. Because the ionization behavior of Cu and Zn is not the same, f_{Zn} cannot be assumed to be equal to f_{Cu}, and thus the relation between f_{Cu} and f_{Zn} is estimated by taking the Napierian logarithm of equations (1) and (2) and ratioing the two equations:

$$\frac{ln\left(\frac{^{66}Zn}{^{64}Zn}\right)_{Measured} - ln\left(\frac{^{66}Zn}{^{64}Zn}\right)_{True}}{ln\left(\frac{^{65}Cu}{^{63}Cu}\right)_{Measured} - ln\left(\frac{^{65}Cu}{^{63}Cu}\right)_{True}} = \frac{f_{Zn}}{f_{Cu}} \frac{ln\left(\frac{M_{66}}{M_{64}}\right)}{ln\left(\frac{M_{65}}{M_{63}}\right)} \qquad (3)$$

By plotting $ln\left(\frac{^{66}Zn}{^{64}Zn}\right)_{Measured}$ vs $ln\left(\frac{^{65}Cu}{^{63}Cu}\right)_{Measured}$ for the standard solution data generated during a session of analyses, the $\frac{f_{Zn}}{f_{Cu}}$ ratio can be estimated from the slope of this diagram (see for example Fig. 9 in Maréchal et al. 1999). The calculated f_{Zn} can then be used to calculate $\left(\frac{^{66}Zn}{^{64}Zn}\right)_{true}$ (and vice-versa for Cu isotopic measurements), provided that there is enough drift in the mass bias during an analytical session. This correction is coupled with a standard bracketing method that consists of measuring a standard before and after each sample, whereby the same correction is applied to both the standard and sample ratios. Once all isotope ratios are corrected for mass discrimination, the data are usually reported using the delta notation:

$$\delta^{65}Cu = \left[\frac{\left({}^{65}Cu/{}^{63}Cu\right)_{sample}}{\left({}^{65}Cu/{}^{63}Cu\right)_{NIST-SRM-976}} - 1\right] \times 1000 \quad (4)$$

$$\delta\,^{x}Zn = \left[\frac{\left({}^{x}Zn / {}^{64}Zn \right)_{sample}}{\left({}^{x}Zn / {}^{64}Zn \right)_{JMC-Lyon}} - 1 \right] \times 1000 \quad (5)$$

With x=66, 67, 68 or 70.

The double spike approach to mass discrimination was first described for Zn by Bermin et al. (2006), and involves the addition of a mixture of a tracer solution of known exotic isotopic composition to each sample (e.g. Dodson 1963; Rudge et al. 2009; John 2012). Equations that relate three measured and mass-bias corrected isotope ratios, for ^{66}Zn/^{64}Zn, ^{67}Zn/^{64}Zn and ^{68}Zn/^{64}Zn in terms of mixing, the exponential mass discrimination law, and natural mass-dependent fractionation relative to a standard, are solved to obtain the isotopic composition of the sample. The quality of data obtained with any double spike depends on the spike isotopes used and the sample/spike ratio in the mixture created, which control the magnification of analytical uncertainties propagated through the double spike algebra; hence, optimal spike compositions and abundances need to be deduced, although there is a range for both over which good isotopic data are obtainable. Other considerations include the potential for isobaric interference. Thus, although the optimal Zn spike is a mixture of ^{66}Zn and ^{70}Zn, practical applications have used a ^{64}Zn-^{67}Zn spike (e.g. Bermin et al. 2006; Conway et al. 2013). Bermin et al. (2006) showed that such a spike yields precise and accurate sample isotopic compositions over about a factor 20 range in sample/spike ratios in the mixture. Over a 2 year period, on a Neptune at ETH Zürich, the δ^{66}Zn of IRMM-3702 standard gave +0.300 ±0.058‰ relative to JMC Lyon (2SD, n =

163). For comparison, standard-sample bracketing standard precisions are of a similar magnitude (i.e. long term 2SD quoted by Chen et al., 2013, is δ^{66}Zn ± 0.04‰) but this is on samples with relatively high Zn concentrations (~100ppm) and relies heavily on very stable instrument running conditions.

All of the Zn isotopic variations measured in terrestrial samples that have been analyzed to date follow a mass-dependent law, i.e., $\delta^{70}\text{Zn}/3 \approx \delta^{68}\text{Zn}/2 \approx \delta^{67}\text{Zn}/1.5 \approx \delta^{66}\text{Zn}$. By contrast, extra-terrestrial mass-independent isotopic effects on ^{66}Zn of over 1500ppm have been observed in refractory inclusions (Loss and Lugmair 1990; Völkening and Papanastassiou 1990) and, more recently, these isotope anomalies have been discovered in bulk primitive meteorites, albeit of a much smaller magnitude (20-70ppm Savage et al. 2014). The survival of these anomalies is perhaps surprising, given the volatile behavior of Zn during solar system condensation. These will be discussed further below.

Because it only has two isotopes, mass independence in Cu isotope variations measured in terrestrial samples cannot be discerned, although there is no reason to assume that such variations occur in this realm. For extra-terrestrial samples, Luck et al. (2003) showed that the Cu isotope variations correlate with Δ^{17}O anomalies in bulk primitive meteorites, which suggests that the variations measured between solar system materials may not be completely generated by 'mass-dependent' fractionation processes.

A number of different reference standards have been used for Cu and Zn isotopic measurements; NIST SRM 976 for Cu isotopes and the JMC 3-0749C (usually called JMC-Lyon) are the two standards used in the original work of Maréchal et al. (1999). Though neither standard is still commercially available they are still the most commonly cited as references. Following Maréchal et al. (1999) other standards have been developed and used in a routine manner in different laboratories . Data for those that have been measured by a number of different laboratories are summarized in Table 1. Other standards relevant to more specific areas of research have been detailed in Cloquet et al. (2008). We suggest, for the sake of consistency, that future data should always be normalized with respect to NIST SRM 976 for Cu and JMC Lyon for Zn. New reference standards for both Cu and Zn will need to be developed soon, and for Zn a round-robin analysis programme of one such new standard is under way (C. Archer, ETH Zürich, pers. comm.). When these new reference standards come on line, we recommend maintaining the isotopic compositions of the original references at zero, with a reference value for new standards set relative to that, as recently proposed for Mo isotopes (Nägler et al. 2014), so that old data can be directly compared with new.

ZINC AND COPPER ISOTOPE FRACTIONATION FACTORS FROM *AB INITIO* METHODS

A considerable amount of progress has been made in calculating isotope fractionation factors between free metal ions and inorganic complexes in aqueous solution, laying the basis for an understanding of surface terrestrial fluids. Almost all the Cu and Zn in the oceans, in rivers and in soils is organically-complexed or sorbed to the surfaces of oxyhydroxides and clays (see section on low temperature processes later in the chapter), rather than being found as a free metal ion. There is therefore an urgent need to build on the existing theoretical work to extend the calculations to species and processes that represent those that are most important at the surface of the Earth.

The equilibrium constant of an isotopic exchange reaction can be theoretically obtained as the Reduced Partition Function Ratio (RPFR or β) of isotopologues (e.g. Schauble 2004). Here we will summarize the isotopic enrichment factors that have been calculated for aqueous solutions and molecules relevant to Zn and Cu in biogeochemistry. We also provide new results for certain molecules that were missing from the published studies (see Tables 2, 3, 4) using the method described in Fujii et al. (2014).

The isotope enrichment factor is evaluated from the reduced partition function ratio (*s/s*')*f* (Bigeleisen and Mayer 1947), also denoted β, such that,

$$ln \frac{s}{s'} f = \sum \left[ln\, b(u_i') - ln\, b(u_i) \right] \tag{6}$$

where

$$ln\, b(u_i) = -ln\, u_i + \frac{u_i}{2} + ln\left(1 - e^{-u_i}\right) \tag{7}$$

and

$$u_i = \frac{h\nu_i}{kT} \tag{8}$$

In the latter expression, ν stands for vibrational frequency, *s* for the symmetry number of the considered compound, *h* for Plank's constant, *k* for the Boltzmann constant, and *T* for the absolute temperature. The subscript *i* denotes the *i*th normal mode of molecular vibration, and primed variables refer to the light isotopologue. The isotope enrichment factor due to molecular vibrations can be evaluated from the frequencies ν_i summed over all normal modes.

The ln β values of Cu(I) and Cu(II) species (Seo et al. 2007; Fujii et al. 2013; Sherman 2013; Fujii et al. 2014; Telouk et al. 2015) are shown in Tables 2 and 3. The inorganic aqueous Cu species are represented in Figure 1. At low pH, positive δ^{65}Cu is found in copper sulfates and carbonates, relative to other inorganic species like hydrated Cu^{2+} and chlorides. At pH ~6, ^{65}Cu is enriched in $CuSO_4$ and $CuHCO_3^+$, while ^{63}Cu is enriched in the other inorganic species like Cu^{2+} and $CuCl^+$ (Fig. 1). With increasing pH, $Cu(OH)_2$ and $CuCO_3$ become the prevalent species (Zirino and Yamamoto 1972). At high pH, δ^{65}Cu is positive in Cu hydroxides and negative in carbonates. At a typical pH of seawater (8.22; Macleod et al. 1994), isotope fractionation among inorganic species favors ^{63}Cu in $CuCO_3$ and ^{65}Cu in $Cu(OH)_2$. However, Cu in soil solutions, rivers and seawater is overwhelmingly complexed to organics (McBride 1981; Coale and Bruland 1988; Moffett and Brand 1996; Shank et al. 2004; Grybos et al. 2007; Vance et al. 2008; Ryan et al. 2014), and the above calculations for inorganic species are relevant only to the tiny inorganic pool of Cu. Little et al. (2014b) and Sherman et al. (2015) show how heavy Cu in simple organic complexes controls seawater Cu isotopes. Note that the interpretation strongly depends on the speciation diagram applied (Fujii et al. 2013). Powell et al. (2007) uses small hydrolysis constants, which depress the role of hydroxides in Cu isotope fractionation; isotope fractionation may therefore not be seen in Cu(II) hydroxide, but Cu in $CuCO_3$ should nevertheless remain isotopically light with respect to the remaining inorganic pool of Cu in seawater, and much lighter than the dominant organically-complexed pool.

Since sulfide-bearing euxinic seawater systems are reducing, isotope fractionation of Cu caused by the co-presence of Cu(I) becomes important (Fujii et al. 2013). The ln β value of sulfides is 1-2‰ lower than Cu(II) carbonates, hydroxides, and hydrated Cu^{2+}. This suggests that the dominant organically-complexed pool, as well as minor Cu^{2+}, Cu(II) chlorides, carbonates, and hydroxides will all be isotopically heavier than sulfides. The speciation of Cu(I) under hydrothermal conditions (Mountain and Seward 1999) indicates that the prevailing species are CuCl, $CuCl_2^-$, CuHS, and $Cu(HS)_2^-$. Increasing complexation of Cu(I) chlorides and sulfides results in decreasing ln β. The ln β values of Cu(II) chlorides and sulfides at 573 K are 0.2-0.5‰ higher than those of corresponding Cu(I) species (Fujii et al. 2013; Fujii et al. 2014). Under hydrothermal conditions, the δ^{65}Cu value of Cu(I) may be 0.2-0.5‰ lower than that of Cu(II) with a ±0.1‰ range of variation among Cu(I) species.

As an application to plant uptake, δ^{65}Cu for Cu phosphates, citrates, hydroxides, and hydrated Cu^{2+} ions was estimated as a function of pH (Fujii et al., 2014). At neutral pH, the major Cu(II) species are phosphates and citrates, and a range of ~0.5‰ can be expected for δ^{65}Cu. This range overlaps with observations on higher plants (Weinstein et al. 2011; Jouvin et al. 2012). A reduction of Cu^{2+} to Cu^{+} by a reductase within roots has also been reported by Jouvin et al. (2012). Since the range of ln β values for Cu(I) species is ~2‰ smaller than those of Cu(II) species at 298 K, a fractionation of -0.84 to -0.11‰ between roots and nutrient solutions (Jouvin et al. 2012) may be expected.

A variety of metabolic processes may induce Cu isotope fractionation. A positive δ^{65}Cu of 1.5‰ was found in both sheep kidney (Balter and Zazzo 2011) and mouse kidney

(Albarède et al. 2011), which may be interpreted in terms of isotope exchange reactions among Cu(I) and Cu(II) species. Oxalic acid is a ubiquitous toxic organic acid in bodily fluids. High oxalate contents in urine and plasma may be correlated with kidney damage. Ascorbate is efficiently converted to oxalate when the coexisting copper concentration is high (Hayakawa et al. 1973). The δ^{65}Cu of the Cu species relative to the bulk solution as a function of Eh and extent of oxalate formation has been estimated (Fujii et al. 2013); δ^{65}Cu of Cu ascorbate varies from –1.0 to +0.5‰ when Eh increases from –1 V to +1 V, but its mole fraction remains very small, while the heavy isotope is enriched (+0.6 to +2.5‰) in the Cu oxalate relative to total Cu. It is expected that degradation of ascorbate and excretion of oxalate should leave isotopically heavy Cu in the kidney. With respect to food, which has a δ^{65}Cu value of about 0‰, if even trace amounts of oxalate form it should leave behind copper with a δ^{65}Cu of ~1.4‰ (δ^{65}Cu at 0‰ extent of oxalate formation). This value is very close to the δ^{65}Cu (1.5‰) found in sheep (Balter and Zazzo 2011) and mice (Albarède et al. 2011) kidneys.

Variations in Cu isotopes among Cu^{2+}-amino acid complexes have been estimated (Fujii et al. 2014). The ln β of Cu^{2+} complexes with O and N-donor amino acids is ~1‰ (at the body temperature of 310 K typical for mammals) higher than those with S-donor amino acids. In a same donor amino acid complex, δ^{65}Cu of ~1‰ may be created via Cu^{2+}/Cu^{+} redox processes in biological activity. This latter study also theoretically estimated the β of Cu lactates. The extent of ^{65}Cu preference over ^{63}Cu in Cu lactates with respect to Cu bound to cysteine is more than 1‰. From a study on the ^{65}Cu/^{63}Cu ratios in the serums of cancer patients, a δ^{65}Cu alarm threshold was found to be at -0.35‰. The decrease of δ^{65}Cu in the serum of cancer patients is assigned to the extensive oxidative chelation of copper by cytosolic lactate (Telouk et al. 2015).

The ln β values of Zn(II) species (Fujii et al. 2010; Black et al. 2011; Fujii et al. 2011; Fujii and Albarède 2012; Fujii et al. 2014) are shown in Table 4 and some species are represented in the Figure 2. It is known that Zn sulfate and carbonate create larger ln β. The fivefold and sixfold coordination of Zn in carbonate complexes, for which carbonates are treated as monovalent and divalent ligands, results in large ln β (Fujii et al. 2011; Fujii et al. 2014). At circumneutral pH the dominant inorganic species of free Zn^{2+} shows small isotope fractionation relative to the total inorganic pool. Zinc sulfate is enriched in ^{66}Zn, whereas Zn chlorides are enriched in ^{64}Zn with a Δ^{66}Zn ~0.5‰ being expected between Zn sulfate and chloride. With increasing pH, $Zn(OH)_2$ and $ZnCO_3$ become the dominant species. Small amounts of free Zn^{2+} and $ZnCl^+$ still exist at pH = 8.2. In seawater, a fractionation Δ^{66}Zn of ~1‰ is expected between Zn carbonate and chloride. Zinc hydroxides and sulfates do not play an important role for Zn isotope fractionation for pH ≥ 8.2. It is again noted, however, that the free and inorganically-complexed pool of both Cu and Zn in soil solutions, rivers and seawater is very minor (in seawater, on the of order 2%; McBride 1981; Coale and Bruland 1988; Moffett and Brand 1996; Shank et al. 2004; Grybos et al. 2007; Vance et al. 2008; Ryan et al. 2014) and most is organically complexed. As such, the above discussion is only relevant to the minor free metal and inorganically-complexed pool.

The role of sulfides is central to a broad range of geological scenarios. The status of sulfur in ancient oceans in particular is still an outstanding issue (Canfield 1998).

Hydrothermal vent solutions discharging either at mid-ocean ridges (Edmond et al. 1979) or along subduction zones (Mott et al. 2004) comprise additional environments dominated by sulfides. Fujii et al. (2011) evaluated the isotope fractionation among the different Zn sulfide species present in geological fluids between 298 and 573 K (Fig. 2). At the high P_{CO2} conditions of hydrothermal solutions, Zn precipitated as sulfides is isotopically nearly unfractionated with respect to a low-pH parent fluid. In contrast, negative δ^{66}Zn, down to at least -0.6‰, can be expected in sulfides precipitated from solutions with pH > 9. Zinc isotopes in sulfides and rocks therefore represent a potential indicator of mid to high pH in ancient hydrothermal fluids (Pons et al. 2011).

Citric acid also plays an important role in the transport of trace metals in the soil-plant system. Citrate is released from the roots of vascular plants and acts as a biological chelating agent for the uptake of metals from soil. Isotope fractionation induced by higher plants has been found for Zn (Weiss et al. 2005; Moynier et al. 2009b). In a pioneering study of isotope fractionation of Zn in the soil-plant system, Weiss et al. (2005) found that Zn was isotopically lighter in the shoots relative to the roots, with a δ^{66}Zn difference of -0.13 to -0.26‰. The origin of this isotope fractionation may be isotopic exchange between Zn(II) phosphates in roots and citrates (or malates) in plants (Fujii and Albarède 2012).

The ln β values for optimized structures of Zn^{2+}-amino acid complexes have been calculated (Fujii et al. 2014). Heavy isotopes tend to bind to O-donor ligands, whereas light isotopes are positively fractionated by S-donor ligands (Balter et al. 2013; Moynier et al. 2013a). This is clearly seen in complexes with identical coordination number (four and six). Isotope fractionation correlated with N-donor ligands may be intermediate between

O-donor and S-donor systems or even stronger than with O-donor ligands. Besides the donor type, coordination number is important, implying that four-fold complexation gives larger ln β values relative to complexes with six-fold coordination. The ln β of $Zn(His)^{2+}$ complexes is 0.2 to 0.6‰ larger than that of $Zn(Cys)^{2+}$. This matches the observation that organs rich in proteins with histidine residues show larger δ^{66}Zn than organs in which proteins rich in cysteine residues dominate (Moynier et al. 2013a).

ZINC AND COPPER IN EXTRA-TERRESTRIAL SAMPLES AND IGNEOUS ROCKS

Chondritic Reference Frame and meteorites. Luck et al. (2003; 2005) were the first to measure Cu and Zn isotopes in a selection of carbonaceous and ordinary chondrites by MC-ICP-MS. The carbonaceous chondrite data show resolvable isotopic variation for both Zn and Cu isotopes between the different groups (e.g. CI, CV, CO, CM…) with the latter system showing the largest variability ($0.16<\delta^{66}Zn<0.52$ and $-1.44<\delta^{65}Cu<-0.09$, Fig. 3 and 4). For both systems, each carbonaceous group has a distinct isotope composition (Fig. 3 and 5). There is also a broad positive co-variation between the Cu and Zn isotope compositions of the carbonaceous chondrites, with the CI chondrites defining the heaviest compositions in both systems. The most robust average composition for the CI chondrites has been obtained from the average composition of 6 large chips of the Orgueil meteorite as well as samples from Ivuna and Alais and is $\delta^{65}Cu = 0.05\pm0.16$‰ and $\delta^{66}Zn = 0.46\pm0.08$‰ (Barrat et al. 2012).

For the ordinary chondrites, Zn isotopes define the larger range ($-1.30<\delta^{66}Zn<0.76$, Fig. 4), compared to Cu ($-0.51<\delta^{65}Cu<0.10$, Fig. 3), although the difference between groups (H, L, LL) is much clearer in the Cu system, whereas the variations in Zn isotopes in ordinary chondrites seem to be controlled by degree of parent body metamorphism, as well as subsequent secondary alteration on the Earth's surface (i.e., 'falls' are much less variable than 'finds').

Luck et al. (2003) showed that the $\delta^{65}Cu$ composition of carbonaceous and ordinary chondrites varies systematically with their mass-independent $\Delta^{17}O$ value ($\delta^{18}O-0.52*\delta^{17}O$, Fig. 3) and $^{58}Ni/^{65}Cu$ ratio, although the two groups fall on distinct trends. They interpreted this phenomenon as revealing the presence of at least two, and potentially three, distinct Cu isotope reservoirs in the early solar system, which subsequently mixed via nebular processing to create the distinct chondritic bodies. They further suggested, based on the relationship with $^{58}Ni/^{65}Cu$ ratio, that the range of Cu isotope compositions was potentially defined early in solar system history by the heterogeneous distribution of a phase enriched in the short-lived radionuclide ^{63}Ni, which decays to ^{63}Cu.

Luck et al. (2005) discovered a negative correlation between $\delta^{66}Zn$ and Mg/Zn in carbonaceous chondrites and un-equilibrated ordinary chondrite falls (Fig. 5). This was taken as robust evidence against evaporation as the origin of the variability of Zn abundance between chondrites groups (with the exception of EL6, see later), and rather suggested that the variation in the volatile element content of chondrite parent bodies was fixed by nebular processes. This argument was later developed by Albarède (2009) to suggest that the volatile element abundance in chondrites was inherited from nebular conditions during accretion, and that the Earth must have accreted "dry" and acquired its volatile elements via later impact events.

Enstatite chondrites are the most reduced type of chondrites and the only group that shares similar isotopic anomaly patterns with Earth for most elements (e.g. O, Cr, Ni, Ti; Moynier and Fegley 2015). For Cu isotopes, the high (EH) and low (EL) iron groups have identical average compositions (δ^{65}Cu ≈ -0.25‰; Savage et al. 2015b), falling in the center of the chondritic range, although the more volatile depleted EL define a larger range (Fig. 3). Enstatite chondrites of types EH and EL3 (low thermal metamorphic grade) have a similar Zn isotopic composition (0.15‰<δ^{66}Zn<0.31‰, Moynier et al. 2011) to that of carbonaceous chondrites, unequilibrated ordinary chondrites and current estimates of BSE (Fig. 4A). On the other hand, those EL chondrites which experienced strong thermal metamorphic alteration (EL6) are highly enriched in the heavier isotopes (δ^{66}Zn up to 7.35‰, Fig. 4B) and are highly depleted in Zn and other moderately volatile elements. The enrichment in the heavier isotopes of Zn is evidence that the origin of the volatile element depletion between EL3 and EL6 chondrites was due to volatilization during thermal metamorphism (Moynier et al. 2011). Why such large enrichments in heavy Zn are not reflected by the Cu isotope composition of EL6 chondrites is puzzling; however, it should be noted that the amount of Cu loss between EH and EL6 is much less significant than the amount of Zn loss; also there are no EL3 Cu isotopic measurements – it could be that EL3 chondrites have a lighter Cu isotope composition than EH, and that the similarity between EH and EL6 is merely coincidence. This question remains unanswered.

Ureilites are ultramafic achondrites which are widely considered as mantle restites. Ureilites with different shock degrees and volatile element abundances show a positive correlation between δ^{66}Zn (with values up to 1 ‰) and 1/Zn, whereby samples with the lowest Zn content have the heaviest Zn isotopic compositions (Moynier et al. 2010b). This was taken as evidence that, as with EL6 meteorites and terrestrial tektites (see later), the variations in the abundance of Zn (isotopes) between ureilite samples is controlled by evaporation processes. In addition, the more depleted samples also exhibited a higher shock state, suggesting an impact may have been responsible for the heating event.

The HED (howardites, eucrite, diogenites) meteorites, presumably derived from the asteroid 4-Vesta, have highly variable δ^{66}Zn (-2 to +1.7‰, Paniello et al. 2012b). On the other hand, unbrecciated eucrites ($1.6<\delta^{66}$Zn$<$ 6.22‰, n=4) and diogenites (0.94‰$<\delta^{66}$Zn$<$ 1.6‰, n=3) are all isotopically heavy and are all more depleted in Zn (and other moderately volatile elements) than brecciated HED suggesting that some volatile loss by evaporation occurred during the formation of the Vestan crust.

Iron meteorites are mostly composed of Fe and Ni and are enriched in siderophile elements compared to chondrites. The so-called magmatic groups (or fractionally crystallized iron groups) are thought to represent the cores of disrupted asteroids while the silicate-bearing groups have a more complex history, and may have formed as pools of impact-produced melt near the base of a regolith on a chondritic parent body (Wasson and Wang 1986). Luck et al. (2005) found that the IIIAB magmatic iron meteorites show very limited isotopic variations of both Cu and Zn, while silicate-bearing iron meteorites from group IA and IIICD are enriched in the heavier isotopes of Zn by up to 3.7‰ (although their Cu isotopes are mostly unfractionated). Bridgestock et al. (2014) have expanded the set of Zn isotopic data in the silicate bearing IA irons and in the IIAB and IIIAB groups with high precision Zn concentration determined by isotope dilution. They found that, in general, all iron meteorites are isotopically heavy in Zn relative to terrestrial/carbonaceous chondrites, and that the δ^{66}Zn is negatively correlated with 1/Zn for each individual group. They also showed that chromites are Zn-rich and isotopically light (δ^{66}Zn~0) and proposed that the correlation observed between δ^{66}Zn and 1/Zn correspond to the segregation of chromite from metal. Chen et al. (2013a) and Bishop et al. (2012) measured the Cu and Zn isotope compositions of a large set of irons, including Zn-poor iron meteorite groups such as IVA and IVB, and did not find any particular enrichments in the heavier isotopes relative to other iron meteorite groups, suggesting that the low volatile element contents recorded in these meteorites is not related to evaporation during the parent body history. Bishop et al. (2012) found that, as observed in chondrites by Luck et al. (2003), δ^{65}Cu correlates with Δ^{17}O for silicate bearing iron meteorites. Such a correlation between mass-dependent and non-mass dependent isotopic fractionation must reflect mixing between at least two solar nebula components (see above); hence, the variations in the Cu isotopic composition of the silicate-bearing iron meteorites originates from nebular processes rather than from planetary differentiation effects. Bishop et al. (2012) further proposed that the same may be true for magmatic iron meteorites (which do not contain silicates and so for which it is not possible to determine the Δ^{17}O) and that Cu isotopes could be used to determine genetic connections between meteorite groups. Chen et al. (2016) measured the Cu isotope composition of the IVB (magmatic) iron meteorites and found a very large range of variation (-5.84 ‰ < δ^{65}Cu < -0.24 ‰). The IVB irons are the most volatile depleted iron meteorites, with Cu concentration depletions several orders of magnitude larger than other iron meteorites groups and Ni/Cu ratios of ~10^5. Chen et al. (2016) show that the Cu isotope variations are controlled by neutron capture due to galactic cosmic ray irradiation by a reaction on ^{62}Ni to form ^{63}Ni, which decays to ^{63}Cu ($t_{1/2} \approx 100$ yrs).

Williams and Archer (2011) reported the Cu isotopic composition of phase separates (metal, troilite and silicate) from a variety of iron meteorites and coupled these with Fe isotope composition of the same phases. They found a large range of Cu isotope variations among metals and troilites (~ 10‰ variations) and also within the calculated metal-troilite fractionation factor (≤~5‰ variations) suggesting a kinetic control on the isotopic fractionation between the different phases. However, the most equilibrated samples display the smallest metal/troilite fractionation factor of ~0.5‰, with the metal phase being enriched in the heavier Cu isotope.

Mass-independent Zn anomalies in extra-terrestrial material. In terms of nucleosynthesis, Zn is classed as an iron peak (IP) element, along with Ca, Ti, Cr, Ni and of course, Fe. These elements have the highest nuclear binding energies per nucleon, and the ‘iron-(abundance)-peak’ is defined by the heaviest nuclides for which nuclear fusion becomes is energetically unfavourable during element synthesis (^{56}Ni, which decays to ^{56}Fe). As such, IP elements are only formed in the cores of massive stars or by explosive nucleosynthesis, where formation of some of the nuclides is dominated by nuclear statistical (quasi)equilibrium during explosive nucleosynthesis (NSE/QSE; see Wallerstein et al., 1997, for a review). The measurement of so-called isotope anomalies (identification of isotope reservoirs that do not fall on the terrestrial fractionation line) of the iron peak elements in extra-terrestrial materials have afforded many important insights into the stellar sources of material into the solar system, early solar system processes, and the building blocks of the terrestrial planets (e.g. Birck 2004; Moynier and Fegley 2015).

Of the IP element isotope systems, Zn isotope anomalies are, arguably, the least well constrained with (at the time of writing), less than 10 studies available in the literature. The initial work (using TIMS, Loss and Lugmair 1990; Völkening and Papanastassiou 1990) focused on the analysis of refractory inclusions from primitive meteorites (those phases thought to be the first to condense from a cooling nebula gas). Previously measured Ca, Ni and Cr anomalies in these materials (see Birck 2004 and refs therein) were modelled by Hartmann et al. (1985) in terms of nuclear statistical equilibrium, which also predicted relatively large ^{66}Zn excesses. Although Loss and Lugmair (1990) and Volkening and Pappanastassiou (1990) measured resolvable ^{66}Zn anomalies, these were much smaller than those predicted by the models, and this was explained as a result of the higher volatility of Zn compared to the other IP elements; i.e. by the time Zn began to condense, mixing in the solar nebula had diluted most anomalous Zn. Nevertheless, the presence of anomalous Zn in refractory inclusions is extremely puzzling, because Zn should not condense at all during their formation, and so all Zn in these inclusions must have been introduced by secondary processes. This implies that Zn isotope anomalies survived the hot initial stage of the solar system, potentially as a distinct sulphide phase, but this is a long standing and poorly understood issue (e.g. Chou et al. 1976).

TIMS measurements could not resolve any Zn anomalies at the bulk meteorite scale, and this was apparently confirmed by the first MC-ICP-MS measurements, which showed that bulk chondrites plotted within error of the terrestrial mass fractionation line in δ^{66}Zn vs. δ^{68}Zn space (Luck et al. 2005) – seemingly confirming that Zn condensed too late for resolvable anomalies to be detected at this scale. The requirement of such large ^{66}Zn excesses to accompany other neutron rich IP anomalies, particularly ^{48}Ca, was also relaxed with the advancement of nucleosynthesis models into so-called quasi-equilibrium (e.g., Meyer et al. 1998). Nevertheless, the first paper to specifically investigate Zn isotope anomalies on the bulk meteorite scale was Moynier et al. (2009a), which utilized MC-ICPMS. The advantages of MC-ICPMS over TIMS, regarding the detection of Zn anomalies, are the much better precision attainable, the ability to accurately measure ^{67}Zn, which always suffered from an unidentified interference on TIMS and, finally, the ability to switch individual amplifier resistances to increase the dynamic range of the instrument. Moynier et al. (2009a) used a smaller resistance amplifier on the ^{64}Zn detector to allow for higher concentration samples to be analysed, with the specific aim of investigating potential ^{70}Zn heterogeneity in bulk solar system materials – important as this can constrain the distribution of ^{60}Fe (a short-lived radionuclide) in the solar nebula. At the precisions attained in their study (±100 ppm), no resolvable ^{66}Zn, ^{67}Zn or ^{70}Zn anomaly patterns were measured (when normalized to ^{68}Zn/^{64}Zn), which indicated relatively homogeneous distribution of Zn isotopes, and also ^{60}Fe; however, there were some hints in their anomaly patterns that, with further improvements in precision, anomalies in ^{66}Zn or ^{67}Zn may be present and measureable.

With techniques modified from Moynier et al. (2009a) and with analytical precision at the ±10ppm level, Savage et al. (2014) showed for the first time that carbonaceous chondrites do have resolvable ^{66}Zn and ^{68}Zn excesses (when normalized to ^{67}Zn/^{64}Zn), and, also that enstatite and potentially ordinary chondrites have smaller ^{66}Zn deficits; this is consistent with the sense of ^{48}Ca, ^{50}Ti, ^{54}Cr and ^{62}Ni anomalies measured in the same samples (Trinquier et al. 2009, Steele et al., 2012, Dauphas et al. 2014; Moynier and Fegley 2015; Schiller et al. 2015). The complementary excesses and deficits exhibited by the carbonaceous and enstatite/ordinary chondrites, the more volatile nature of Zn, and the correlations between Zn and other iron-peak anomalies adds further credence to the 'unmixing' hypothesis of solar nebula evolution, where specific phases were remobilized via thermal processing in a previous well-mixed nebula cloud (e.g. Trinquier et al. 2009; Schiller et al. 2015). Sequential leaching experiments show that the Zn anomalies are not limited to one phase, although this is most likely due to post-formation remobilization of Zn. One important insight from this dataset is that Earth is not similar to enstatite chondrites, in terms of Zn isotope budget, adding to a slowly growing group of isotope systems (O, Ti, Mo) which bring in to question the 'enstatite chondrite' Earth model (e.g. Moynier and Fegley 2015). Now that Zn isotope anomalies have been discovered in bulk primitive meteorites, there is potential to discover such anomalies in other solar system materials, and the new insights from this system could be hugely important for our understanding of our solar system.

Bulk Silicate Earth composition. The estimation of the isotopic composition of the bulk silicate Earth is not trivial since both Zn and Cu are fractionated during partial melting of the mantle, hence during differentiation processes their isotopes may be fractionated also. In addition, as both Zn and Cu are trace elements, metasomatism or low-temperature alteration could overwhelm any primitive signal that a rock once held. Therefore, in order to estimate the Cu and Zn isotopic compositions of the bulk silicate Earth (BSE) it is necessary to 1) choose pristine samples; 2) constrain the extent to which igneous differentiation processes fractionate the isotopes, and; 3) analyze as wide a variety of mantle derived samples as possible.

The first modern Cu and Zn isotope estimates of BSE were based on the average composition of MORB samples taken from three ocean basins: δ^{65}Cu = 0‰ and δ^{66}Zn = 0.25‰ (Ben Othman et al. 2006). The reason that no precision is given is that these data are given in a conference abstract; nevertheless, for the following decade, these estimates were the accepted values (the abstract was never written up and no further systematic studies were performed).

It is only recently that further investigations into this area have been made. Since Cu is highly incompatible and strongly chalcophile, its behavior during mantle melting is controlled by the fusion of sulfides (Lee et al. 2012); for partial melting degrees <25%, residual sulfides may be retained in the source and could potentially create isotopic fractionation. In order to test the possible effect of partial melting on the isotopic composition of Cu, Savage et al. (2015b) measured komatiites (ultra-mafic lavas formed by >25% partial melting; δ^{65}Cu = 0.06±0.06‰, 2sd, n=14) and compared these to fertile orogenic lherzolites (mantle samples that have undergone the least melt depletion: δ^{65}Cu=0.07±0.09‰, 2sd, n=16: Ben Othman et al. 2006; Ikehata and Hirata 2013), as well as a representative selection of both mid-ocean ridge and ocean island basalts. All groups have identical Cu isotope compositions (Fig. 6) which suggests that during mantle melting there is limited Cu isotope fractionation expressed in the melt. Savage et al. (2015a) therefore used all this data to propose a δ^{65}Cu=0.07±0.10‰ (2sd) for the BSE. Furthermore, these authors measured the Cu isotope compositions of two magmatic differentiation sequences, from Kilauea Iki, Hawaii, and Hekla, Iceland, systems. Both suites define a large range of SiO_2 and MgO contents and evolved from a cogenetic source with limited contaminations by crustal materials. The samples from Kilauea Iki showed no variation away from BSE with increasing degree of differentiation, as would be expected given the lack of sulfide fractionation in this system. In comparison, the samples from Hekla show more variability, which seems to be related to the removal of sulfides in the magma chamber. However, these variations are limited (range of compositions from Hekla $-0.08‰<\delta^{65}Cu<0.20‰$) and, crucially, the basalts from Hekla are identical to BSE. This indicates that significant igneous differentiation generates only limited Cu isotope fractionation, further confirmed by the similarity of I-type granite ($\delta^{65}Cu=0.03\pm0.15‰$, 2sd: Li et al. 2009) to BSE.

Liu et al. (2015) reached similar conclusions to Savage et al. (2015b) by comparing a large set of both unmetasomatised cratonic and orogenic peridotites with MORB, and OIB and proposed a $\delta^{65}Cu=0.06\pm0.20‰$ (2sd) for the BSE. Their data for metasomatised peridotites were much more variable, demonstrating the susceptibility of Cu-depleted rocks to secondary isotope fractionation; this was also seen in large negative Cu isotope excursions in Kilbourne Hole peridotites which correlate with LREE enrichment, and with large positive komatiite Cu isotope enrichments which only occur in those samples whose Cu contents do not plot on olivine control lines (Savage et al. 2015a). This suggests that Cu isotopes could be further utilized as a tracer of recycled materials in the mantle and, for instance, island arc material; indeed, Liu et al. (2015) provide a large set of arc basalt data whose range is much larger than that defined by both MORB and OIB (Fig. 6).

Compared to the Cu isotope system, fewer studies have attempted to address the behavior of Zn isotopes during igneous processes. Chen et al. (2013a) evaluated the extent to which Zn isotopes are fractionated during igneous processes by the same set of samples as Savage et al. (2015a) for Cu isotopes, those of Kilauea Iki, USA, and Hekla Volcano, Iceland. Both sets of samples show ~0.1 per mille isotopic variation but only the δ^{66}Zn of the Kilauea Iki samples vary systematically, correlating with the degree of differentiation (MgO contents) with the most evolved samples enriched in the heavier isotopes (see Fig. 7). These isotopic variations are interpreted as the result of crystallization of isotopically light olivines, and Ti-oxides at the very end of the differentiation sequence (Chen et al. 2013b). Chen et al. (2013b) combined the data from mafic rocks from Herzog et al. (2009), and their own data to determine the δ^{66}Zn of the BSE to be 0.28 ± 0.08‰. More recently, Sossi et al. (In review) have shown that ultramafic rocks comprising unmetasomatised peridotites from the Balmuccia massif and komatiites with ages varying from 3.5 to 2.7Ga are all isotopically lighter than basalts and complement the δ^{66}Zn vs MgO trend defined by Chen et al. (2013b). Sossi et al. (In review) used the average of these ultramafic samples to determine the most up to date δ^{66}Zn composition of the BSE to be 0.15 ± 0.05‰. Telus et al. (2012) showed that most granites are not isotopically fractionated in Zn with regards to the BSE value, but pegmatites and some granites are isotopically heavy (up to ~0.9‰). Telus et al. (2012) interpreted these heavy isotopic compositions in terms of fluid exsolution and suggest that Zn isotopes can be used to trace fluid exsolution in rocks.

Isotopic fractionation during core formation. Given that both Zn and Cu can partition in measureable quantities into the metal phase during metal-silicate equilibration, there is the potential that both isotope systems could reveal insights into the physiochemical conditions of Earth's differentiation into a planet with a metallic core and silicate mantle. However, for both Zn and Cu, their isotope partitioning behavior is only now being investigated via experimental studies – but there is huge potential for further work.

In the case of Zn, Bridgestock et al. (2014) showed that there appears to be no isotope effect associated with metal silicate equilibration. This indicates that, even if there is measureable Zn in Earth's core, partitioning into this reservoir would not leave its isotopic fingerprints on Earth's mantle. This is consistent with the similarity of the BSE composition with those of carbonaceous, unequilibrated ordinary and EH chondrites (see above).

The case of Cu is more complicated. A series of metal-silicate experiments performed by Savage et al. (2015b) indicated that the heavier Cu isotope prefers to enter the metal phase. This would suggest (given that 2/3 of Earth's Cu is in the core) that bulk Earth is isotopically heavier than the value estimated for BSE (see above). The problem is that there are no primitive meteorites thus far measured which match this isotopically heavy composition (in fact, the Cu isotope composition of BSE is still heavier than most chondrites; Fig. 3). Assuming that the bulk Earth is chondritic, i.e., the bulk Earth has a lighter Cu isotope composition than its mantle, this could imply a number of possibilities:

1) Cu is also a moderately volatile element, depleted in Earth's mantle relative to chondrites. It could be that impact-driven volatilization created this depletion, which would preferentially lead to the loss of light Cu, leaving a heavy residue. However, as Zn and to a lesser extent Cu isotopes in chondrites have shown,

Earth’s volatile depletion was more likely caused by nebula processes (see above).

2) Earth’s mantle Cu isotope composition is not in equilibrium with its core: it could be that late addition of Cu to the Earth, during the final stages (i.e. the giant impact) or post-core formation (i.e. the late veneer) may have set the BSE composition. In the case of the late veneer, there is not enough mass delivered by this process to account for all the Cu in the mantle today. In the case of the giant impactor, this is dependent on the composition of the impactor – even if it was CI-like (e.g. Schonbachler et al. 2010), the disruption created by this event would still have led to phase equilibration in the following magma ocean.
3) Earth contains a hidden, isotopically light Cu reservoir. Savage et al. (2015b) performed sulfide-silicate Cu isotope fractionation experiments, and found that, in this instance, the sulfide phase preferentially takes the lighter isotope of Cu; hence, rather than 2/3 of Cu being held in the core, this reservoir may be split into an isotopically heavy metal and isotopically light sulfide (relative to BSE). One possibile sulfide reservoir is that of a ‘Hadean Matte’ (O'Neill 1991; Lee et al. 2007), an Fe-O-S phase that remains as the final liquid after the crystallization of a magma ocean. Modelling this in terms of [Cu] and δ^{65}Cu suggests that, if such a reservoir formed and eventually was admixed into the core (it would sink through the mantle due to its higher density), it could add up to ~0.8wt.% S to the core (Savage et al. 2015b).

Although there are caveats associated with each of the above models, Cu isotopes could be a powerful tool in tracing the fate of sulfides in various igneous and planetary processes, but the framework to understand this fractionation is still required, and more experimental work is required.

Isotopic fractionation by evaporation on Earth. While the Zn and Cu isotopic database for terrestrial igneous rocks is very limited, tektites are extremely fractionated (Moynier et al. 2009c). Tektites are terrestrial natural glasses produced during a hypervelocity impact of an extraterrestrial projectile onto the Earth's surface, and are extremely depleted in volatile elements, e.g., they are among the driest terrestrial samples (<0.02% of water). Moynier et al. (2009c) found that tektites are extremely enriched in the heavier isotopes of Zn, up to 2.5 ‰ and attributed this enrichment to kinetic isotopic fractionation during evaporation. Copper can be even more fractionated than Zn, with δ^{65}Cu up to 12.5 ‰ found in some European tektite samples (Rodovka et al. In review). The difference of behavior between Cu and Zn has been explained by isotopic fractionation in a diffusion-limited regime, where the magnitude of the isotopic fractionation is regulated by the competition between the evaporative flux and the diffusive flux at the diffusion boundary layer (Moynier et al. 2010a). Copper diffuses much faster than Zn (due to the difference in ionic charge in silicates of Zn^{2+} vs. Cu^{+}), hence the larger isotopic fractionation in Cu than in Zn in tektites is due to the significant difference in their respective chemical diffusivity.

The Moon. The isotopically heavy lunar regolith (2.2‰<δ^{66}Zn < 6.4‰ and 2.6‰<δ^{65}Cu <4.5‰) reflects billions of years of evaporation due to solar wind sputtering and micrometeorite impact gardening (Moynier et al. 2006; Herzog et al. 2009). On the other hand, the low-Ti (δ^{66}Zn = 1.31 ± 0.13‰) and high-Ti basalts (δ^{66}Zn = 1.39 ± 0.39) have a more limited isotopic variations and are systematically ~1 ‰ heavier than the BSE for Zn

(Paniello et al. 2012a; Day and Moynier 2014; Kato et al. 2015). The only data available for Cu isotopes (δ^{65}Cu =0.5±0.1‰, Herzog et al. 2009) suggests that there is a similar enrichment in the heavy Cu isotope in lunar? rocks, but this will need further investigation in the future. Since the isotopically heaviest carbonaceous chondrite group (CI) has a δ^{66}Zn = 0.46‰ and δ^{65}Cu = 0.05‰ (Luck et al. 2003, 2005; Barrat et al. 2012), mixing with chondrites does not explain the Zn or Cu isotopic composition of the lunar basalts. In addition, lunar plutonic rocks (alkali and magnesian suite samples) are isotopically heavier than the mare basalts (δ^{66}Zn up to 6.27‰) suggesting that the volatile loss could have occurred in two stages: during the proto-lunar disk stage, where a fraction of lunar volatiles accreted onto Earth, and from degassing of a differentiating lunar magma ocean, implying the possibility of isolated, volatile-rich regions in the Moon's interior (Kato et al. 2015).

ZINC AND COPPER IN LOW TEMPERATURE GEOCHEMISTRY

Since the pioneering work of Maréchal et al. (1999; 2000), and Francis Albarède's chapter on Cu and Zn isotopes in the first RiMG volume on non-traditional stable isotopes (Albarède 2004), a considerable amount of effort has gone into understanding and applying isotope variations of these two elements in samples from Earth's surface. As with the development of any relatively new isotope system, documentation of stable isotope variations in nature has been coupled with experimental and theoretical studies aimed at characterizing isotopic fractionations associated with key surface Earth processes. Copper-Zn stable isotope geochemistry of the surface Earth environment has been part of reviews by Cloquet et al. (2008) and Wiederhold (2015). An emerging new interest lies in the application of Zn and Cu isotopes to the study of biological pathways and changes in metabolism associated with diseases. These applications are here treated in chapter X (Albarède et al. 20XX, this volume).

The data obtained to date for important surface Earth reservoirs are summarized in Figure 8. One of the first order features of Cu-Zn isotope geochemistry that this compilation confirms is the contrast between the relative homogeneity of samples whose isotopic characteristics are determined by high temperature processes, versus the variability in materials formed and equilibrated at low temperatures. Thus, igneous rocks (excluding ultramafic rocks) show a very tight distribution, with δ^{66}Zn = 0.30±0.07‰ (n = 77, 1SD) and δ^{65}Cu = 0.08±0.17‰ (n = 287) which overlaps with the BSE estimate presented earlier in this chapter (note that these averages were taken using all igneous rock data available in the literature, without screening for the possibility of secondary alteration/metasomatism – hence they are slightly different, and have poorer precisions, to those defined in the section above). Another first-order feature of the data in Figure 8 is that sediments that have undergone physical, but minimal chemical, processing through the fluid envelopes of the surface Earth (i.e. clastic sediments from rivers, lakes, oceans, as well as aerosols/dust), have average Cu and Zn isotope signatures that are identical to high temperature igneous rocks, and are not much more variable. In contrast, environmental samples that *have* seen such biogeochemical processing record a roughly 2.5‰ range in Cu and Zn isotopes, or about 30-40 times the analytical precision. Ore minerals that formed at high temperatures exhibit a range of roughly 1‰ that is also more or less centred on the peak in igneous rocks (Fig. 8, black bars at bottom). In contrast, the isotope compositions of minerals from the supergene environment, containing Cu that has undergone (possibly multiple) oxidation and reduction cycles, exhibit huge (~20‰) variability (e.g. Maréchal et al. 1999; Larson et al. 2003; Mason et al. 2005; Mathur et al. 2005; Markl et al. 2006; Asael et al. 2007; Mathur et al. 2009; Mathur et al. 2010).

In the following sections we first review the experimental constraints on the size and sign of isotope fractionations of Cu and Zn associated with key surface, low temperature, processes. Secondly, we discuss the origin of, and geochemical constraints available from, Cu and Zn isotope variability in “natural” samples – i.e. those not significantly impacted by human activities. This large subject is separated into sub-sections on (1) the weathering-soil-plant system, and (2) the oceans, their inputs, outputs and internal cycling. In this section we also briefly outline the very few studies that have sought to apply Cu-Zn isotopes in Earth history, and outline the prospects for the future of such a pursuit. Isotopic variations, and their expression in environmental samples, superimposed by human activity on this natural biogeochemical cycling represent a somewhat distinct topic, and are treated in a third section. For convenience, and since ore minerals often represent the starting material from which pollution of the Anthropocene environment derives, the very large variability seen in ore minerals is also dealt with in this third section.

Experimental constraints on fractionation mechanisms

A survey of the literature reveals four general isotope fractionation mechanisms causing the roughly 2.5‰ variation in both Cu and Zn isotopes in environmental samples, as well as the much greater degree of variability in supergene Cu ore minerals:

1. Equilibrium isotope distributions between Cu in different oxidations states;

2. Equilibrium isotope distribution between dissolved aqueous species;

3. Equilibrium and kinetic effects caused by interactions between solids – abiotic as well as living cells - and aqueous solutions (sorption, precipitation);

4. Kinetic and equilibrium effects related to uptake into the cells of living microbes and higher plants.

The sign and magnitude of these fractionations are summarized in Figure 9 and are discussed in turn below. Though the separate processes bulleted above makes discussion more convenient, distinction between these fractionation mechanisms is not often sharp. To some extent this lack of clarity represents some confusion in the literature. Thus, for example, all metals sorb to the external surfaces of microbial cells, and to some extent the roots of higher plants. This is a somewhat distinct phenomenon from uptake into the cells for metabolic use in enzymes and proteins. When metal uptake is studied in microbiological or hydroponic plant growth experiments, the vast majority of the metals in solution in the media are bound to an added organic complexant, such as EDTA. This leaves only a small pool of free metal ion, which is often regarded as the pool that is available for uptake. The isotopic composition of the metal taken up can be lighter than the bulk experiment, for example where uptake is transport (diffusion)-limited (e.g. John et al. 2007b), or it can be heavier, for example for some plant species that actively bind external metals using phytosiderophores (e.g. Arnold et al. 2010a).

On the other hand, in experiments where organic complexants have not been added, the free metal ion pool is often many orders of magnitude more concentrated. In this case the metals sorb to external surfaces. Though sometimes described as "uptake" in the literature, there is almost certainly no metabolic function of the metals in this case. Such sorption often involves binding to deprotonating functional groups such as carboxyls and amines, so that the fractionation factors measured in these experiments are more relevant to categories 2 and 3 above than 4. On the other hand, there is sometimes genuine uncertainty over whether a pool of metals associated with a cellular experimental product is intra-cellular or sorbed on external surfaces. Some researchers have been able to distinguish between these two mechanisms using experiments with living (active metabolic uptake) versus dead (passive adsorption) cells, or by removing the extra-cellular pool using a desorptive wash prior to analysis (e.g. John et al. 2007b; Navarette et al. 2011). Finally, Cu uptake into microbial cells has been interpreted as involving reduction of external Cu(II) to internal Cu(I) – i.e. a component of 1 above (e.g. Zhu et al. 2002; Navarette et al. 2011; Jouvin et al. 2012; Ryan et al. 2013).

Changes in oxidation state. Zinc does not undergo changes in oxidation state at Earth surface conditions. Thus, although a substantial isotope fractionation has been characterized in an electroplating experiment involving reduction of aqueous Zn (II) to Zn metal (Kavner et al. 2008), this is unlikely to be relevant to natural systems. For copper, on the other hand, the transition between Cu(I) and Cu(II) happens at redox conditions relevant to the Earth's surface, and Cu occurs in both reduced and oxidized forms in Earth materials. Further, it is clear that the redox transition involves large isotope fractionations. This fractionation was first characterized by Zhu et al. (2002) in experiments that found $\Delta^{65}Cu_{Cu(II)-Cu(I)}$ = 4‰ for the reduction of aqueous Cu(II) to a Cu(I) iodide precipitate at 20°C (here and throughout $\Delta^{65}Cu_{x-y} = \delta^{65}Cu(\text{phase x}) - \delta^{65}Cu(\text{phase y})$). Ehrlich et al. (2004) followed this up with experiments involving the precipitation of Cu(I)S (covellite) from an aqueous Cu(II) solution and found $\Delta^{65}Cu_{Cu(II)aq-Cu(I)S} = 3.06\pm0.14‰$ at 20°C. Furthermore, and importantly, they contrasted this large fractionation with the small one ($\Delta^{65}Cu_{Cu(II)aq-Cu(II)(OH)2} = 0.27\pm0.02‰$) for Cu(II) hydroxide precipitation from a $Cu(II)_{aq}$ solution. This finding, as well as that by Maréchal and Sheppard (2002) of small (0.2-0.4‰) isotopic differences between Cu(II) in solution versus malachite, strongly suggests that it is the change in oxidation state, and not the phase change, that causes the large isotopic shift seen in these and other redox experiments. These results were further confirmed by Mathur et al. (2005), who found that Cu (I) in chalcocite (Cu_2S) and chalcopyrite ($CuFeS_2$) was 1.3 and 2.74‰ lighter than aqueous Cu(II) in abiotic batch oxidative leach experiments. In analogous experiments inoculated with *Thiobacillus ferrooxidans* the heavy oxidized Cu was located in amorphous Cu-Fe oxide minerals surrounding bacterial cells.

Zhu et al. (2002) found that Cu incorporated into proteins expressed in bacteria and yeast cells was 1.0-2.1‰ lighter than in the parent solutions and media, and used these findings to suggest that the biogenic uptake of light Cu also involved reduction. Likewise, Navarette et al. (2011) interpret Cu isotope variations in media from which live bacterial cells remove Cu as due to cellular uptake (as opposed to sorption, which induces a different fractionation in their experiments, as observed in dead cells). This is associated with preferential uptake of the light isotope – by up to 4.4‰ - and was also interpreted to involved reduction of Cu(II). As noted in this study, if this reduction occurs within the cell, the changes seen in the media require that there is also efflux of heavy Cu from the cells, allowing equilibration of the two Cu pools. As discussed later in this section, uptake of isotopically light Cu by bacteria and higher plants probably also involves reduction by a reductase protein (e.g. Navarette et al. 2011; Weinstein et al. 2011; Jouvin et al. 2012; Ryan et al. 2013).

Organic complexation. Copper forms very strong inner sphere complexes (conditional stability constants up to 10^{25}) with functional groups in organic matter (McBride 1981; Grybos et al. 2007; Ryan et al. 2014). Virtually all Cu in the operationally-defined dissolved phase (that fraction passing through a 0.45μm filter) of rivers and the oceans is bound in these organic complexes (e.g. McBride 1981; Coale and Bruland 1988; Moffett and Brand 1996; Shank et al. 2004; Grybos et al. 2007; Vance et al. 2008; Ryan et al. 2014), such that inorganically-complexed and free Cu^{2+} ion concentrations are 2-5 orders of magnitude lower than total dissolved Cu. Similarly, up to 98% of the "dissolved" Zn in many natural waters is also complexed to organic ligands, though with stability constants that are of order 10^9-10^{11} (e.g. Wells et al. 1998; Bruland 1999; John et al. 2007b). Grybos et al. (2007) suggest that two important processes compete to control transition element behavior in soils: binding to organic complexes, both in condensed organic matter and in an aqueous phase, versus sorption to the surfaces of secondary minerals such as clays and Fe-Mn oxyhydroxides. The last decade of research on Cu-Zn isotopes has revealed that this competition is almost certainly key for isotope distributions, not only in soils but also between the dissolved and particulate phases in rivers and the oceans (e.g. Vance et al. 2008; Bigalke et al. 2010a; b; Bigalke et al. 2011; Little et al. 2014b; Vance et al. 2016). In quantifying the isotopic fractionations between an (often) aqueous organically-complexed pool and the sorbed pool, the universal approach has thus far been to measure the isotopic separation between each of these and a dissolved free metal ion (Cu^{2+}, Zn^{2+}) pool. Each of these, therefore, are here dealt with separately.

Ban et al. (2002) were the first to quantify the isotopic impact of this important process, finding $\Delta^{66}Zn_{EDTAZn\text{-}Zn2+}$ ~ 0.2‰ (here and throughout $\Delta^{66}Zn_{x\text{-}y} = \delta^{66}Zn_{(phase\ x)} - \delta^{66}Zn_{(phase\ y)}$). Jouvin et al. (2009) used Donnan membranes to separate free Zn from that complexed to humic acid. These authors found no fractionation at pH ≤5.4, but $\Delta^{66}Zn_{Humic\text{-}Zn2+}$ = +0.24±0.06‰ at pH 6.1-7.2. The variable fractionation as a function of pH was interpreted in terms of the partitioning of the bound Zn between high affinity (HA, bound to phenols) and low affinity (LA, bound to carboxylate groups) sites, and the fact that, at equilibrium, isotopically heavy Zn is partitioned into the strongly-bound species. Zinc is increasingly bound to the HA sites at higher pH (50:50 LA and HA at pH around 6.1-6.2). Based on calculated mass balance between the species, Jouvin et al. (2009) proposed a fractionation factor, $\alpha_{HAS\text{-}Zn2+}$, of 1.0004. Bigalke et al. (2010a) performed the same experiment for Cu at pH 2-7. In the case of Cu there is no apparent isotopic difference between LA and HA sites, and only 11-35% of the bound Cu is in HA sites. For both, $\Delta^{65}Cu_{Humic\text{-}Cu2+}$ = +0.26±0.11‰. More recently, Ryan et al. (2014) measured the Cu isotope fractionation between free Cu and a range of soluble organic ligands. They see a “strong” positive correlation between the isotopic fractionation and the value of the stability constant for each complex. Thus for natural riverine fulvic acid (log K = 8) $\Delta^{65}Cu_{complex\text{-}free}$ = +0.14±0.11‰, whereas for desferrioxamine B (DFOB logK = 24.7) $\Delta^{65}Cu_{complex\text{-}free}$ = +0.84±0.30‰.

Sorption to abiotic substrates. As with the fractionations associated with organic complexation outlined above, isotopic effects associated with sorption have also been measured experimentally relative to a dissolved free metal ion pool. Pokrovsky et al. (2005) measured Zn isotope fractionations upon sorption from simple aqueous solutions of low ionic strength (0.01M), where Zn is speciated as a hexaquocomplex, and where the sorption equilibrium can often be envisaged as (omitting the solvating waters in the aqueous species):

$$>MeOH^0 + Zn^{2+} = MeO\text{-}Zn^+ + H^+$$

They found a small preference for the light isotopes of Zn (by about ~0.18-0.23‰) on goethite and birnessite (δ-MnO_2) surfaces, and for the heavy isotopes (by about ~0.11-0.14‰) on pyrolusite (β-MnO_2) and aluminium oxides. Zinc sorbed to hematite exhibited the largest isotopic separation from dissolved free Zn, with $\Delta^{66}Zn_{sorbed\text{-}free}$ = +0.61‰ when sorption starts at pH 5.5, but decreasing to zero at higher pH as sorption increases. Not all the results of this pioneering study have been reproduced. Indeed in all subsequent studies, sorbed Zn has been found to be universally heavy relative to the aqueous free metal ion pool. Bryan et al. (2015) discuss possible reasons for these discrepancies, including the possibility of kinetic effects in short duration experiments. Moreover, theoretical considerations (e.g. Schauble 2004) suggest that the lower co-ordination of the metal sorbed on these surfaces (e.g. Peacock and Sherman 2004; Balistrieri et al. 2008; Juillot et al. 2008) should prefer the heavy isotope.

Balistrieri et al. (2008) find heavy Cu and Zn sorbed onto ferrihydrite, in a study incorporating both natural data from streams draining a metal sulphide deposit and experimental results. The experiments were also done with low ionic strength solutions (0.008M). The sorption experiments only lasted 2-3 hours, but in this case the sorption of heavy isotopes as well as a close-to-linear relationship between the fraction of dissolved metal and isotopic composition rule out a kinetic effect. Again, however, only the aqueous phase was measured so that the mass balance was not confirmed. This study also mixed water draining a mine (acidic and metal-rich) with water from the river (uncontaminated and alkaline) it drains into. Overall, aqueous Cu and Zn concentrations decrease as pH increases and as they are sorbed onto ferrihydrite, and the aqueous phase becomes light. The $\Delta_{\text{sorbed-solution}}$ values are +0.73±0.08‰ for Cu and +0.52±0.04‰ for Zn. Despite potential variation in aqueous speciation with pH, these sorption experiments are well modeled by a single process, which they suggest to be a change in co-ordination and bond length – octahedral co-ordination in solution with Me-O bond distances of 2.0-2.4Å, versus tetrahedral-co-ordination on ferrihydrite and other Fe oxides and bond lengths of 1.8-2Å. Pokrovsky et al. (2008) corroborate the finding of sorption of heavy Cu, finding $\Delta^{65}\text{Cu}_{\text{sorbed-solution}}$ = 0.8±0.2‰ for goethite and1.0±0.2‰ for gibbsite.

Juillot et al. (2008) confirmed this result for Zn sorption to ferrihydrite ($\Delta^{66}\text{Zn}_{\text{sorbed-solution}}$ = +0.53‰). These authors also obtained $\Delta^{66}\text{Zn}_{\text{sorbed-solution}}$ for goethite = +0.29‰. In these experiments ionic strength was kept at 0.1M using KNO_3 and some solids were measured to close the mass balance. Moreover, time-dependent experiments found light Zn taken up onto ferrihydrite in the first hour, before the observations settled down to a constant heavy value at about 18 hours, possibly explaining the light value found in the Pokrovsky et al. (2005) study. These authors also interpret their results in terms of changes in co-ordination and bond-length. The smaller fractionation for goethite is ascribed to the fact that bond-lengths are shorter on the surface relative to solution, even though Zn is octahedrally co-ordinated on goethite, versus tetrahedral co-ordination on ferrihydrite.

Recently, Bryan et al. (2015) conducted a much more extensive study of Zn isotopic fractionation during sorption to poorly crystalline Mn oxyhydroxide, which dominates the sorption of many metals, including Zn, in the marine environment (e.g. Koschinsky and Hein 2003; Wasylenki et al. 2011; Little et al. 2014b). Isotopic fractionations were monitored as a function of equilibration time, ionic strength of the solution, speciation of inorganic zinc in the aqueous phase, and degree of loading of the Mn oxide surface. The Zn isotopic composition of both solid and dissolved phase were measured, allowing an assessment of overall experimental mass balance as well as of the relative importance of kinetic versus equilibrium fractionation. For low ionic strengths there is a small kinetic effect ($\Delta^{66}Zn_{sorbed\text{-}dissolved}$ ~ -0.2‰) for experimental durations up to 48 hours, but for equilibration times greater than 100 hours fractionations are within uncertainty of zero ($\Delta^{66}Zn_{sorbed\text{-}dissolved} = +0.05\pm0.08$‰). For high ionic strength solutions heavy isotopes are always preferentially adsorbed, but there is a strong dependence on surface loading, with $\Delta^{66}Zn_{sorbed\text{-}solution} = +2.74$‰ for low surface loadings (8%), reducing to +0.16‰ for high. The authors interpret this variation in terms of a change in co-ordination from tetrahedral to octahedral as surface loading increases from tetrahedral for Mn oxide with Zn/Mn = 0.008 to octahedral at Zn/Mn = 0.128 (Manceau et al. 2002). The difference in behavior at different ionic strengths is partially attributed to the fact that in the low ionic strength experiments the surface loadings were also high (Zn/Mn ~ 0.2). There may also be an effect of speciation. The authors suggest that it is free Zn^{2+} that is sorbed. The isotopic composition of free Zn is predicted to change as ionic strength and the proportions of inorganic carbonate and chloride complexes of Zn, with different equilibrium fractionations relative to free Zn (Fujii et al. 2010, 2014; Black et al. 2011), change. For

Zn sorption to kaolinite (Guinoiseau et al., 2016), qualitatively similar variation in $\Delta_{\text{sorbed-free aqueous ion}}$ (Fig. 9) has been interpreted as a shift from outer sphere complexation of Zn in basal exchange sites at low pH, when edge sites are protonated, to inner sphere complexation on edge sites, and larger fractionations, at higher pH and ionic strength.

Sorption/binding to biological suurfaces. Both elements under consideration here are essential nutrients for plants and animals, but they are toxic at high concentrations in both the terrestrial and marine realm (e.g. Anderson and Morel 1978; Flemming and Trevors 1989; Marschner 1995; Moffett and Brand 1996; Sold and Behra 2000; Peers and Price 2006; Broadley et al. 2007; Yruela 2009; Sinoir et al. 2012; Bruland et al. 2014). Thus, there are important interactions with the cells of living matter that induce significant isotope fractionations. As noted earlier a careful distinction must be made, one that is not always made in the literature (though see John et al. 2007b; Navarette et al. 2011), between metals that are sorbed or bound to the surfaces of microbial cells and plant roots, and those taken up for metabolic utilization. In terms of basic chemical and isotopic mechanisms, the former process is more akin to the binding to the functional groups of both organic matter and inorganic surfaces discussed in previous sections, and usually favours the heavy isotopes. The latter may favour either the light isotope, if governed by a transport-limited, kinetic, process (e.g. John et al. 2007b) or if it involves reduction as may be the case for Cu (e.g. Zhu et al. 2002; Navarette et al. 2011), or the heavy, if it occurs through active uptake by phytosiderophores (e.g. Arnold et al. 2010a).

Gélabert et al. (2004; 2006) conducted experiments that characterized the nature of interactions between marine and freshwater diatoms and aqueous Zn, including isotope fractionation. The aqueous phase (the medium) in these experiments had inorganic Zn concentrations of 0.3-20 μM. With no organic complexant stabilizing Zn in solution, the process studied is sorption, not "uptake". Zinc sorption was strongly controlled by organic layers covering the silica frustule, specifically by carboxylate and silanol groups, with the amount of Zn sorbed to an organic-free silica skeleton being factor five less than cell with organic surface layers. They find $\Delta^{66}Zn_{diatomcell\text{-}medium} = +0.1‰$ to +0.5‰ in the presence or absence of organic layers. Coutaud et al. (2014) conducted experiments that characterized fractionation upon uptake and release by and from a "phototrophic biofilm" (an aggregate of micro-organisms embedded in a exopolysaccharide matrix) and see adsorption of heavy isotopes to a much greater degree than this – by up to 1.2±0.4‰ relative to solution. Some of these fractionations for sorption to cells are very similar to those measured for those outlined earlier for complexation of Zn to organic functional groups, which may be the dominant binding process (Gélabert et al. 2004; Gelabert et al. 2006). They are also often similar to those found for externally-bound Zn in culturing experiments by John et al. (2007b) that were primarily targeted at documenting fractionation upon uptake into the cells themselves.

Three additional studies have been aimed at quantifying and understanding the sorption of Cu and Zn onto cells, but differ in their interpretation of the exact driver of the fractionations observed, specifically whether it was sorption or biological uptake. Pokrovsky et al. (2008), in experiments with Cu sorption onto abiotic metal surfaces and onto bacterial and diatom cells at low ionic strength (0.01-0.1M), see virtually no fractionation upon sorption to bacterial cells at circumneutral pH (5.1-6.1, Δ^{65}Cu = mostly 0±0.3‰). They see light Cu sorbed onto the cells of soil bacteria at pH 1.8-3.3 (by up to 1.8‰). The rationale given for the sorption of light Cu in this case relates to an outer-sphere monodentate complex likely to form between Cu and phosphoryl groups – with apparently longer bond distances - on bacterial surfaces at low pH.

Navarette et al. (2011), on the other hand, contrast two sets of Cu uptake experiments with live versus dead cells of *E. coli* and *B. subtilis*. When the cells are alive the solution gets much heavier as it loses Cu to the cells, with $\Delta^{65}\mathrm{Cu}_{\mathrm{cells\text{-}solution}}$ as low as -2.6‰ and -4‰ at different pH values. On the other hand, when cells were dead, the solution was lighter, and only by about 0.4‰. As with the small fractionations of Zn in the Gélabert et al. (2004; 2006) experiments, it is likely that the latter process is analogous to the complexation of Cu to organic functional groups outlined earlier (e.g. Bigalke et al. 2010c; Ryan et al. 2014). The uptake of light Cu by live cells, on the other hand, is interpreted in terms of active intra-cellular complexation. Navarette et al. (2011) confirm this finding in experiments where the aqueous Cu is stabilised by organic complexants so that it is not sorbed. They again document large separation factors, with $\Delta^{65}\mathrm{Cu}_{\mathrm{cells\text{-}solution}}$ = -1.2 to -4.4‰, depending on species and the nature of bacterial consortia used in each experiment. The authors suggest that the light uptake may be due either to a kinetic fractionation – irreversible incorporation – or to an equilibrium reduction to Cu(I) within the cell. If the latter is important there has to be communication with the outside of the cell to allow the efflux of the oxidized Cu back to the solution. The theme of a paper by Kafantaris and Borrok (2014) is similar, in this case applied to Zn, in that their objective was to try to understand the relative importance of surface complexation versus intracellular incorporation. For experiments with high Zn/bacterial cells ratios, Zn sorption varies with increasing pH in a very similar way to abiotic experiments, presumably due to increased deprotonation of cell surface organic functional groups and consequent binding of Zn. Zinc isotopic data are best fitted by an equilibrium model with a separation factor $\Delta^{66}Zn_{cells-solution}$ +0.46‰. In contrast, this study found heavy Zn in solutions at low Zn/bacterial cells ratios, with $\Delta^{66}Zn_{cells-solution}$ = -2.5‰. This is interpreted in terms of the complexation of Zn in the dissolved phase by organic exudates, generating two pools of Zn, a complexed (heavy) and a free (light) pool, with the light free Zn pool sorbing onto cell surfaces. This would, however, require an isotope separation factor between organically-complexed and free Zn of 2-3‰, an order of magnitude greater than that found in experiments to date (Ban et al. 2002; Jouvin et al. 2009). On the other hand, these authors also used an electrolyte wash to remove extra-cellular Zn in an attempt to quantify intra-cellular inventories and isotopic composition, and also found Zn isotopes in cells to be slightly, to very, heavy relative to the aqueous phase. It should be noted, however, that these experiments were conducted at Zn concentrations 3-4 orders of magnitude greater than found in nature, perhaps at levels where Zn is toxic. Moreover, precipitates containing high levels of Zn on cell surfaces, probably not removed by their wash, is likely at these high concentrations.

Metabolic uptake by algae and higher plants. Primary production by photosynthesis on Earth is roughly equally split between higher plants on land and algae in the oceans (Field et al. 1998). As noted earlier, Cu and Zn are both essential micronutrients for photosynthesizing organisms and are indeed required for enzymes and proteins in all organisms, but are also both toxic to plants and algae at very high concentrations. There have been a relatively small number of studies characterizing fractionation of Cu and Zn isotopes during uptake by plants – as opposed to absorption or binding to external surfaces as discussed in the previous section.

John et al. (2007b) report culturing experiments with the diatom *Thalassiosira oceanica* across a range of free Zn ion concentrations, controlled in their media by the addition of complexant EDTA, representative of coastal and open ocean waters. In order to document fractionation during uptake, such culturing studies must remove externally adsorbed Zn by washing prior to analysis, and John et al. (2007b) find that the externally-sorbed Zn isolated in this way has an isotopic composition that is 0.1-0.5‰ heavier than the medium, consistent with other studies where binding of Zn to diatom external surfaces has been specifically targeted (Gelabert et al. 2006). In contrast, Zn in washed cells (targeting the internalized cellular Zn pool) is isotopically lighter than the medium. John et al. (2007b) document a range in fractionations, from $\Delta^{66}Zn_{\text{diatom-medium}}$ = -0.2‰ at low medium free Zn concentrations to -0.8‰ at high, with a step-like transition at free Zn concentrations that are in the range for natural seawater, at around 10^{-10}M. The authors ascribe these two different fractionations to two different Zn uptake systems – high and low affinity. These two systems are well-documented in previous culturing studies (e.g. Sunda and Huntsman 1992), with the high affinity pathway up-regulated when available Zn is low but saturated at high seawater/medium Zn concentrations. The low affinity pathway likely involves diffusive transport across the cell membrane, thus favouring the light isotope. John and Conway (2014) document the same magnitude of fractionation upon uptake into a different kind of phytoplankton – the marine flagellate chlorophyte

Dunaliella tertiolecta. The $\Delta^{66}Zn_{cells-medium}$ = -0.76±0.02‰ obtained is the same as for the low affinity uptake system in the diatom experiments, consistent with the high free Zn concentrations in their medium.

There have been more studies focusing on fractionations of Cu and Zn isotopes upon uptake into higher plants. Taken as a whole, these studies have documented a number of important features of plant uptake systems for Cu and Zn: (1) all plants have a bulk Cu isotope composition that is lighter than the external pool (c.f. bacterial uptake of Cu in Navarette et al. (2011), discussed earlier), leading to the suggestion that Cu reduction upon uptake is an important process; (2) bulk plant Zn isotopic compositions are both lighter and heavier than the external bioavailable pool, perhaps depending on whether free Zn or a complex is taken up; (3) all plants preferentially transfer the lighter isotopes of Zn upwards into stems and leaves, whereas early studies document preferential upward translocation of both light and heavy Cu isotopes.

Before discussing the details of experimental isotopic studies for Cu and Zn in higher plants, it is useful to briefly set the context in terms of plant uptake systems and the constraints that have come from the better studied Fe isotopic system (see Russel et al. 2003 for useful summaries; Jouvin et al. 2012). For Fe, two fundamentally different uptake strategies lead to different isotope fractionations (e.g. Guelke and Von Blanckenburg 2007). Iron acquisition by Strategy I (non-graminaceous) plants involves the uptake of a free metal ion and requires a reduction step that favours uptake of isotopically light Fe. Analogously uptake of free Cu via transporters such as COPT1 has been described (e.g. Sancenon et al. 2004; Jouvin et al. 2012), and would also require reduction of soil Cu (II) to Cu (I) by a reductase enzyme. For Zn there is no oxidation state change involved. As with the diatom studies outlined above, Strategy I uptake of Zn may involve both a low and high affinity uptake system (see Jouvin et al. 2012). Low affinity uptake, active at external bioavailable Zn concentrations in excess of perhaps 10^{-7}M (e.g. Wang et al. 2009; Jouvin et al. 2012), involves diffusive transport via ion channels and electrogenic pumps, favouring the light isotope. High affinity Strategy I uptake involves zinc-iron-permease (ZIP) proteins that bind free Zn from the external pool at the cell membrane, probably favouring the heavy isotope, and facilitate its uptake and transmembrane transport. In contrast, Strategy II uptake (graminaceous plants), under metal-deficient conditions, can actively complex soil Fe (III) to a phytosiderophore derived from their root – with no reduction step and a small positive isotope fractionation for Fe (e.g. Guelke and Von Blanckenburg 2007; Moynier et al. 2013b). Uptake of Zn and Cu in "phytosiderophores", organic complexes that will favour the heavy isotope as discussed in earlier, have been discussed in the isotopic literature as outlined below.

The pioneering study of Weiss et al. (2005) showed that the roots of tomato, rice and lettuce were all slightly enriched in the heavy isotopes of Zn relative to the bulk nutrient solution in which they were grown – by 0.1-0.2‰. In contrast, the shoots, housing 75-85% of the Zn inventory of the plant, were isotopically light relative to the same nutrient solution – by 0.25-0.5‰, so that the bulk plants contain light Zn relative to the external pool. The simplest explanation of this observation requires the uptake of isotopically light Zn, through ion channels or electrogenic pumps, coupled to the preferential upward transfer of even lighter Zn, leaving the residual root pool heavy. Fujii and Albarède (2012) re-interpreted these observations using *ab initio* calculations and suggested that the fractionation is controlled by the difference in Zn speciation between the root system (isotopically heavy Zn-phosphates) and the upper parts, rich in isotopically light citrates and malates. It is noteworthy that the predicted isotopic signal of Strategy I behavior is found in a Strategy II plant like rice. In a follow up study, however, Arnold et al. (2010a) demonstrate that rice grown in soil rather than hydroponically is isotopically *heavy* relative to the soil, particularly under Zn deficiency. They attribute this to uptake of Zn bound to a "Zn-phytosiderophore". On the other hand, Tang et al. (2012) also observe Zn in plants that is up to ~0.6‰ heavier than in soils, but reject the phytosiderophore hypothesis because the species concerned do not release them. Instead, they favour uptake of heavy isotopes by ZIPs. The upwards transfer of light Zn has been confirmed by later studies (e.g. Moynier et al. 2009b; Caldelas et al. 2011; Jouvin et al. 2012; Tang et al. 2012).

This earlier work on Zn uptake by plants has been followed up by a series of more targeted studies aimed at more detailed investigation of the mechanisms by which plants take up Zn and its isotopes, especially with regard to speciation and including Zn uptake by zinc hyperaccumulators from contaminated soils (Aucour et al., 2011, 2015; Houben et al., 2014; Couder et al., 2015).

Weinstein et al. (2011) first measured the isotopes of Cu in plants, documenting light isotopes in every part of Strategy II plants – by 0.3-0.8‰ - relative to the soils in which they were grown. They also document significant transfer of light Cu upwards from the roots, or from the initial stock of Cu in lentils grown from seed without further Cu addition. In all cases, the topmost and youngest leaves contain the lightest Cu. These findings were confirmed by Jouvin et al. (2012). Though the latter study found a difference between Strategy I ($\Delta^{65}Cu_{\text{plant-nutrient solution}}$ = -0.84 to -0.47‰) and Strategy II ($\Delta^{65}Cu_{\text{plant-nutrient solution}}$ = -0.48 to -0.11‰), all of them took up the light isotope, suggesting that reduction of Cu (II) is an important factor in the uptake of Cu by all plants whether the Cu is complexed or not. Like the previous two studies, Ryan et al. (2013) observe much lighter Cu in plants than the soils in which they were grown, and a very clear difference between Strategy I ($\Delta^{65}Cu_{\text{whole plant-nutrient solution}}$ = -1.02±0.37‰) and Strategy II ($\Delta^{65}Cu_{\text{whole plant-nutrient solution}}$ = -0.15±0.11‰) plants. However, in contrast to the previous two studies, their Strategy II plants have a fairly constant isotopic composition in different parts of the plant while for Strategy I the heavier isotope preferentially moves upwards (shoots 0.87-1.35‰ heavier, leaves 0.53-0.98‰ heavier). These authors rationalize their observations in terms of the upward transfer of Cu in organic complexes like nicotinamine, which would indeed preferentially transport the heavy isotope (Ryan et al. 2014), if translocation upwards was not close to quantitative.

Cu-Zn isotopes in the weathering-soil-plant system

Soils represent the interface between the solid Earth and its fluid envelope, the place where chemical weathering of primary minerals and precipitation of secondary minerals begin, the substrate for plant growth, and the locus for the initial partitioning of elements between solid material and the aqueous phase that drains into groundwater, rivers and, eventually, the oceans. In addition, transfer of chemical elements between the atmosphere and soils occurs through the ablation, transport and deposition of dust. As such, soils are sites of complex processes that involve Cu and Zn transfer and isotopic fractionation via all of the mechanisms detailed in the previous section. For ease of discussion here we separate these processes as follows: (1) isotopic effects associated with leaching and dissolution of primary minerals; (2) the partitioning of Cu and Zn and their isotopes between a dissolved pool, often complexed to soluble organics, and a pool sorbed to secondary minerals; (3) overprinting of weathering processes via the addition of atmospheric aerosol to soils; (4) uptake into plants and associated isotope fractionations in the upper organic-rich levels of soils. Anthropogenic addition of Cu and Zn to soils is a fifth important process but is dealt with in the section on the Anthropocene later in this chapter.

Weathering release of Cu and Zn from primary minerals. To our knowledge there are only two studies that have characterized Cu-Zn isotope compositions upon release from primary minerals to an experimental leachate designed to simulate the weathering process. Fernandez and Borrok (2009) measured isotopic compositions of fluids released during oxidative leaching experiments on rocks containing sulphides (pyrite, chalcopyrite, galena, sphalerite). Copper released is 2‰ heavier than the starting rocks at pH 2 and 5. Zinc released is both heavier and lighter than the primary sulphide, depending on the precise rock/mineral being leached, but only by order 0.2‰. For Cu the release of heavy isotopes is almost certainly related to an oxidation state change, from Cu(I) in the sulphides to Cu(II) in the leachates. Weiss et al. (2014) conducted experiments on leaching of biotite granite using 0.5M HCl and oxalic acid. Zinc mobilized into the aqueous phase in the first hour was as light as -1.2‰ relative to starting material, with 30-40% of the initial rock Zn pool released. The Zn in solution then moved back towards the initial rock, but never got beyond 0.1 -0.3‰ lighter after 168 hours (with 45-75% of the original starting Zn mobilised). The early, very negative, fractionations are interpreted as being kinetic.

Cu-Zn isotopes of soils and the impact of sorption and aqueous complexation. Though experimental studies are a useful template for the interpretation of field data, real weathering of rocks in soils is more complex for two main reasons. Firstly, Cu and Zn are not necessarily located in sulphide minerals such as in the Fernandez and Borrok (2009) experimental leaching study. Where this *is* the case the results obtained from field studies are consistent with the experiments. Thus Mathur et al. (2012) studied Cu isotopes in soils and soil waters developed on black shales in Pennsylvania USA, where a very large proportion of the Cu is located in pyrite. Loss or gain of an element of interest (*i*) during the soil development process is often expressed in terms of a tau (τ) value (Chadwick et al. 1990), which normalizes the concentration (C) of the element in a particular soil horizon (*h*) to both that in the parent material (*p*) and to the concentration of an immobile element (*j*, often Nb, Zr or Ti):

$$\tau_{i/j} = \left[\frac{(C_i/C_j)_h}{(C_i/C_j)_p} - 1 \right]$$

Tau values greater than zero denote addition of the element of interest relative to the immobile element, and values less than zero loss. Unfortunately, not all studies of Cu and Zn isotopes in soils report tau values (Viers et al. 2007; Mathur et al. 2012; Liu et al. 2014; Vance et al. 2016), but they are essential for identifying net loss or gain of an element given changes in mass that occur during soil development. Tau values for the Mathur et al. (2012) soils are about -0.5, implying loss of 50% of the original Cu in the rock, while δ^{65}Cu is about 0.5-1‰ lighter than the original Cu. In contrast, soil pore waters are all enriched in the heavy isotope, by 0.7-1.7‰. The authors attribute these findings to the preferential mobilization of heavy isotopes due to the oxidative leaching of pyrite, consistent with an abundance of experimental data, including those of Fernandez and Borrok (2009).

Secondly soil solutions, and the interactions between this aqueous phase and the residual solids in the soil, are more complex than those in the experimental studies described above. Mathur et al. (2012) discuss other possible interpretations of their Cu isotopic data, such as organic complexation in solution with a preference for the heavy isotope, but dismiss their relevance to that particular setting given the dominance of pyrite as a reservoir for Cu in the parent rock. However, in many soil settings it is the equilibrium partitioning of both Cu and Zn and their isotopes between dissolved organic complexes in an aqueous phase versus sorption to residual secondary minerals in the soil that appears to dominate trace metal distributions (e.g. Grybos et al. 2007), and the isotopic patterns seen for both Cu-Zn (Bigalke et al. 2010b; Bigalke et al. 2011; Vance et al. 2016) and other metals (e.g. Wiederhold et al. 2007).

No soil has yet been studied where conditions are reducing enough for the large isotope fractionations between Cu(I) and Cu(II) to be relevant. However, environmentally-relevant redox conditions *do* control the availability of Fe-Mn oxyhydroxides phases as a substrate for sorption. Figure 10a,b documents the isotopic impact of this control in soils distributed across three sites on the island of Maui, Hawaii, that have seen different annual rainfall amounts and in which there is a transition from well-drained conditions that retain Fe oxides to waterlogged conditions that do not (Vance et al. 2016). If Fe oxides are retained in the soils, depletion of Cu and Zn is accompanied by preferential loss of the heavy isotopes of Cu and slight preferential loss of the heavy isotopes of Zn. When Fe oxides disappear the remaining Cu and Zn is almost completely stripped from the soil and residual isotopic compositions move towards heavy values. Patterns consistent with those seen in Hawaii are also observed by Bigalke et al. (2010c; 2011). The most likely interpretation is that heavy Cu is mobilized into aqueous organic complexes, while the oxides in the soil preferentially sorb the light isotopes. As noted earlier, both soluble organic complexes and sorption show a preference for heavy isotopes relative to free Cu ion in aqueous solution, so that this interpretation requires that the preference of the organic complexes for heavy Cu is greater than that of sorption. This in turn, would require the dissolved complexes to bind Cu at least as strongly as the strongest organic ligands in the experiments of Ryan et al. (2014), but there is evidence from the partitioning of Cu isotopes between the aqueous and particulate phases in rivers (Vance et al. 2008 , discussed below) that this is indeed the case. The data for Zn in Figure 10a,b document a much more subtle isotopic effect in free-draining soils, mirroring more subtle differences between the dissolved and particulate load of rivers (e.g. Chen et al. 2008; Chen et al. 2009; Little et al. 2014a, also discussion below), and consistent with the fact that the isotopic effects of aqueous complexation versus sorption to mineral surfaces may cancel each other out. Figure 10a,b also show such an effect when Cu and Zn are almost completely stripped away in water-logged conditions. As the Fe oxyhydroxides are removed, the isotopic composition tends towards heavier values, perhaps reflecting the retention of a very small residual pool on aluminium hydroxides or on condensed organic matter or the addition of dust (see below).

Addition of atmospheric aerosol to soils. There have been few studies of the impact of atmospheric aerosol deposition on soils, and all but one of these concern anthropogenic aerosol deposition (discussed in a later section). Deposition of natural aerosol dust from the atmosphere has the potential to confound and overprint weathering signals. Here we illustrate the impact of such a process again using data from the relatively un-polluted Hawaiian Islands from Vance et al. (2016). The geochemical impact of the deposition of Asian desert-derived dust on Hawaiian soils is well-documented for many elements (e.g. Kurtz et al. 2001; Vance et al. 2016 and references therein). Its impact on Cu and Zn isotopes is illustrated in Figure 10c,d. Tau data for very young (300 years) soils from the island of Hawaii further help to define the weathering depletion trend illustrated in Figure 10a,b (thick solid black arrow). However, soils with ages in the range 20-150 kyr show deviations from this tau pattern that fall on arrays that are consistent with the addition of Asian dust (thick dashed arrows). The potential impact of this on Cu isotopes is illustrated by the dashed arrows in Figure 10d, but the precise trajectory on this plot depends on the relative concentrations of Cu in the dust versus those in the soil when the dust was added. In general, it might be expected that dust addition would tend to buffer soil Cu and Zn isotopes back to about 0‰ and +0.3‰ respectively, the average Cu and Zn isotope compositions in natural atmospheric aerosol (c.f. Fig. 8). However, Weiss et al. (2007) document a heavier Zn isotopic composition for background (un-contaminated) dust deposition in Finland, δ^{66}Zn = +0.9‰, while Dong et al. (2013) found variations of up to 0.5‰ in δ^{65}Cu among the different size fractions of Asian dust, with some samples of the >63μm fraction giving isotopic values = 0.4-0.5‰. The fact that natural atmospheric aerosol may be isotopically heavier than the lithogenic values for Cu and Zn isotopes may indicate either a significant contribution from a non-lithogenic source or isotope fractionation during atmospheric processing.

The impact of plants on soil Cu and Zn isotopes. The surface organic-rich layers of soils are often enriched in the light isotopes of both Cu and Zn (e.g. Weiss et al., 2007; Bigalke et al., 2010a, 2011; Liu et al., 2014; Vance et al., 2016). Though an interpretation in terms of addition from the atmosphere has been discussed (e.g. Bigalke et al. 2010b; Bigalke et al. 2011), another likely process relates to the concentration of the light isotopes in these surface layers by plant growth and decay. Viers et al. (2007) was the first study to highlight the potential importance of plant cycling for Zn, while Bigalke et al. (2010b; 2011) conclude that light Cu in the upper organic layers of soils is likely attributable to decaying plant material. Likewise, Liu et al. (2014) point to light Cu and high TOC in the upper layers of soils from Hainan, China, as evidence for plant activity. However, in these particular soils Cu is uniformly depleted in the upper relative to deeper soil horizons, whereas the other soils where isotopically light Cu and Zn in the upper organic horizons has been attributed to plants are definitely (Vance et al. 2016) or probably (Bigalke et al. 2010b; Bigalke et al. 2011) enriched relative to those underneath. Thus the Liu et al. (2014) data may be more consistent with the loss of heavy Cu by mobilization in aqueous organic complexes, as for the Hawaiian soils discussed above. Schulz et al. (2010) observed the effect of “biolifting” on the distribution and isotopic composition of Fe in soils from Santa Cruz, California. Biolifting is the process by which plant roots and symbiotic fungi (mycorrhizae) transport an element from deep in the regolith to the shallow soil. Vance et al. (2016) observed increasing τ_{Cu} and τ_{Zn} coupled to increasing τ_P with soil age in the uppermost horizons of Scottish soils, but decreases at depth, suggesting movement of Cu and Zn upwards with increasing soil development (eg. Fig. 10e). As with the experimental studies of plants discussed earlier, these authors document significantly lighter Zn in plant material than in soils, suggesting that biolifting and fractionation by vegetation can also explain some aspects of soil δ^{66}Zn and δ^{65}Cu (e.g. Fig. 10f) for the surface layers of these soils. In contrast, Viers et al. (2015) find little variation in soil Zn isotope compositions related to plant activity in Siberian permafrost soils, which they attribute to the homogenizing impact of seasonal freezing front migration. Plants developed on these latter soils exhibit Zn isotope compositions both lighter and heavier than the bulk soil, possibly due to climate-driven changes in speciation of the plant-available pool.

Summary. Figure 11 presents Cu-Zn isotopes in soils in the form of integrated tau values and isotopic compositions for whole soil profiles (where tau data are also available: Viers et al. 2007; Mathur et al. 2012; Liu et al. 2014; Vance et al. 2016), in order to make a summary assessment of the degree of loss and isotopic fractionation that occur in this setting. Such an assessment is important for the significance of weathering and other pedogenic processs in global biogeochemical budgets, and sets the scene for the discussion of one of the main inputs to the oceans, rivers, in the next section. It is already relatively clear from this still small dataset that soils lose heavy Cu during the weathering process, whether it is because of oxidation of sulphides (e.g. Mathur et al. 2012) or through retention of light Cu isotopes on residual Fe-Mn oxides coupled to the mobilization of heavy Cu in aqueous organic complexes (Bigalke et al. 2010b; Bigalke et al. 2011; Vance et al. 2016). In contrast, the isotopic impact of chemical weathering on Zn is much more subdued, with the majority of soils retaining very slightly heavy Zn. It should be noted that the real impact of weathering removal on its own would be more pronounced than these data suggest, given that nearly all these soils will have seen the addition of some dust, buffering the isotopic composition closer to the parent rock than would otherwise be the case. The main point of presenting the summary in Figure 11 is that it predicts that the complementary aqueous reservoir to the residual solids in soils, the dissolved phase of rivers, should be significantly heavier than the average continental crust for Cu, and not very different from the latter for Zn. It will be seen in the next section that this prediction is borne out for estimates of the Cu and Zn isotope composition of the dissolved riverine flux to the oceans obtained from measurements of the dissolved pool in large and small, relatively unpolluted, rivers (Vance et al. 2008; Little et al. 2014a).

The oceans: inputs, outputs and internal cycling of Cu and Zn isotopes

The oceanic dissolved pool and authigenic metals extracted from it to be delivered to sediments represent the ultimate fate of Cu and Zn mobilized on the continents via weathering and erosion, discussed in the previous section. Measurements of the Cu and Zn isotope composition of the dissolved pool of the oceans is extremely challenging due to the low abundances of both metals in seawater (concentrations of order 10^{-10}-10^{-9}M). This presents difficulties related to clean sampling and analysis, in addition to the problem of obtaining large ion currents for the precise measurement of isotope ratios. The challenge is to achieve efficient, low blank, chemical extraction and purification of Cu and Zn from large volumes (of order 0.1-10 litres) of seawater, containing up to 8 orders of magnitude more interfering ions such as Mg and Na. The availability of the double spike approach for Zn eliminates concerns over isotope fractionation artefacts during the chemical extraction process, but this approach is not available for Cu. The isotope geochemistry of seawater started with the pioneering work of Bermin et al. (2006) and Vance et al. (2008), but has gained momentum recently and is likely to grow in importance over the next decade for two principal reasons. The first is the inception of the GEOTRACE programme (www.geotraces.org), an international collaboration involving many chemical oceanographers worldwide that is now providing large, cleanly-collected, seawater samples for a huge body of work aimed at reaching a quantitative understanding of trace elements and their isotopes in seawater. The second is the development of a key new methodology, using Nobias chelate PA-1 resin (e.g. Conway and John 2014; Takano et al. 2014; Conway and John 2015; Vance et al. In review). This new approach is capable of producing a very clean transition metal fraction from seawater, that can then be taken on to the usual anion column for the purification of separate Cu and Zn (as well as Fe, Cd, Mo) fractions.

The data currently available from these endeavours is summarized in Figure 12 and 13. Two principal scientific themes have emerged both from this early work on the dissolved pool of the oceans themselves, as well as from Cu-Zn isotopic characterization of the inputs and outputs: (1) the overall mass balance of Cu and Zn cycling through the oceans as a whole; (2) the cycling of Cu and Zn within the oceans, by biological uptake and regeneration, and through interaction with the surfaces of both biological and abiotic particulates, often termed “scavenging”. We discuss each of these in turn below. The work done so far on Cu and Zn isotopes in rivers, atmospheric aerosols, hydrothermal systems, as well as the chemical sediments that represent the outputs from the dissolved pool, are all tied up with the first of these topics and are discussed as part of it.

The overall oceanic budget of Cu and Zn in the oceans. The dissolved pool of the oceans is conventionally regarded as being in steady state with regard to inputs and outputs. Though there are both isotopic and elemental records and models for long residence time elements such as Sr and Mg that suggest the contrary (e.g. Vance et al. 2009; Coggon et al. 2010; Pogge von Strandmann et al. 2014), long-term records of Cu and Zn isotopes in the oceans (Little et al. 2014a) demonstrate a temporal constancy that makes this a useful starting point here.

Vance et al. (2008) and Little et al. (2014a) have characterized the isotopic composition of the dissolved pool of rivers for Cu and Zn isotopes, including relatively unpolluted large and small catchments such as the Amazon and the Kalix (Arctic Circle, Sweden). A key finding for Cu is that the dissolved pool of rivers is isotopically heavier than the continental crust as sampled in high temperature igneous rocks and clastic sediments (Fig. 8), with a discharge- and [Cu]-weighted average δ^{65}Cu of about +0.7‰. This result is common to a number of transition metals, including Mo (Archer and Vance 2008) and Ni (Cameron and Vance 2014), which are also all characterized by weak positive relationships between isotope composition and reciprocal metal concentration. In the case of Cu, at least one small river carries a particulate load with δ^{65}Cu = -0.4 to -0.6‰, and the two pools balance to suggest an estimated total load that is about the same as the rocks being weathered. Vance et al. (2008) attributed this difference between the dissolved and particulate load to a roughly 1.2±0.4‰ equilibrium isotopic fractionation between heavy Cu in dissolved aqueous organic complexes and light Cu in particulate material. Though this suggestion is qualitatively consistent with the fact that the small number of soil systems so far analysed seem to lose heavy Cu (Fig. 11), and with the experimental finding that organic complexes preferentially sequester the heavy isotope of Cu (Fig. 10: Bigalke et al. 2010a; Ryan et al. 2014), the fractionation seen between the dissolved and particulate phases in rivers is much larger. Little et al. (2014a) found that Zn isotopes in a subset of the same large and small rivers is less variable, and that the discharge- and [Zn]-weighted riverine flux to the oceans, at about +0.33‰, is very close to the continental crust (Fig. 8). This finding is also completely consistent with the very subtle isotopic variations seen in soils (Fig. 11), and with the fact that there is likely to be minimal isotopic difference between dissolved aqueous organic complexes of Zn and that sorbed to surfaces (Fig. 9 and references in the caption).

Other work on rivers has concentrated on rather small catchments, often with a focus on modification of riverine processes due to human activities such as smelting and agriculture (see Anthropocene section). However Ilina et al. (2013), in a study of pristine rivers in subarctic watersheds (NW Russia), also found heavy Cu in the dissolved load (δ^{65}Cu = +0.46±0.05‰), and used ultrafiltration to demonstrate that this isotopic composition characterizes the riverine load down to <1kDa, even though 40-60% of the Cu in the rivers they studied is colloidal. Szynkiewicz and Borrok (2015) document a much wider range of Zn isotope compositions (δ^{66}Zn = -0.57 to +0.41‰) than in the global survey of Little et al. (2014a) in streams of the Rio Grande catchment (USA), which they attribute to preferential removal of the light isotope from the dissolved load by adsorption onto particulates. Though part of a study of a river estuary that is at least partially anthropogenically-disturbed, particulate and dissolved Cu isotopes in the Gironde estuary show $\Delta^{65}\mathrm{Cu}_{\mathrm{particulates\text{-}dissolved}}$ around +0.4‰ for Cu (Petit et al. 2013). Finally, Chen et al. (2008; 2009), though also in a study primarily aimed at using Zn isotopes to study pollution sources in the River Seine, France, observe rather subtle isotopic differences between the particulate and dissolved load.

Little et al. (2014a) in an assessment of the overall oceanic mass balance of Cu and Zn isotopes, present and summarise further data on the size and isotopic composition of the likely inputs. This paper suggests that the dissolved riverine load is dominant for both, but uncertainties remain. It is conventionally assumed that the metal load of hydrothermal fluids is precipitated and scavenged very close to mid-ocean ridges, and Little et al. (2014a) conclude that the flux that gets past this trap is likely to be very small indeed. However, the recent finding that substantial amounts of iron are transported 1000s of km from hydrothermal systems across the deep Pacific (Resing et al. 2015) may prompt a re-assessment of that conclusion. We know very little about the isotopic composition of end-member hydrothermal fluids, though the [Zn]-weighted δ^{66}Zn in the only study so far (John et al. 2008) is very close to basalts, the continental crust and rivers, at around +0.25‰. Similarly the [Zn]-weighted average δ^{66}Zn of thermal springs and fumaroles from one Caribbean volcano is +0.34‰ (Chen et al. 2014b). Dust, transported through the atmosphere from the continents, was estimated to represent only about 10% of the total input for both Cu and Zn in Little et al. (2014a), whereas Takano et al. (2014) estimate this source to be slightly larger than rivers for Cu. Much of this discussion depends on two inter-related uncertainties. Firstly, the Takano et al. (2014) dust estimate is derived from the Cu concentration of rainwater over Japan, taken to characterize the wet deposition flux of dust Cu to the Earth's surface. However, this rain is likely to be anthropogenically contaminated. Though the residence time of Cu in the oceans is not well-constrained it is certainly of order 10^3-10^4 years, so that it seems unlikely that 100-200 years of this flux is relevant to the whole ocean budget at all. A second uncertainty relates to the size of the dust flux to the oceans itself, and in particular solubility of Cu in that dust. Little et al.

(2014a) use a solubility of 27%, likely relevant for mineral dust (Desbouefs et al. 2005), but anthropogenic aerosol may contain a more soluble pool of metals, possibly explaining the high Cu concentrations in Japanese rain.

These uncertainties are important, because the available data for sources and sinks point to missing budget terms (Little et al. 2014a). The isotopic composition of the input to the oceanic dissolved pool for Zn is fairly well-constrained despite large uncertainties on the amount of *total* Zn, simply because the isotopic composition of average rivers, dust and hydrothermal systems are all around +0.25 to +0.33 (Fig. 8). This is significantly lighter than the deep ocean dissolved pool and requires at least one sink from the oceans that is isotopically light. For Cu, the input shown on Figure 13 is that from Little et al. (2014a). If dust is much more important than suggested in that paper, and more like 60% of the total input as in Takano et al. (2014), and with an average δ^{65}Cu in dust of +0.04‰ (Fig. 8) then the total input would be substantially lighter than the dissolved pool of the oceans, so that at least one isotopically *heavy* sink is required.

The current level of knowledge on the isotopic composition of these sinks is summarized in Figure 8 and Figure 12 and 13. For Zn, all the sinks in the open oxic ocean are heavy. One that is likely to be quantitatively important, and the one that we know most about (Little et al. 2014ab; Bryan et al. 2015), is that which occurs via scavenging of Zn to particulate Fe-Mn oxides and delivery with them to sediment. This sink, as recorded in Fe-Mn crusts, has an isotope composition = +0.94±0.14‰ (Marechal et al. 2000; Little et al. 2014a, see also metalliferous sediments in Dekov et al. 2010), about 0.5‰ heavier than the deep oceans. This is qualitatively consistent with (1) the finding of Little et al. (2014b) that Zn and Cu are both very clearly associated with Mn oxide in these samples and (2) that of

Bryan et al. (2015) that Zn sorbed to Mn oxide is heavier than a dissolved pool. However, Zn/Mn ratios in crusts suggest low surface loading, for which Bryan et al. (2015) document an isotopic fractionation upon sorption from a high ionic strength solution in which Zn is inorganically-speciated of as great as +2.7‰. The solution to this quantitative discrepancy put forward by Little et al. (2014b) and Sherman et al. (2015) – see schematic in Figure 14 - is that, in the dissolved pool, the free metal Zn ion that is likely to be sorbed is actually much lighter than the total dissolved pool because of the fact that most of the oceanic dissolved pool of Zn is organically-complexed, which would be heavier than the free ion (Fig. 10 Jouvin et al. 2009).

Organic complexation is likely to be even more important, quantitatively and isotopically, for Cu. Fe-Mn crusts are isotopically lighter than the oceanic dissolved pool by about 0.2‰ (Fig. 13 Little et al. 2014a). No experiments have yet characterized isotope fractionation of Cu upon sorption to Mn oxide surfaces, but experiments for other oxides have universally documented sorption of the heavy isotopes from an aqueous phase containing free Cu(II) (Fig. 10 Balistrieri et al. 2008; Pokrovsky et al. 2008; Navarette et al. 2011). As pointed out by Little et al. (2014b) and Sherman et al. (2015), sorption of the heavy isotope would be consistent with the change in co-ordination state of Cu (e.g. Schauble 2004) from V in solution to dominantly III-IV on birnessite (δ-MnO_2). But this is inconsistent in sign, never mind magnitude, with the observation of light Cu in natural Fe-Mn crusts. However, Cu again, in all aqueous solutions at the surface of the Earth is ubiquitously complexed to organics (e.g. Coale and Bruland 1988), so that this conundrum probably has a solution similar to the Zn problem. In other words, the free ion that is sorbed is likely to be lighter than the total, as also shown schematically in Figure 14.

Returning to the whole ocean mass balance, at the level of knowledge discussed above there is clearly a substantial budgetary problem for Zn isotopes if the oceans are in steady state. The open ocean outputs are heavier than the dissolved pool while the inputs are light, implying that the oceans should be moving to lighter isotopic compositions through time, which is not seen in records (e.g. Little et al. 2014a). The solution to this problem is likely to lie in a sink for Zn into organic-rich sediments. Very recently, Little et al. (2016) have shown that sediments deposited beneath upwelling continental margins, rich in organic carbon due to high photic zone productivity, carry substantial authigenic Zn enrichments and that this Zn is isotopically light. Light Zn isotopes in organic-rich sediment could either be delivered there via uptake of light Zn into phytoplankton in the photic zone, sinking and preservation of the organic matter (e.g. John et al. 2007b; Peel et al. 2009). An alternative is suggested by the data of Vance et al. (In review) for the sulphidic Black Sea. In this setting Zn behaves very like Mo: sulphidisation leads to removal of Zn as particle reactive sulphide species that are isotopically light – by 0.6-0.7‰ (consistent with ab initio calculations: Fujii et al. 2011, see earlier in this chapter) – pushing the residual dissolved pool very heavy (Fig. 8). Pore waters within organic-rich sediments also become sulphidic just beneath the sediment-water interface, due to reduction of pore water sulphate when respiration depletes oxygen and other oxidants (e.g. Froelich et al. 1979). In the Black Sea this process is near-quantitative so that authigenic Zn in sediments is the same as the open ocean dissolved pool, but a non-quantitative version of the same process within the sediments of upwelling continental margins could close the oceanic Zn isotope budget.

As noted earlier, what we currently know about the Cu isotope budget also requires an as yet unidentified sink, in this case isotopically heavy. But we know too little about the oceanic Cu isotope budget to say much more at this stage.

Cycling of Cu and Zn isotopes within the oceans. The discussion in the previous section emphasized the homogeneity of Cu and Zn isotope compositions in the deep ocean (Figs. 12, 13), but there is clearly a great deal of variability *within* the oceanic dissolved pool, in the top 1000m and particularly for Zn, where the roughly 2‰ range is greater than any other Earth reservoir (Fig. 8). One of the most impressive features of ocean chemistry is the massive drawdown of Zn in the surface ocean, with concentrations there that are sometimes as low as 0.03 nM, more than 2 orders of magnitude lower than the highest concentrations in the deep ocean (Fig. 12 and references therein). For Cu, the surface-deep contrast is smaller, at a maximum of about factor 10 (Fig. 13 and references therein). Thus it is no surprise, if this drawdown is associated with even a small isotope fractionation, that there is substantial variability in the small residual dissolved pool of the upper ocean. The reasons for isotopic variability have focused on two explanations of both the surface ocean drawdown and the isotopic variation: (1) a kinetic fractionation leading to preferential uptake of the light isotope into phytoplankton cells in the photic zone; (2) reversible and non-reversible scavenging of Cu and Zn in both the surface and deep ocean.

For Cu, scavenging is the process that is often regarded as dominant. Though Cu is an important component of enzymes and proteins in phytoplankton (e.g. Peers and Price 2006), it is not limiting to phytoplankton growth and at high concentrations it is toxic (e.g. Moffett and Brand 1996). Indeed, the organic ligands that bind Cu in the dissolved phase of the oceans (and at least to some degree elsewhere on Earth) are probably exuded by phytoplankton to reduce the concentrations of free Cu^{2+} ion beneath the threshold for toxicity at around 10^{-12}M – some 3 orders of magnitude beneath *total* oceanic Cu concentrations (e.g. Moffett and Brand 1996). This dichotomy between the requirement for small amounts of Cu by phytoplankton, coupled to toxicity at high concentrations, has led to Cu being dubbed the "Goldilocks element" of ocean biogeochemistry (e.g. Thomson and Ellwood 2014). The approximately linear increase in Cu concentrations with depth (Fig. 13) is reminiscent of that attributed to reversible scavenging for some other oceanic metals (e.g. Bacon and Anderson 1982), and Little et al. (2013) demonstrated that depth profiles of Cu concentrations are very well modeled by such a process. In support of this, Takano et al. (2014) interpret a good positive relationship between Cu isotope composition and oxygen availability in the deep ocean in terms of preferential scavenging of the light isotope to Fe-Mn oxides, a suggestion that is consistent with what we know of the isotope composition of Cu in Fe-Mn crusts (Little et al. 2014a). Thompson and Ellwood (2014) concur with Vance et al. (2008) and Little et al. (2014a,b) in highlighting the importance of organic ligands in this process: without them, if Cu existed as a free metal ion in seawater, it seems almost certain that sorption would remove the heavy isotope (Balistrieri et al. 2008; Pokrovsky et al. 2008; Little et al. 2014b; Sherman et al. 2015).

Little et al. (2013) showed that, in contrast to Cu, Zn concentrations are not at all well modeled by a reversible scavenging process and conclude that biogeochemical cycling, uptake into phytoplankton at the surface and regeneration by respiration at depth, must be the key process. If this is the case, and if Zn uptake into phytoplankton is associated with a kinetic isotope fractionation that favours uptake of the light isotope (Fig. 10 John et al. 2007b; John and Conway 2014), then the expectation is that drawdown of Zn in the surface ocean should be associated with residual heavy isotopic compositions in the dissolved pool of the upper ocean. An initial examination of Figure 12 seems to imply, if anything, the opposite. John and Conway (2014) suggest that scavenging must play at least some role. These authors conducted a cell degradation experiment in an attempt to simulate regeneration of organic material by respiration, and found that the Zn released was 0.27±0.11‰ lighter than the cell inventory. They suggest that this is due to the preferential re-adsorption of the heavy isotopes onto residual organic particles, implying a $\Delta^{66}Zn_{adsorbed-dissolved}$ = +0.58‰. However, these experiments contained very high aqueous Zn concentrations and no ligand to complex it, very different from the real ocean where a large portion of the Zn in the dissolved pool is complexed to organic ligands.

We suggest that the main control on oceanic Zn distributions remains to be unequivocally established but that biological uptake and regeneration, with whatever isotope fractionation it is associated with, will turn out to be the key process. In making this suggestion, which will require further work to substantiate, we suggest that the following observations from the data we currently have are going to be key. First, the main oceanic region in which Zn is taken up into cells and exported to the deep is the Southern Ocean. Diatoms dominate the ecology in this region and their cells contain an order of magnitude more Zn than average oceanic phytoplankton (Twining and Baines 2013). Given that diatoms dominate the export of carbon to the deep ocean (e.g. Armbrust 2009), they must completely dominate the export of Zn. Second, the Zn isotopic data for the Southern Ocean (Fig. 12 Zhao et al. 2014) show no isotopic shift in the surface across a 2 order of magnitude drop in Zn concentration away from the locus of upwelling and as diatoms take it up, suggesting the massive uptake of Zn by diatoms in this region causes no isotope fractionation. Third, when the depth profiles in Figure 12 are examined in more detail it is clear that the surface-most point is isotopically heaviest, and the isotopically light Zn that is clearly seen in this figure occupies depths beneath the surface, at 50-200m (e.g. Zhao et al. 2014). All of these observations are most consistent with very shallow upper ocean recycling of Zn by non-diatom phytoplankton and associated with small isotope fractionations, superimposed on a quantitatively much more important deep export that is controlled by diatoms in the Southern Ocean but that imparts no isotopic variability.

Applications to Earth history. There have been a small number of applications of Zn isotopes in the study of the oceans through Earth history (Pichat et al. 2003; Kunzmann et al. 2013; Pons et al. 2013). Though these have been hampered by a limited understanding of the modern cycle, there is now great potential for such applications given that this understanding has now reached quite an advanced stage through the datasets described in this review. A bridge between attempts to understand the modern cycle and the recent and deep past is provided by the study of the systematics of Zn isotopes in the biological components of core-top sediments, as in Andersen et al. (2011) and Hendry and Andersen (2013). Two studies have sought to harness Zn isotopes in marine carbonate as a monitor of photic zone primary productivity on both kyr timescales in the Quaternary, targeted at understanding upwelling supply of Zn to the photic zone as controlled by climate (Pichat et al. 2003), and on the much longer timescales represented by the recovery from Snowball Earth glaciations, focused on tracking the recovery of the biosphere through the hypothesized burial of isotopically light photosynthesized Zn. Pons et al. (2013), by contrast, link secular changes in Zn isotopes in Banded Iron Formations (BIFS) to relationships between the geochemical cycle of phosphate and isotopic fractionation of Zn isotopes, a phenomenon for which, in all the studies of the modern cycle summarized earlier, evidence has yet to emerge. The burial of light Zn with organic carbon (Little et al., 2016) and the likely control of this burial by sequestration of the light isotope into sulphide in pore waters suggested by the Black Sea data of Vance et al. (In review) together suggest that the future of successful applications of paleo-Zn isotopes probably lies in the investigation of the links between the biosphere and redox in the ancient oceans. Similarly, a very recent study of Cu isotopes in black shales from across the Great Oxidation Event at 2.7-2.1 Ga (Chi Fru et al., 2016) presents a viable interpretation in terms of removal of the light isotope of Cu into Fe formations before 2.2 Ga and the lack of this removal thereafter. It is not clear, however, whether this interpretation is unique, given what we still have to learn about the controls on other outputs of Cu from the modern ocean, such as to organic-rich sediments and in the sulphidic environments that likely dominated the oceans after the demise of BIFS. Finally, Pons et al. (2011) found that Zn isotopes in 3.8 Ga serpentinites from Isua are depleted in heavy isotopes compared to the BSE (δ^{66}Zn down to -0.5‰), while serpentinites from modern ophiolites and mid-ocean ridges are isotopically similar to the BSE, at around +0.3‰. Theoretical calculations (Fujii et al. 2011) show that the incorporation of isotopically light Zn in serpentinites requires that the serpentinisation reactions occurred at high-pH, with a fluid rich in carbonate at medium temperature (100-300 °C). In addition, Pons et al. (2011) point out that these are the conditions that are found in modern mud volcano environments such as the Mariana's forearc, where the serpentinites are also isotopically light (δ^{66}Zn down to -0.3‰). Pons et al. (2011) further suggest that Zn isotopes could be used as a pH proxy for ancient hydrothermal fluids.

Cu and Zn isotopes in the Anthropocene

A significant effort has gone into the identification and quantification of human disturbance of the natural Earth surface cycles of Cu and Zn, including via their stable isotopes (see recent review in Fekiacova et al., 2015). Approximately 25% of the Zn and 30% of the Cu released annually to the atmosphere derives directly from human activities such as agriculture, manufacturing and waste management (Rauch and Pacyna, 2009). Absolute anthropogenic emissions of Zn are close to double those of Cu (Rauch and Pacyna, 2009) and most of the isotopic work on environmental tracing of these emissions has focused on Zn. Virtually all the estimated Cu emitted to the atmosphere annually is thought to derive from non-ferrous metal production (70%) and fossil fuel combustion. For Zn about 70% is also from non-ferrous metal production, 16% from fossil fuel combustion, with 4-5% each via steel and cement production and waste disposal. In terms of riverine transport, Chen et al. (2014a) estimate that excess anthropogenic Cu and Zn in the Seine at Paris represent 15-20% of the total at low water, with little excess over continental crustal concentrations at high water stage.

Zn and Cu isotopes in ore bodies and industrial products. An important starting point is the variability in, and processes responsible for, Cu and Zn isotopes in the mineral ores processed during the smelting that is responsible for about 70% of the emissions to the atmosphere. Though we briefly outline this topic here, it should be emphasized that industrial products and emissions – in the end and at least of Zn – do not reflect the massive variability seen in mineral ores (Fig. 8), implying homogenization of these isotope compositions during processing.

Larson et al. (2003) first documented the large Cu isotope variations in ore minerals in the weathering/supergene environment (δ^{65}Cu = - 3 to +2.5‰), while also noting that variability in primary high-temperature minerals was more subdued. These twin results have been confirmed by subsequent studies (Graham et al. 2004; Mason et al. 2005; Markl et al. 2006; Asael et al. 2007; Asael et al. 2009; Mathur et al. 2009; Mathur et al. 2010): primary ore minerals predominantly in the 0±0.5‰ range, while the range of Cu isotope compositions for the supergene environment has broadened to -16.5 to +10‰. As first noted by Larson et al. (2003) and confirmed subsequently, redox-induced fractionations almost certainly control the huge variability seen in the supergene environment, where oxidative leaching of high-temperature reduced Cu minerals in the vadose zone is followed by precipitation of reduced minerals beneath the water table (Larson et al. 2003; Ehrlich et al. 2004; Mathur et al. 2005). As noted by Sherman (2013), however, the variability in the natural minerals is much greater than the fractionation factors measured in experiments, so that multiple cycles of oxidation and reduction, or Rayleigh fractionation or open system behavior, or all three, must be in operation. Though redox processes are certainly dominant, Markl et al. (2006) also suggest there may be a component to fractionation controlled by phase changes between fluid and solid mineral. Asael et al. (2009) further suggest that the nature of the ligand-bonding in solution is also important, confirmed by Sherman et al. (2013) and Fujii et al. (2013) using *ab-initio* calculations to show that aqueous Cu complexes have a δ^{65}Cu range of 1.3‰ (see earlier in this chapter).

There have been fewer studies of Zn isotope variation in ore minerals and, without redox chemistry, the variability is more subdued. Mason et al. (2005) document a range in δ^{66}Zn of 0.63‰ in a volcanic-hosted massive sulphide ore deposit, attributed to a Zn isotopic difference between co-existing sphalerite and chalcopyrite as well as Rayleigh fractionation during precipitation from a hydrothermal fluid. Wilkinson et al. (2005) and Gagnevin et al. (2012) also explain variability in Zn isotopic data for sphalerite from the Irish ore fields (-0.17 to +1.33‰) as due to a kinetic fractionation and Rayleigh fractionation during progressive precipitation from fluids percolating up from the basement.

To our knowledge, the isotope composition of the final industrial products of these metals has only been measured for Zn. The main result of this study (John et al. 2007a) was that the variability seen in a small number of industrial products, which are mostly -0.4 to +0.2‰, was much less than in the raw ore minerals. In addition, the average δ^{66}Zn of the products measured is identical – at +0.19±11‰ (2SD, n =14) - to the average for ore minerals in the Wilkinson et al. (2005) and Mason et al. (2005) studies – at +0.15‰. Sivry et al. (2008) note that the extraction yields for Zn processing are higher than 95%, so that a similarity between the final product and average initial ore is perhaps not surprising.

Dispersal of anthropogenic Cu and Zn via the atmosphere. A number of studies have sought to use Zn isotopes (but only one to use Cu: Thapalia et al. 2010) to trace emissions of Zn to the atmosphere in the urban environment (e.g. waste combustors) and in the vicinity of mining and smelting activities through the analysis of lichens and anthropogenic aerosols (Cloquet et al. 2006; Dolgopolova et al. 2006; Gioia et al. 2008; Mattielli et al. 2009), ombrotrophic peat cores (Weiss et al. 2007), and in soils or sediments from rivers and lakes (Sivry et al. 2008; Sonke et al. 2008; Juillot et al. 2011; Aebischer et al. 2015). Though source signatures are not always easily partitioned into natural and anthropogenic (e.g. Cloquet et al. 2006), and though post-depositional processes can induce substantial isotope variability that obscures initial source signatures (e.g. Weiss et al. 2007; Juillot et al. 2011, though c.f. Sonke et al. 2008), a systematic feature *has* often emerged from studies of smelting activities (see recent review in Yin et al., 2016). Generally, the slag residues, or tailings, are typically enriched in the heavy isotopes of Zn, while the fine dust and aerosol emitted from smelter chimney stacks tends to be isotopically light (Dolgopolova et al. 2006; Sivry et al. 2008; Sonke et al. 2008; Juillot et al. 2011). In contrast, Ochoa Gonzalez and Weiss (2015) find that heavy isotopes are emitted to the atmosphere during coal combustion while the light isotopes are retained in bottom ashes, an observation that may allow the fingerprinting of sources of Zn pollution from different activities.

Mattielli et al. (2009) provide the most extensive discussion of the causes and consequences of isotopic fractionation during the processing of Zn ores. These authors document a change in the size and Zn isotopic composition of aerosols away from the main chimney, with δ^{66}Zn = +0.01 to +0.19‰ at ≤1km, and -0.52 to -0.02‰ at 2-5 km. They attribute the light Zn in aerosols to the high temperatures in the smelter (up to 1300K), leading to fractionation during volatilization/condensation (see above section on Isotopic fractionation by evaporation on Earth). Their main chimney dust samples have the lightest δ^{66}Zn, at -0.67±0.10‰. In contrast Sivry et al. (2008) document Zn in tailings at a smelter with δ^{66}Zn = +0.18 to +1.49‰, a signal also seen in polluted downstream sediments (+0.83 to +1.38‰). Similarly, Juillot et al. (2011) measure δ^{66}Zn = +0.81±0.20‰ for slags at a French smelter and see a shift towards this isotope signature in heavily contaminated top soils within 500m of the smelter. Consistent with this, Thapalia et al. (2010) document a step towards lighter Zn isotopes in lake sediment ~ 100km from a smelter after it became active. This is perhaps the only study of a Cu isotope archive of anthropogenic activity, showing a subtle shift to heavier Cu isotopes (δ^{65}Cu from +0.77±0.05 to +0.94±0.10‰) due to human activity.

Processes affecting Cu and Zn isotopes in polluted rivers. A small number of studies have been undertaken of Cu and Zn isotopes in two classes of polluted rivers: (1) rivers that are clearly affected by mining, including acid mine drainage and (2) rivers in areas that have been intensely developed for agriculture and industrial activities more generally. Borrok et al. (2008) studied dissolved Cu and Zn and their isotopes in small streams located in 6 historical mining areas in the US and Europe. It should be noted that the Cu and Zn concentrations in these mining-impacted streams, not unexpectedly, are up to 4 orders of magnitude greater than those in the relatively unpolluted rivers studied in Vance et al. (2008) and Little et al. (2014a). The δ^{66}Zn data covers the range +0.02 to +0.46‰ and exhibits a diel cycle that may be related to uptake by microorganisms. The range of δ^{65}Cu is -0.7 to +1.4‰, similar to that in non-mining-impacted rivers. Kimball et al. (2009) document Cu in acid mine drainage that has δ^{65}Cu about 1.5‰ heavier than the primary minerals, attributing this fractionation to oxidation of reduced Cu(I) in the minerals. More recently, Wanty et al. (2013, 2015) have documented Zn isotope fractionations associated with biomediated precipitation of hydrozincite in streams draining mining areas.

Chen et al. (2008; 2009) present an array of data for the dissolved and particulate phase of the River Seine, including time-series data in Paris as well as contaminated waters draining roofs and waste water treatment plants. Dissolved Zn concentrations in the Seine increase continuously downstream from 1 to 74 nM, while δ^{66}Zn decreases from a high in the headwaters of Aube tributary (0.58‰) to +0.09‰ at the estuary. The decreasing δ^{66}Zn values as anthropogenic Zn is added downstream, particularly in Paris, is consistent with generally light Zn isotope compositions in roadway and roof runoff, and plant-treated and waste water (-0.06±0.05‰). Fertilizers showed heavier Zn isotope values at +0.19 to +0.42‰, leading these authors to suggest that fertilizer Zn is strongly retained in soil. Data for suspended particulate matter presented a similar picture: δ^{66}Zn decreases from +0.3 to 0.08‰ downstream, associated with a 4-fold increase in concentration. Time-series samples in Paris show an inverse relationship between enrichment factor and isotopes. Chen et al. (2009) interpret the results as due to more or less conservative mixing of silicate and anthropogenic particles, ruling out sorption as an important process generating isotopic variability.

Acknowledgments: FM acknowledges funding from the European Research Council under the H2020 framework program/ERC grant agreement #637503 (Pristine), as well as the financial support of the UnivEarthS Labex program at Sorbonne Paris Cité (ANR-10-LABX-0023 and ANR-11-IDEX-0005-02), and the ANR through a chaire d’excellence Sorbonne Paris Cité. FM would like to thank Francis Albarède, James Day, Emily Pringle, Paolo Sossi and Damien Guinoiseau for discussions. Three anonymous reviewers and editor Fang-Zhen Teng greatly improved the text.

REFERENCES

Aebischer, S, Cloquet, C, Carignan, J, Maurice, C, Pienitz, R (2015) Disruption of the geochemical metal cycle during mining: multiple isotope studies of lake sediments dfrom Schefferville, subarctic Québec. Chem. Geol. 412: 167-178

Albarède F (2004) The stable isotope geochemistry of copper and zinc. *In*: Rev Mineral Geochem. Vol 55. Johnson CM, Beard BL, Albarède F, (eds). Mineralogical Society of America, p 409-427

Albarède F (2009) Volatile accretion history of the terrestrial planets and dynamic implications. Nature 461:1227-1233, doi:Doi 10.1038/Nature08477

Albarède F, Telouk P, Lamboux A, Jaouen K, Balter V (2011) Isotopic evidence of unaccounted for Fe and Cu erythropoietic pathways. Metallomics 3:926-933, doi:Doi 10.1039/C1mt00025j

Albarède F, Balter V, Jaouen K, Lamboux A (2011) Applications of the stable isotopes of metals to physiology. The 38th Meeting of the Federation of Analytical Chemistry and Spectroscopy Societies (FACSS), Reno (abstract).

Albarède et al. (20XX, this volume) Emerging applications of non-traditional isotopes in biomedical research Rev. Mineral. Geochem. XX:xxxx

Amira S, Spångberg D, Hermansson K (2005) Distorted five-fold coordination of Cu^{2+}(aq) from a Car-Parrinello molecular dynamics simulation. Phys Chem Chem Phys 7:2874-2880

Andersen MB, Vance D, Archer C, Anderson RF, Ellwood MJ, Allen CS (2011) The Zn abundance and isotopic composition of diatom frustules, a proxy for Zn availability in ocean surface seawater. Earth Planet Sci Lett 301:137-145, doi:10.1016/j.epsl.2010.10.032

Anderson D, Morel F (1978) Copper sensitivity of Gonyaulax tamarensis. Limnol Oceanogr 23:283–295

Archer C, Vance D (2002) Mass discrimination correction in multiple collector plasma source mass-spectrometry: an example using Cu and Zn isotopes. J Anal At Spectrom, 64:356-365

Archer C, Vance D (2004) Mass discrimination correction in multiple-collector plasma source mass spectrometry: an example using Cu and Zn isotopes. J Anal At Spectrom 19:656-665, doi:Doi 10.1039/B315853e

Archer C, Vance D (2008) The isotopic signature of the global riverine molybdenum flux and anoxia in the ancient oceans. Nature Geoscience 1:597-600

Armbrust EA (2009) The life of diatoms in the world’s oceans. Nature 459:185-192

Arnold T, Kirk GJD, Wissuwa M, Frei M, Zhao FJ, Mason TFD, Weiss DJ (2010a) Evidence for the mechanisms of zinc uptake by rice using isotope fractionation. Plant Cell Environ 33:370-381, doi:Doi 10.1111/J.1365-3040.2009.02085.X

Arnold T, Schonbachler M, Rehkamper M, Dong SF, Zhao FJ, Kirk GJD, Coles BJ, Weiss DJ (2010b) Measurement of zinc stable isotope ratios in biogeochemical matrices by double-spike MC-ICPMS and determination of the isotope ratio pool available for plants from soil. Anal Bio Chem 398:3115-3125, doi:Doi 10.1007/S00216-010-4231-5

Asael D, Matthews A, Bar-Matthews M, Halicz L (2007) Copper isotope fractionation in sedimentary copper mineralization (Timna Valley, israel). Chem Geol 243:238-254

Asael D, Matthews A, Oszczepalski S, Bar-Matthews M, Halicz L (2009) Fluid speciation controls of low temperature copper isotope fractionation applied to the Kupferschiefer and Timna ore deposits. Chem Geol 262:147-158

Aucour, AM, Pichat, S, Macnair, MR, Oger, P (2011) Fractionation of stable isotope zinc isotopes in the zinc hyperaccumulator *Arabidopsis halleri* and nonaccumulator *Arabidopsis petrasea*. Environ Sci Technol 45: 9212-9217

Aucour, AM, Bedell, J-P, Queyron, M, Magnin, V, Testemale, D, Sarret, G (2015) Dynamics of Zn in an urban wetland soil-plant system: coupling isotopic and EXAFS approaches. Geochim Cosmochim Acta 160: 66-69

Bacon MP, Anderson RF (1982) Distribution of thorium isotopes between dissolved and particulate forms in the deep sea. J Geophys Res 87:2045-2056

Balistrieri LS, Borrok DM, Wanty RB, Ridley WI (2008) Fractionation of Cu and Zn isotopes during adsorption onto amorphous Fe(III) oxyhydroxide: Experimental mixing of acid rock drainage and ambient river water. Geochim Cosmochim Acta 72:311-328, doi:DOI 10.1016/j.gca.2007.11.013

Balter V, Zazzo A (2011) An animal model (sheep) for Fe, Cu, and Zn isotopes cycling in the body. Mineralogical Magazine 75:476

Balter V, Lamboux A, Zazzo A, Telouk P, Leverrier Y, Marvel J, Moloney AP, Monahan FJ, Schmidt O, Albarède F (2013) Contrasting Cu, Fe, and Zn isotopic patterns in organs and body fluids of mice and sheep, with emphasis on cellular fractionation. Metallomics 5:1470-1482, doi:10.1039/c3mt00151b

Ban Y, Aida M, Nomura M, Fujii Y (2002) Zinc isotope separation by ligand-exchange chromatography using cation exchange resin. J Ion Exch 14:46-52

Barrat JA, Zanda B, Moynier F, Bollinger C, Liorzou C, Bayon G (2012) Geochemistry of CI chondrites: Major and trace elements, and Cu and Zn Isotopes O. Geochim Cosmochim Acta 83:79-92

Ben Othman D, Luck JM, Bodinier JL, Arndt NT, Albarède F (2006) Cu-Zn isotopic variations in the Earth's mantle. Geochim Cosmochim Acta 70:46

Benfatto M, D'Angelo P, Della Longa S, Pavel NV (2002) Evidence of distorted fivefold coordination of the Cu^{2+} aqua ion from an x-ray-absorption spectroscopy quantitative analysis. Phys Rev B 65:174205

Bentahila Y, Ben Othman D, Luck J-M (2008) Strontium, lead and zinc isotopes in marine cores as tracers of sedimentary provenance: a case study around Taiwan orogeny. Chem Geol 62-82

Bermin J, Vance D, Archer C, Statham PJ (2006) The determination of the isotopic composition of Cu and Zn in seawater. Chem Geol 226:280-297, doi:10.1016/j.chemgeo.2005.09.025

Bersuker IB (2006) The Jahn-Teller effect;. Cambridge Univ. Press, New York

Bigalke M, Weyer S, Wilcke W (2010a) Copper Isotope Fractionation during Complexation with Insolubilized Humic Acid. Environ Sci Technol 44:5496-5502, doi:Doi 10.1021/Es1017653

Bigalke M, Weyer S, Wilcke W (2010b) Stable Copper Isotopes: A Novel Tool to Trace Copper Behavior in Hydromorphic Soils. Soil Sci Soc Am J 74:60-73, doi:DOI 10.2136/sssaj2008.0377

Bigalke M, Weyer S, Kobza J, Wilcke W (2010c) Stable Cu and Zn isotope ratios as tracers of sources and transport of Cu and Zn in contaminated soil. Geochim Cosmochim Acta 74:6801-6813, doi:DOI 10.1016/j.gca.2010.08.044

Bigalke M, Weyer S, Wilcke W (2011) Stable Cu isotope fractionation in soils during oxic weathering and podzolization. Geochim Cosmochim Acta 75:3119-3134

Bigeleisen J, Mayer MG (1947) Calculation of equilibrium constants for isotopic exchange reactions. J Chem Phys 15:261-267

Birck JL (2004) An overview of isotopic anomalies in extraterrestrial materials and their nucleosynthetic heritage. *In*: Rev Mineral Geochem. Vol Rev. Mineral. 55. Johnson CM, Beard BL, Albarède F, (eds). Min. Soc. Amer., Washington, p 26-63

Bishop MC, Moynier F, Weinstein C, Fraboulet JG, Wang K, Foriel J (2012) The Cu isotopic composition of iron meteorites. Meteoritics Planet Sci 47:268-276, doi:Doi 10.1111/J.1945-5100.2011.01326.X

Black J, Kavner A, Schauble E (2011) Calculation of equilibrium stable isotope partition function ratios for aqueous zinc complexes and metallic zinc. Geochim Cosmochim Acta 75:769-783

Borrok DM, Wanty RB, Ridley WI, Wolf R, Lamothe PJ, Adams M (2007) Separation of copper, iron, and zinc from complex aqueous solutions for isotopic measurement. Chem Geol 242:400-414, doi:10.1016/j.chemgeo.2007.04.004

Borrok DM, Nimick DA, Wanty RB, Ridley WI (2008) Isotopic variations of dissolved copper and zinc in stream waters affected by historical mining. Geochim Cosmochim Acta 72:329-344

Bridgestock LS, Williams H, Rehkamper M*, et al.* (2014) Unlocking the zinc isotope systematics of iron meteorites. Earth Planet Sci Lett 400:153-164

Broadley MR, White PJ, Hammond JP, Zelko I, Lux A (2007) Zinc in plants. New Phytologist 173:677-702

Bruland KW (1999) Complexation of zinc by natural organic ligands in the central North Pacific. Limnol Oceanogr 34:269-285.

Bruland KW, Middag R, Lohan MC (2014) Controls of trace metals in seawater. Treatise in Geochemistry 8:19-51

Bryan AL, Dong S, Wilkes EB, Wasylenki LE (2015) Zinc isotope fractionation during adsorption onto Mn oxyhydroxide at low and high ionic strength. Geochim Cosmochim Acta 157:182-197

Caldelas C, Dong SF, Araus JL, Weiss DJ (2011) Zinc isotopic fractionation in Phragmites australis in response to toxic levels of zinc. J Exp Bot 62:2169-2178, doi:Doi 10.1093/Jxb/Erq414

Cameron V, Vance D (2014) Heavy nickel isotopic composition of rivers and the oceans. Geochim Cosmochim Acta 129:195-211

Canfield DE (1998) A new model for Proterozoic ocean chemistry. Nature 396:450-453.

Chaboy J, Muñoz-Páez A, Merkling PJ, Sánchez Marcos E (2006) The hydration of Cu^{2+}: Can the Jahn-Teller effect be detected in liquid solution? J Chem Phys 124:064509

Chadwick OA, Brimhall GH, Hendricks DM (1990) From a black box to a gray box - a mass balance interpretation of pedogenesis. Geomorphology 3:369-390

Chaussidon et al. (20XX, this volume) In-situ analysis of non-traditional isotopes by SIMS and LA-MC-ICPMS Rev. Mineral. Geochem. XX:xxxx

Chen H, Nguyem BM, Moynier F (2013a) Zinc isotopic composition of iron meteorites: Absence of isotopic anomalies and origin of the volatile element depletion. Meteorit Planet Sci 48:2441-2450

Chen H, Savage P, Teng FZ, Helz RT, Moynier F (2013b) No zinc isotope fractionation during magmatic differentiation and the isotopic composition of the bulk Earth. Earth Planet Sci Lett 369:34-42

Chen H, Moynier F, Humayun M, Bishop MC, Williams J (2016) Cosmogenic effects on Cu isotopes in IVB iron meteorites. Geochim Cosmochim Acta 182:145-154

Chen J, Gaillardet J, Louvat P (2008) Zinc isotopes in the Seine River waters, France: a probe of anthropogenic contamination. Environ Sci Technol 43:6494-6501

Chen J, Gaillardet J, Louvat P, Huon S (2009) Zn isotopes in the suspended load of the Seine River, France: isotopic variations and source determination. Geochim Cosmochim Acta 73:4060-4076

Chen J, Gaillardet J, Bouchez J, Louvat P, Wang Y-N (2014a) Anthropophile elements in river sediments: overview from the Seine River, France. Geochem Geophys Geosyst 15:4526-2546

Chen J, Gaillardet J, Dessert C, Villemant B, Louvat P, Crispi O, Birck J-L, Wang Y-N (2014b) Zn isotope compositions of the thermal spring waters of La Soufrière volcano, Guadeloupe Island. Geochim Cosmochim Acta 127:67-82

Chen S, Liu Y, Hu J, Zhang Z, Hou Z, Huang F, Yu H (2016) Zinc isotopic composition of NIST683 and whole rock reference materials. Geostandards and Geoanalytical Research. doi: 10.1111/j.1751-908X.2015.00377.x

Chou C-L, Baedecker PA, Wasson JT (1976) Allende inclusions: volatile-element distribution and evidence for incomplete volatilization of presolar solids. Geochim Cosmochim Acta 40:85-94

Chi Fru, E, Rodriguez, NP, Partin, CA, Lalonde, SV, Andersson, P, Weiss, DJ, El Albani, A, Rodushkin, I, Konhauser, KO (2016) Cu isotopes in marine black shales record the Great Oxidation Event. Proc Natl Acad Sci USA, in press, doi:10.1073/pnas.1523544113

Cloquet C, Carignan J, Libourel G (2006) Isotopic composition of Zn and Pb atmospheric depositions in an urban/periurban area of northeastern France. Environ Sci Technol 40:6594-6600

Cloquet C, Carignan J, Lehmann MF, Vanhaecke F (2008) Variation in the isotopic composition of zinc in the natural environment and the use of zinc isotopes in biogeosciences: a review. Anal Bio Chem 390:451-463

Coale KH, Bruland KW (1988) Copper complexation in the northeast Pacific. Limnol Oceanogr 33:1084-1101

Coggon RM, Teagle DAH, Smith-Duque CE, Alt JC, Cooper MJ (2010) Reconstructing past seawater Mg/Ca and Sr/Ca from mid-ocean ridge flank calcium carbonate veins. Science 327:1114-1117

Conway TM, Rosenberg AD, Adkins JF, John SG (2013) A new method for precise determination of iron, zinc and cadmium stable isotope ratios in seawater by double-spike mass spectrometry. Anal Chim Acta 793:44-52

Conway TM, John SG (2014) The biogeochemical cycling of zinc and zinc isotopes in the North Atlantic Ocean. Glob Biogeochem Cycles 28:1111-1128

Conway TM, John SG (2015) The cycling of iron, zinc and cadmium in the North East Pacific Ocean - Insights from stable isotopes. Geochim Cosmochim Acta 164:262-283, doi:10.1016/j.gca.2015.05.023

Couder, E, Mattielli, N, Drouet, T, Smolders, E, Delvaux, B, Iserentant, A, Meeus, C, Maerschalk, C, Opfergelt, S, Houben, D (2015) Transpiration flow controls Zn transport in *Brassica napus* and *Lolium multiflorum* under toxic levels as evidenced from isotopic fractionation. Comptes Rendus Geoscience 347: 386-396

Coutaud A, Mehuet M, Viers J, Rols J-L, Pokrovsky OS (2014) Zn isotope fractionation during interaction with phototrophic biofilm. Chem Geol 390:46-60

Dauphas N, Chen JH, Zhang J, Papanastassiou DA, Davis AM, Travaglio C (2014) Calcium-48 isotopic anomalies in bulk chondrites and achondrites: Evidence for a uniform isotopic reservoir in the inner protoplanetary disk. Earth Planet Sci Lett 407:96-108, doi:10.1016/j.epsl.2014.09.015

Day JM, Moynier F (2014) Evaporative fractionation of volatile stable isotopes and their bearing on the origin of the Moon. Philosophical transactions Series A, Mathematical, physical, and engineering sciences 372:20130259, doi:10.1098/rsta.2013.0259

de Almeida KJ, Murugan NA, Rinkevicius Z, Hugosson HW, Vahtras O, Ågrena H, Cesar A (2009) Phys Chem Chem Phys 11:508-519

Dekov, VM, Cuadros, J, Kamenov, GD, Weiss, D, Arnold, T, Basak, C, Rochette, P (2010) Metalliferous sediments from the H.M.S. Challenger voyage (1872-1876). Geochim Cosmochim Acta 74: 5019-5038

Desbouefs KV, Sofikitis A, Losn R, Colin JL, Ausset P (2005) Dissolution and solubility of trace metals from natural and anthropogenic aerosol particulate matter. Chemosphere 58:195-203

Dodson MH (1963) A theoretical study of the use of internal standards for precise isotopic analysis by the surface ionization technique: Part I. General first-order algebraic solutions. J Sci Instrum 40:289–295

Dolgopolova A, Weiss DJ, Seltmann R, Kober B, Mason TFD, Coles BJ, Stanley C (2006) Use of isotope ratios to assess sources of Pb and Zn dispersed in the environment during mining and ore processing within the Orlovka-Spokoinoe mining site (Russia). App Geochem 21:563-579, doi:10.1016/j.apgeochem.2005.12.014|ISSN 0883-2927

Dong S, Weiss DJ, Strekopytov S, Kreissig K, Sun Y, Baker AR, Formenti P (2015) Stable isotope ratio measurements of Cu and Zn in mineral dust (bulk and size fractions) from the Taklimakan Desert and the Sahel and in aerosols from the eastern tropical North Atlantic Ocean. Talanta 114:103-109

Dreibus G, Palme H (1996) Cosmochemical constraints on the sulfur content in the Earth's core. Geochim Cosmochim Acta 60:1125-1130

Edmond JM, Measures C, Mangum B, Grant B, Sclater FR, Collier R, Hudson A, Gordon LI, Corliss JB (1979) On the formation of metal-rich deposits at ridge crests. Earth Planet Sci Lett 46:19-30

Ehrlich S, Butler I, Halicz L, Rickard D, Oldroyd A, Matthews A (2004) Experimental study of copper isotope fractionation between aqueous Cu(II) and covellite, CuS. Chem Geol 209:259-269

Fekiakova S, Cornu S, Pichat S (2015) Tracing contamination sources in soils with Cu and Zn isotope ratios. Science of the total environment 517:96-105

Fernandez A, Borrok DM (2009) Fractionation of Cu, Fe and Zn isotopes during weathering of sulfide-rich rocks. Chem Geol 264:1-12

Field CB, Behrenfeld MJ, Randerson JT, Falkowski P (1998) Primary production of the biosphere: integrating terrestrial and oceanic components. Science 281:237-240

Flemming CA, Trevors JT (1989) Copper toxicity and chemistry in the environment – a review. Air Soil Pollut 44:143-158

Froelich PN, Klinkahmmer GP, Bender ML, Luedtke NA, Heath GR, Cullen D, Dauphin P, Hammond D, Hartman B, Maynard V (1979) Early oxidation of organic matter in pelagic sediments of the eastern equatorial Atlantic: suboxic diagenesis. Geochim Cosmochim Acta 43:1075-1090

Fujii T, Albarède F (2012) Ab Initio Calculation of the Zn Isotope Effect in Phosphates, Citrates, and Malates and Applications to Plants and Soil. Plos One 7, doi:ARTN e30726DOI 10.1371/journal.pone.0030726

Fujii T, Moynier F, Telouk P, Abe M (2010) Experimental and Theoretical Investigation of Isotope Fractionation of Zinc between Aqua, Chloro, and Macrocyclic Complexes. J Phys Chem A 114:2543-2552, doi:Doi 10.1021/Jp908642f

Fujii T, Moynier F, Pons ML, Albarède F (2011) The origin of Zn isotope fractionation in sulfides. Geochim Cosmochim Acta 75:7632-7643, doi:Doi 10.1016/J.Gca.2011.09.036

Fujii T, Moynier F, Abe M, Nemoto K, Albarède F (2013) Copper isotope fractionation between aqueous compounds relevant to low temperature geochemistry and biology. Geochim Cosmochim Acta 110:29-44, doi:10.1016/j.gca.2013.02.007

Fujii T, Moynier F, Blichert-Toft J, Albarède F (2014) Density functional theory estimation of isotope fractionation of Fe, Ni, Cu, and Zn among species relevant to geochemical and biological environments. Geochim Cosmochim Acta 140:553-576, doi:10.1016/j.gca.2014.05.051

Fulton EA, Parslow JS, Smith ADM, Johnson CR (2004) Biogeochemical marine ecosystem models II: the effect of physiological detail on model performance. Ecol Model 173:371-406, doi:Doi 10.1016/J.Ecolmodel.2003.09.024

Gagnevin D, Boyce AJ, Barrie CD, Menuge JF, Blakemann RJ (2012) Zn, Fe and S isotope fractionation in a large hydrothermal system. Geochim Cosmochim Acta 88:183-198

Gélabert A, Pokrovsky OS, Schott J, Boudou A, Fertet-Mazel A, Mielczarski J, Mielczarski E, Mesmer-Dudons N, Spalla O (2004) Study of diatoms/aqueous solution interface. I. Acid-base equilibria and spectroscopic observation of freshwater and marines species. Geochim Cosmochim Acta 68:4039-4058

Gélabert A, Pokrovsky OS, Viers J, Schott J, Boudou A, Feurtet-Mazel A (2006) Interaction between zinc and freshwater and marine diatom species: Surface complexation and Zn isotope fractionation. Geochim Cosmochim Acta 70:839-857, doi:10.1016/j.gca.2005.10.026

Gioia, S, Weiss, D, Coles, B, Arnold, T, Babinski, M (2008) Accurate and precise zinc isotope ratio measurements in urban aerosols. Anal Chem 80: 9776-9780

Ghidan OY, Loss RD (2011) Isotope fractionation and concentration measurements of Zn in meteorites determined by the double spike, IDMS-TIMS techniques. Meteoritics Planet Sci 46:830-842, doi:Doi 10.1111/J.1945-5100.2011.01196.X

Graham S, Pearson N, Jackson S, Griffin W, O'Reilly SY (2004) Tracing Cu and Fe from source to porphyry: in situ determination of Cu and Fe isotope ratios in sulfides from the Grasberg Cu-Au deposit. Chem Geol 207:147-169

Grybos M, Davranche M, Gruau G, Petitjean P (2007) Is trace metal release in wetland soils controlled by organic mobility or Fe-oxyhydroxides reduction? J Colloid Interface Sci 324:490-501

Guelke M, Von Blanckenburg F (2007) Fractionation of stable iron isotopes in higher plants. Environmental Science & Technology 41:1896-1901, doi:Doi 10.1021/Es062288j

Hartmann D, Woosley SE, El Eid MF (1985) Nucleosynthesis in neutron-rich supernova ejecta. Astrophys J 297:837-845

Guinoiseau, D, Gélabert, A, Moureau J, Louvat, P, Benedetti, MF (2016) Zn isotope fractionation during sorption onto kaolinite. Environ Sci Technol 50: 1844-1852

Hayakawa K, Minami S, Nakamura S (1973) Kinetics of the oxidation of ascorbic acid by the copper(II) ion in an acetate buffer solution. Bull Chem Soc Jpn 46:2788.

Hendry KR, Andersen MB (2013) The zinc isotopic composition of siliceous marine sponges: investigating nature's sediment traps. Chem Geol:33-41

Herwartz D, Pack A, Friedrichs B, Bischoff A (2004) Identification of the giant impactor Theia in lunar rocks. Science 344:1146-1150

Herzog GF, Moynier F, Albarède F, Berezhnoy AA (2009) Isotopic and elemental abundances of copper and zinc in lunar samples, Zagami, Pele's hairs, and a terrestrial basalt. Geochim Cosmochim Acta 73:5884-5904, doi:DOI 10.1016/j.gca.2009.05.067

Houben D, Sonnet P, Tricot G, Matielli N, Couder E, Opfergelt S (2014) Impact of root-induced mobilization of zinc on stable Zn isotope variation in the soil-plant system. Environ Sci Technol 48:7866-73

Ikehata K, Hirata T (2013) Evaluation of UV-fs-LA-MC-ICP-MS for Precise in situ Copper Isotopic Microanalysis of Cubanite. Anal Sci 29:1213-1217

Ilina SM, Viers J, Lapitsky SA, Mialle S, Mavromatis V, Chmeleff J, Brunet P, Alekhin YV, Isnard H, Pokrovsky OS (2013) Stable (Cu, Mg) and radiogenic (Sr, Nd) isotope fractionation in colloids of boreal organic-rich waters. Chem Geol 434:63-75

John SG, Park JG, Zhan ZT, Boyle EA (2007a) The isotopic composition of some common forms of anthropogenic zinc. Chem Geol 245:61-69

John SG, Geis R, Saito M, Boyle EA (2007b) Zn isotope fractionation during high-affinity zinc transport by the marine diatom Thalassiosira oceanica. Limnol Oceanogr 52:2710-2714

John SG, Rouxel OJ, Craddock PR, Engwall AM, Boyle EA (2008) Zinc stable isotopes in seafloor hydrothermal vent fluids and chimneys. Earth Planet Sci Lett 269:17-28

John SG, Conway TM (2014) A role for scavenging in the marine biogeochemical cycling of zinc and zinc isotopes. Earth Planet Sci Lett 394:159-167

Jouvin D, Louvat P, Juillot F, Marechal CN, Benedetti MF (2009) Zinc Isotopic Fractionation: Why Organic Matters. Environ Sci Technol 43:5747-5754, doi:10.1021/es803012e

Jouvin D, Weiss D, Mason T, Bravin M, Louvat P, Zhao F, Ferec F, Hinsinger P, Benedetti M (2012) Stable Isotopes of Cu and Zn in Higher Plants: Evidence for Cu Reduction at the Root Surface and Two Conceptual Models for Isotopic Fractionation Processes. Environ Sci Technol 46:2652–2660

Juillot F, Maréchal C, Ponthieu M, Cacaly S, Morin G, Benedetti M, Hazemann JL, Proux O, Guyot F (2008) Zn isotopic fractionation caused by sorption on goethite and 2-Lines ferrihydrite. Geochim Cosmochim Acta 72:4886-4900

Juillot F, Marechal C, Morin G*, et al.* (2011) Contrasting isotopic signatures between anthropogenic and geogenic Zn and evidence for post-depositional fractionation processes in smelter-impacted soils from Northern France. Geochim Cosmochim Acta 75:2295-2308, doi:Doi 10.1016/J.Gca.2011.02.004

Kafantaris F-C, Borrok DM (2014) Zinc isotope fractionation during surface adsorption and intracellular incorporation by bacteria. Chem Geol 366:42-51

Kato C, Moynier F, Valdes MC, Dhaliwal JK, Day JM (2015) Extensive volatile loss during formation and differentiation of the Moon. Nature Com. 6:7617, doi:10.1038/ncomms8617

Kau L-S, Spira-Solomon DJ, Penner-Hahn JE, Hodgson KO, Solomon EI (1987) X-ray absorption edge retermination of the oxidation state and coordination number of copper: Application to the type 3 site in Rhus vernicifera Laccase and its reaction with oxygen. J Am Chem Soc 109:6433-6442

Kavner A, John SG, Sass S, Boyle EA (2008) Redox-driven stable isotope fractionation in transition metals: application to Zn electroplating. Geochim Cosmochim Acta 72:1731-1741

Kimball BE, Mathur R, Dohnalkova AC, Wall AJ, Runkel RL, Brantley SL (2009) Copper isotope fractionatin in acid mine drainage. Geochim Cosmochim Acta 73:1247-1263

Koschinsky A, Hein JR (2003) Acquisition of elements from seawater by ferromanganese crusts: Solid phase association and seawater speciation. Mar Geol 198:331-351

Kunzmann N, Halverson GP, Sossi PA, Raub TD, Payne JL, Kirby J (2013) Zn isotope evidence for immediate resumption of primary productivity after snowball Earth. Geology 41:27-30

Kurtz AC, Derry LA, Chadwick OA (2001) Accretion of Asian dust to Hawaiian soils: Isotopic, elemental, and mineral mass balances. Geochim Cosmochim Acta 65:1971–1983

Larner F, Rehkaemper M, Coles B, Kreissig K, Weiss D, Sampson B, Unsworth C, Strekopytov S (2011) A new separation procedure for Cu prior to stable isotope analysis by MC-ICP-MS. J Anal At Spectrom 26:1627-1632

Larson PB, Maher K, Ramos FC, Chang Z, Gaspar M, Meinert LD (2003) Copper isotope ratios in magmatic and hydrothermal ore forming environments. Chem Geol 201:337-350

Lee CTA, Yin Q-Z, Lenardic A, Agranier A, O'Neill C, Thiagarajan N (2007) Trace-element composition of Fe-rich residual liquids formed by fractional crystallization: implications for the Hadean magma ocean. Geochim Cosmochim Acta 71:3601-3615

Lee CTA, Luffi P, Chin EJ, Bouchet R, Dasgupta R, Morton DM, Le Roux V, Yin Q-Z, Jin D (2012) Copper Systematics in Arc Magmas and Implications for Crust-Mantle Differentiation. Science 336:64-68, doi:10.1126/science.1217313

Li W, Jackson S, Pearson NJ, Alard O, Chappell BW (2009) The Cu isotopic signature of granites from the Lachlan Fold Belt, SE Australia Chem Geol 258:38-49

Little SH, Vance D, Siddall M, Gasson E (2013) A modelling assessment of the role of reversible scavenging in controlling oceanic dissolved Cu and Zn distributions. Glob Biogeochem Cycles 27:780-791

Little SH, Vance D, Walker-Brown C, Landing WM (2014a) The oceanic mass balance of copper and zinc isotopes, investigated by analysis of their inputs, and outputs to ferromanganese oxide sediments. Geochim Cosmochim Acta 125:673-693, doi:10.1016/j.gca.2013.07.046

Little SH, Sherman DM, Vance D, Hein JR (2014b) Molecular controls on Cu and Zn isotopic fractionation in Fe-Mn crusts. Earth Planet Sci Lett 396:213-222

Little SH, Vance D, McManus J, Severmann S (2016) Critical role of continental margin sediments in the oceanic mass balance of Zn and Zn isotopes. Geology 44: 207-210.

Liu S-A, Teng F-Z, Li S, Wei G-J, Ma J-L, Li D (2014) Copper and iron isotope fractionation during weathering and pedogenesis: insights from saprolite profiles. Geochim Cosmochim Acta 146:59-75

Liu S-A, Huang J, Liu J, Woerner G, Yang W, Tang Y-J, Chen Y, Tang L, Zheng J, Li S (2015) Copper isotopic composition of the silicate Earth. Earth Planet Sci Lett 427:95-103, doi:10.1016/j.epsl.2015.06.061

Lodders K (2003) Solar System abundances and condensation temperatures of the elements. Astrophys J 591:1220-1247

Loss RD, Lugmair GW (1990) Zinc isotope anomalies in Allende meteorite inclusions. Astroph J 360:L59-L62

Loss RD, Rosman KJR, Delaeter JR (1990) The Isotopic Composition of Zinc, Palladium, Silver, Cadmium, Tin, and Tellurium in Acid-Etched Residues of the Allende Meteorite. Geochim Cosmochim Acta 54:3525-3536

Luck JM, Othman DB, Barrat JA, Albarède F (2003) Coupled ^{63}Cu and ^{16}O excesses in chondrites. Geochim Cosmochim Acta 67:143-151

Luck JM, Othman DB, Albarède F (2005) Zn and Cu isotopic variations in chondrites and iron meteorites: Early solar nebula reservoirs and parent-body processes. Geochim Cosmochim Acta 69:5351-5363

Macleod G, Mcneown C, Hall AJ, Russel MJ (1994) Hydrothermal and oceanic pH conditions of possible relevance to the origin of life. Biosphere 24:19-41

Manceau A, Lanson B, Drits VA (2002) Structure of heavy metal sorbed birnessite. Part III: results from powder and polarized extended X-ray absorption fine structure spectroscopy. Geochim Cosmochim Acta 66:2639-2663

Maréchal C, Télouk P, Albarède F (1999) Precise analysis of copper and zinc isotopic compositions by plasma-source mass spectrometry. Chem Geol 156:251-273Maréchal CN, Douchet C, Nicolas E, Albarède F (2000) The abundance of zinc isotopes as a marine biogeochemical tracer. Geochem, Geophys, Geosyst 1:1999GC-000029

Maréchal C, Albarède F (2002) Ion-exchange fractionation of copper and zinc isotopes. Geochim Cosmochim Acta 66:1499–1509

Maréchal CN, Sheppard SMF (2002) Isotopic fractionation of Cu and Zn between chloride and nitrate solutions and malachite or smithsonite at 30° and 50°C (abstr.). Geochim Cosmochim Acta 66:A84

Markl G, Lahaye Y, Schwinn G (2006) Copper isotopes as monitors of redox processes in hydrothermal mineralization. Geochim Cosmochim Acta 70:4215-4228

Marschner H (1995) Mineral nutrition of higher plants. 2nd edition. Academic Press, London.

Mason TFD, Weiss DJ, Horstwood M, Parrish RR, Russell SS, Mullane E, Coles BJ (2004a) High-precision Cu and Zn isotope analysis by plasma source mass spectrometry. Part 1. Spectral interferences and their correction. J Anal At Spectrom 19:209-217

Mason TFD, Weiss DJ, Horstwood M, Parrish RR, Russell SS, Mullane E, Coles BJ (2004b) High-precision Cu and Zn isotope analysis by plasma source mass spectrometry. Part 2. Correcting for mass discrimination effects. J Anal At Spectrom 19:218-226

Mason TFD, Weiss DJ, Chapman JB, Wilkinson JJ, Tessalina SG, Spiro B, Horstwood MSA, Spratt J, Coles BJ (2005) Zn and Cu isotopic variability in the Alexandrinka volcanic-hosted massive sulphide (VHMS) ore deposit, Urals, Russia. Chem Geol 221:170-187

Mathur R, Ruiz J, Titley S, Liermann L, Buss H, Brantley S (2005) Cu isotopic fractionation in the supergene environment with and without bacteria. Geochim Cosmochim Acta 69:5233-5246Mathur R, Titley S, Barra F, Brantley S, Wilson M, Phillips

A, Munizaga F, Maksaev V, Vervoort J, Hart G (2009) Exploration potential of Cu isotope fractionation in porphyry copper deposits. J Geochem exp 102:1-6

Mathur R, Dendas M, Titley S, Phillips A (2010) Patterns in the copper isotope composition of minerals in porphyry copper deposits in southwestern United States. Econ Geol 105:1457-1467

Mathur R, Jin L, Prush V, Paul J, Ebersole C, Fornadel A, Williams JZ, Brantley S (2012) Cu isotopes and concentrations during weathering of black shale of the Marcellus Formation, Huntingdon County, Pennsylvania (USA). Chem Geol 304:175-184

Mattielli N, Petit JC, Deboudt K, Flament P, Perdrix E, Taillez A, Rimetz-Planchon J, Weis D (2009) Zn isotope study of atmospheric emissions and dry depositions within a 5 km radius of a Pb-Zn refinery. Atmos Environ 43:1265-1272

McBride MB (1981) Forms and distribution of copper in solid and solution phases of soil. In: Copper in soils and plants. *In*: Copper in soils and plants. Loneragan J, Robson AD, Graham RD, (ed) Academic Press, NY, p 25-45

McDonough WF (2003) Compositional Model for the Earth's Core. *In*: Treatise on Geochemistry. Vol 2. Holland HD, Turekian KK, (eds). p 547-568

Meyer BS, Krishan TD, Clayton DD (1998) Theory of Quasi-Equilibrium Nucleosynthesis and Applications to Matter Expanding from High Temperature and Density. Astrophys J 498:808-830

Mhin BJ, Lee S, Cho SJ, Lee K, Kim KS (1992) $Zn(H2O)_6^{2+}$ is very stable among aqua-Zn (II) ions. Chem Phys Lett 197:77-80

Moffett JW, Brand LE (1996) The production of strong, extracellular Cu chelators by marine cyanobacteria in response to Cu stress. Limnol Oceanogr 41:288-293

Mott lMJ, Wheat CG, Fryer P, Gharib J, Martin JB (2004) Chemistry of springs across the Mariana forearc shows progressive devolatilization of the subducting plate. Geochim Cosmochim Acta 68:4915-4933

Mountain BW, Seward TM (1999) The hydrosulphide/sulphide complexes of copper(I): experimental determination of stoichiometry and stability at 22c and reassessment of high temperature data. Geochim Cosmochim Acta 63:11-29

Moynier F, Le Borgne M (2015) High precision zinc isotopic measurements applied to mouse organs. Journal of visualized experiments:JoVE:e52479-e52479, doi:10.3791/52479

Moynier F, Fegley B (2015) The Earth's building blocks. *In*: The Early Earth: Accretion and Differentiation. Vol 212. Badro J, Walter MJ, (eds). Wiley, New York, p 27-48

Moynier F, Albarède F, Herzog G (2006) Isotopic composition of zinc, copper, and iron in lunar samples. Geochim Cosmochim Acta 70:6103-6117

Moynier F, Dauphas N, Podosek FA (2009a) A Search for ^{70}Zn Anomalies in Meteorites. Astrophys J 700:L92-L95

Moynier F, Pichat S, Pons ML, Fike D, Balter V, Albarède F (2009b) Isotopic fractionation and transport mechanisms of Zn in plants. Chem Geol 267:125-130, doi:DOI 10.1016/j.chemgeo.2008.09.017

Moynier F, Beck P, Jourdan F, Yin Q-Z, Reimold U, Koeberl C (2009c) Isotopic fractionation of zinc in tektites. Earth Planet Sci Lett 277:482-489

Moynier F, Koeberl C, Beck P, Jourdan F, Telouk P (2010a) Isotopic fractionation of Cu in tektites. Geochim Cosmochim Acta 74:799-807, doi:DOI 10.1016/j.gca.2009.10.012

Moynier F, Beck P, Yin Q, Ferroir T, Barrat JA, Paniello RC, Telouk P, Gillet P (2010b) Volatilization induced by impacts recorded in Zn isotope composition of ureilites. Chem Geol 276:374-379

Moynier F, Paniello RC, Gounelle M, Albarède F, Beck P, Podosek F, Zanda B (2011) Nature of volatile depletion and genetic relationships in enstatite chondrites and aubrites inferred from Zn isotopes. Geochim Cosmochim Acta 75:297-307, doi:Doi 10.1016/J.Gca.2010.09.022

Moynier F, Fujii T, Shaw A, Le Borgne M (2013a) Heterogeneous distribution of natural zinc isotopes in mice. Metallomics 5:693-699

Moynier F, Fujii T, Wang K, Foriel J (2013b) Ab initio calculations of the Fe(II) and Fe(III) isotopic effects in citrates, nicotianamine, and phytosiderophore, and new Fe isotopic measurements in higher plants. Comptes Rendus Geoscience 345:230-240, doi:10.1016/j.crte.2013.05.003

Nägler TF, Anbar AD, Archer C, Goldberg G, Gordon GW, Greber ND, Siebert C, Sohrin Y, Vance, D (2014) Proposal for an international molybdenum isotope measurement standard and data representation. Geostandards and Geoanalytical Research 38, 149-151

Navarette JU, Borrok DM, Viveros M, Ellzey JT (2011) Copper isotope fractionation during surface adsorption and intracellular incorporation by bacteria. Geochim Cosmochim Acta 75:784-799

Ochoa Gonzalez, R, Weiss, D (2015) Zinc isotope variability in three coal-fired power plants: a predictive model for determining isotopic fractionation during combustion. Environ Sci Technol 49: 12560-12567

O'Neill H (1991) The origin of the Moon and the earlyhistory of the Earth-A chemical model. Part 2: The Earth. Geochim Cosmochim Acta 55:1159-1172

Pacyna JM, Pacyna EG (2001) An assessment of global and regional emissions of trace metals to the atmosphere from anthropogenic sources worldwide. Environ Rev 9:269-288

Palme H, O'Neill H (2003) Comochemical Estimates of Mantle Composition. *In*: Treatise on Geochemistry. Vol 2. Holland HD, Turekian KK, (eds). p 1-38

Paniello RC, Day JM, Moynier F (2012a) Zinc isotopic evidence for the origin of the Moon. Nature 490:376-379, doi:10.1038/nature11507

Paniello RC, Moynier F, Beck P, Barrat JA, Podosek FA, Pichat S (2012b) Zinc isotopes in HEDs: Clues to the formation of 4-Vesta, and the unique composition of Pecora Escarpment 82502. Geochim Cosmochim Acta 86:76-87, doi:Doi 10.1016/J.Gca.2012.01.045

Pasquarello A, Petri I, Salmon PS, Parisel O, Car R, Toth E, Powell DH, Fischer HE, Helm L, Merbach AE (2001) First solvation shell of the Cu(II) aqua ion: evidence for fivefold coordination. Science 291:856-859

Peacock CL, Sherman DM (2004) Copper (II) sorption onto goethite, hematite and lepidocrocite: a surface complexation model based on ab initio molecular geometries and EXAFS spectroscopy. Geochim Cosmochim Acta 68:2623-2637

Peel K, Weiss D, Sigg L (2009) Zinc isotope composition of settling particles as a proxy for biogeochemical processes in lakes: insights from the eutrophic Lake Greifen, Switzerland. Limnol Oceanogr Methods 54:1699-1708

Peel K, Weiss D, Chapman J, Arnold T, Coles B (2008) A simple combined sample-standard bracketing and inter-element correction procedure for accurate mass bias correction and precise Zn and Cu isotope ratio measurements. J Anal At Spectrom 23:103-110, doi:10.1039/b710977f

Peers G, Price NM (2006) Copper-containing plastocyanin used for electron transport by an oceanic diatom. Nature 441:341-344

Petit JC, Schäfer J, Coynel A, Blanc G, Deycard VN, Derriennic H, Lanceleur L, Dutruch L, Cossy C, Mattielli N (2013) Anthropogenic sources and biogeochemical reactivity of particulate and dissolved Cu isotopes in the turbidity gradient of the Garonne River (France). Chem Geol 359:125-135

Pichat S, Douchet C, Albarède F (2003) Zinc isotope variations in deep-sea carbonates from the eastern equatorial Pacific over the last 175 ka. Earth Planet Sci Lett 210:167-178

Pogge von Strandmann PAE, Forshaw J, Schmidt DN (2014) Modern and Cenozoic records of seawater magnesium from foraminiferal Mg isotopes. Biogeosciences 11:5155-5168

Pokrovsky OS, Viers J, Freydier R (2005) Zinc stable isotope fractionation during adsorption on oxides and hydroxides. J Colloid Interface Sci 291:192-200

Pokrovsky OS, Viers J, Emnova EE, Kompantseva EI, Freydier R (2008) Copper isotope fractionation during its interaction with soil and aquatic microorganisms and metal oxy(hyd)oxides: Possible structural control. Geochim Cosmochim Acta 72:1742-1757

Pons ML, Quitte G, Fujii T, Rosing MT, Reynard B, Moynier F, Douchet C, Albarède F (2011) Early Archean serpentine mud volcanoes at Isua, Greenland, as a niche for early life. Proc. Natl. Acad. Sci. USA 108:17639-17643, doi:Doi 10.1073/Pnas.1108061108

Pons M-L, Fujii T, Rosing M, Quitté G, Télouk P, Albarède F (2013) A Zn isotope perspective on the rise of continents. Geobiology 11:201-214

Ponzevera E, Quetel CR, Berglund M, Taylor PDP, Evans P, Loss RD, Fortunato G (2006) Mass discrimination during MC-ICPMS isotopic ratio measurements: Investigation by means of synthetic isotopic mixtures (IRMM-007 series) and application to the calibration of natural-like zinc materials (including IRMM-3702 and IRMM-651). Journal of the American Society for Mass Spectrometry 17:1412-1427, doi:10.1016/j.jasms.2006.06.001

Powell KJ, Brown PL, Byrne RH, Gajda T, Hefter G, Sjoberg S, Wanner H (2007) Chemical speciation of environmentally significant metals with inorganic ligands - Part 2: The Cu^{2+}-OH^-, Cl^-, CO_3^{2-}, SO_4^{2-}, and PO_4^{3-} systems. Pure Appl Chem 79:895-950

Rauch, JN, Pacyna, JM (2009) Earth's global Ag, Al, Cr, Cu, Fe, Ni, Pb, and Zn cycles. Glob Biogeochem Cycles 23: GB2001, 10.1029/2008GB003376

Resing JA, Sedwick PN, German CR, Jenkins WJ, Moffett JW, Sohst BM, Tagliabue A (2015) Basin scale transport of hydrothermal dissolved metals across the South Pacific Ocean. Nature 523:200-203

Rodovka Z, Magna T, Zak K, Kato C, Savage P, Moynier F, Skala R (In review) Zinc and copper isotope systematics in sediments from the Ries Impact Structure and central European tektites – implications for material sources and loss of volatiles. Geochim Cosmochim Acta

Rosman KJR (1972) A survey of the isotopic and elemental abundances of zinc. Geochim Cosmochim Acta 36:801-819

Rudge JF, Reynolds BC, Bourdon B (2009) The double spike toolbox. Chem Geol 265:420-431

Russel SS, Zhu X, Guo Y, Belshaw N, Gounelle M, Mullane E (2003) Copper isotope systematics in CR, CH-like, and CB meteorites: a preliminary study (abstr.). Meteorit Planet Sci 38

Ryan BM, Kirby JK, Degryse F, Scheiderich K, McLaughlin MJ (2014) Copper isotope fractionation during equilibration with natural and synthetic ligands. Environ Sci Tech 48:862-866

Ryan BM, Kirby JK, Degryse F, Harris H, McLaughlin MJ, Scheiderich K (2013) Copper speciation and isotopic fractionation in plants: uptake and translocation mechanisms. New Phytologist 199:367-378

Sancenon V, Puig S, Mateu-Andrés I, Dorcey E, Thiele D, Penarrubia L (2004) The Arabidopsis copper transporter COPT1 functions in root elongation and pollen development. J Biol Chem 269:15348-15355

Savage P, Boyet M, Moynier F (2014) Zinc Isotope Anomalies in bulk Chondrites. 77th Meteoritical Society Meeting, Casablanca, Morocco, p 5246

Savage P, Moynier F, Harvey J, Burton K (2015a) The behavior of copper isotopes during igneous processes. AGU conference, San Francisco

Savage P, Moynier F, Chen H, Shofner G, Siebert J, Badro J, Puchtel IS (2015b) Copper isotope evidence for large-scale sulphide fractionation during Earth's differentiation. Geochemical Perspective Letters 1:53-64

Schauble EA (2004) Applying stable isotope fractionation theory to new systems. Rev Mineral Geochem 55:65-111

Schiller M, Paton C, Bizzarro M (2015) Evidence for nucleosynthetic enrichment of the protosolar molecular cloud core by multiple supernova events. Geochim Cosmochim Acta 149:88-102, doi:10.1016/j.gca.2014.11.005

Schonbachler M, Carlson RW, Horan MF, Mock TD, Hauri EH (2010) Heterogeneous Accretion and the Moderately Volatile Element Budget of Earth. Science 328:884-887, doi:DOI 10.1126/science.1186239

Schulz MS, Bullen TD, White AF, Fitzpatrick JF (2010) Evidence of iron isotope fractionation due to biologic lifting in a soil chronosequence. Geochim Cosmochim Acta 74:A927

Seo JH, Lee SK, Lee I (2007) Quantum chemical calculations of equilibrium copper(I) isotope fractionations in ore-forming fluids. Chem Geol 243:225-237

Shank CG, Ckrabal SA, Whitehead RF, G. BA, Keiber RJ (2004) River discharge of strong Cu-binding ligands to South Atlantic Bight Waters. Mar Chem 88:41-51

Sherman DM (2001) Quantum chemistry and classical simulations of metal complexes in aqueous solutions. *In*: Rev Mineral Geochem. Vol 42. p 273-317

Sherman DM (2013) Equilibrium isotopic fractionation of copper during oxidation/reduction, aqueous complexation and ore-forming processes: predictions from hybrid density functional theory. Geochim Cosmochim Acta 118:85-97

Sherman DM, Little SH, Vance D (2015) Reply to comment on "Molecular controls on Cu and Zn isotopic fractionatin in Fe-Mn crusts". Earth Planet Sci Lett 411:313-315

Shields WR, Murphy TJ, Garner EL (1964) Absolute isotopic abundance ratio and the atomic weight of a reference sample of copper. J Res NBS 68A:589-592

Shields WR, Goldich SS, Garner EL, Murphy TJ (1965) Natural variations in the abundance ratio and the atomic weight of copper. J Geophys Res:479-491

Shiller AM, Boyle EA (1985) Dissolved zinc in rivers. Nature 317:49-52

Siebert J, Corgne A, Ryerson FJ (2011) Systematics of metal–silicate partitioning for many siderophile elements applied to Earth's core formation. Geochim Cosmochim Acta 75:1451-1489

Singha Deb AK, Ali SkM, Shenoy KT, and Ghosh SK (2014) Nano cavity induced isotope separation of zinc: density functional theoretical modeling. J Chem Eng Data, 59:2472-2484

Sinoir M, Butler ECV, Bowie AR, Mongin M, Nesterenko PN, Hassler CS (2012) Zinc marine biogeochemistry in seawater: a review. Mar Freshwater Res 63:644-657

Sivry Y, Riotte J, Sonke JE, Audry S, Schäfer J, Vuers J, Blanc G, Freydier R, Dupré B (2008) Zn isotopes as tracers of anthropogenic pollution from Zn ore-smelters. The Riou Mort-Lot River system. Chem Geol 255:295-304

Sold D, Behra R (2000) Long-term effects of copper on the structure of freshwater periphyton communities and their tolerance to copper, zinc, nickel and silver. Aquatic Toxicol 47:181-189

Sonke JE, Sivry Y, Viers J, Fréydier R, Dejonghe L, André L, Aggarwal JK, Fontan F, Dupré B (2008) Historical variations in the isotopic composition of atmospheric zinc deposition from a zinc smelter. Chem Geol 252:145-157

Sossi PA, Halverson GP, Nebel O, Eggins SM (2015) Combined Separation of Cu, Fe and Zn from Rock Matrices and Improved Analytical Protocols for Stable Isotope Determination. Geostandards and Geoanalytical Research 39:129-149, doi:10.1111/j.1751-908X.2014.00298.x

Sossi PA, Nebel O, O'Neil HST, Moynier F (In review) Progressive accretion of Earth's moderately volatile elements revealed by Zn isotopes. Geochemical Perspective Letters.

Steele RCJ, Coath CD, Regelous M, Russell S, Elliott T (2012) Neutron-poor nickel isotope anomalies in meteorites. Astrophys J 758(59) doi:10.1088/0004-637X/758/1/59

Sunda WG, Huntsman SA (1992) Feedback interactions between zinc and phytoplankton in seawater. Limnol Oceanogr Methods 37: 25-40

Szynkiewicz A,_Borrok DB (2016) Isotope variations of dissolved Zn in the Rio Grande watershed, USA: The role of adsorption on Zn isotope composition. Earth Planet Sci Lett 433: 293-302

Takano S, Tanimizu M, Hirata T, Sohrin Y, 10.1038/ncomms6663. IcobcocitoNCd (2014) Isotopic constraints on biogeochemical cycling of copper in the ocean. Nature communications doi: 10.1038/ncomms6663.

Tang Y-T, Cloquet C, Sterckman T, Echevarria G, Carignan J, Qiu R-L, Morel J-L (2012) Fractionation of stable zinc isotopes in the field-grown zinc hyperaccumulator Noccaea caerulescens and the zinc-tolerant plant Silene vulgaris. Environ Sci Technol 46:9972-9979

Tanimizu M, Asada Y, Hirata T (2002) Absolute isotopic composition and atomic weight of commercial zinc using inductively coupled plasma mass spectrometry. Anal Chem 74:5814-5819

Telouk P, Puisieux A, Fujii T, Balter V, Bondanese VP, Morel A-P, G. C, Lamboux A, Albarède F (2015) Copper isotope effect in serum of cancer patients. A pilot study. Metallomics 7:299-308.

Telus M, Dauphas N, Moynier F, Tissot F, Teng FZ, Nebelek PI, Craddock PR, Groat LR (2012) Iron, zinc, magnesium, and uranium isotopic fractionation during continental crust differentiation : The tale from migmatites, granitoids and pegmatites. Geochim. Cosmochim. Acta 97:247-265.

Thapalia A, Borrok DM, van Metre PC, Musgrove M, Landa ER (2010) Zn and Cu isotopes as tracers of anthropogenic contamination in a sediment core from an urban lake. Environ Sci Technol 44:1544-1550

Thomson CM, Ellwood MJ (2014) Dissolved copper isotope geochemistry in the Tasman Sea, SW Pacific Ocean. Mar Chem 165:1-9

Trinquier A, Elliott T, Ulfbeck D, Coath C, Krot AN, Bizzarro M (2009) Origin of Nucleosynthetic Isotope Heterogeneity in the Solar Protoplanetary Disk. Science 324:374-376

Twining BS, Baines SB (2013) The trace metal composition of marine phytoplankton. Ann Rev Earth Planet Sci 5:191-215

Vance D, Archer C, Bermin J, Perkins J, Statham PJ, Lohan MC, Ellwood MJ, Mills RA (2008) The copper isotope geochemistry of rivers and the oceans. Earth Planet Sci Lett 274:204-213, doi:10.1016/j.epsl.2008.07.026

Vance D, Teagle DAH, Foster GL (2009) Variable Quaternary chemical weathering fluxes and imbalances in marine geochemical budgets. Nature 458:493-496

Vance D, Matthews A, Keech A, Archer C, Hudson G, Pett-Ridge J, Chadwick OA (2016) The behaviour of Cu and Zn isotopes during soil development: controls on the dissolved load of rivers. Chem Geol: accepted

Vance D, Little SH, Archer C, Rijkenberg M (In review) Transition metal isotopes as tracers of oceanic metal budgets and cycling. Phil Trans R Soc A

Viers J, Oliva P, Nonelle A, Gelabert A, Sonke J, Freydier R, Gainville R, Dupre B (2007) Evidence of Zn isotopic frationation in a soil-plant system of a pristine tropical watershed (Nsimi, Cameroon). Chem Geol 239:124-137

Viers, J, Prokushkin, AS, Pokrovsky, OS, Kirdyanov, AV, Zouiten, C, Chmeleff, J, Meheut, M, Chabaux, F, Oliva, P, Dupré, B (2015) Zn isotope fractionation in a pristine larch forest on permafrost-dominated soils in Central Siberia. Geochem Trans 16: 10.1186/s12932-015-0018-0

Völkening J, Papanastassiou DA (1990) Zinc isotope anomalies. Astrophys J 358:L29-L32

Wallerstein G, Iben Jr I, Parker P, Boesgaard AM, Hale GM, Champagne AE, Barnes CA, Kaeppeler F, Smith VV, Hoffman RD, Timmes FX, Sneden C, Boyd RN, Meyer BS, Lambert DL (1997) Synthesis of the elements in stars: forty years of progress. Reviews of Modern Physics, 69: 995-1084

Wang P, Zhou DM, Luo XS, Li LZ (2009) Effects of Zn-complexes on zinc uptake by wheat (Triticum aestivum) roots: a comprehensive consideration of physical, chemical and biological processes on biouptake. Plant Soil 316:177-192

Wanty, RB, Ballistrieri, LS, Wesner, JS, Walsters, DM, Schmidt, TS, Podda, F, De Giudici, G, Stricker, CA, Kraus, J, Lattanzi, P, Wolf, RE, Cidu, R (2015) Isotopic insights into biological regulation of zinc in contaminated systems. Proc Earth Planet Sci 13: 60-63

Wanty, RB, Podda, F, De Giudici, G, Cidu, R, Lattanzi, P (2013) Zinc isotope and transition-element dynamics accompanying hydrozincite biomineralization in the Rio Naracauli, Sardinia, Italy. Chem Geol 337-338: 1-10

Wasson JT, Wang JM (1986) A non magmatic origin of group-IIE iron-meteorites. Geochim Cosmochim Acta 50:725-732

Wasylenki LE, Weeks CL, Bargar JR, Spiro TG, Hein JR, Anbar AD (2011) The molecular mechanism of Mo isotope fractionation during adsorption to birnessite. Geochim Cosmochim Acta 75:5019-5031

Weinstein C, Moynier, F., Wang, K., Paniello, R., Foriel, J., Catalano, J., and Foriel, J. (2011) Cu isotopic fractionation in plants. Chem Geol 286:266-271

Weiss DJ, Mason TFD, Zhao FJ, Kirk GJD, Coles BJ, Horstwood MSA (2005) Isotopic discrimination of zinc in higher plants. New Phytologist 165:703-710

Weiss DJ, Rausch N, Mason TFD, Coles BJ, Wilkinson JJ, Ukonmaanaho L, Arnold T, Nieminen TM (2007) Atmospheric deposition and isotope biogeochemistry of zinc in ombrotrophic peat. Geochim Cosmochim Acta 71:3498-3517

Weiss DJ, Boye K, Caldelas C, Fendorf S (2014) Zinc isotope fractionation during early dissolution of biotite granite. Soil Sci Amer 78:171-189

Wells ML, Kozelka PB, Bruland KW (1998) The complexation of "dissolved" Cu, Zn, Cd and Pb by soluble and colloidal organic matter in Narragansett Bay, RI. Mar Chem 62:203-217

Wiederhold JG, Teutsch N, Kraemer SM, Halliday AN, Kretzschmar R (2007) Iron isotope fractionation in oxic soils by mineral weathering and podzolization. Geochim Cosmochim Acta 71:5821-5833, doi:Doi 10.1016/J.Gca.2007.07.023

Wiederhold J (2015) Metal stable isotope signatures as tracers in environmental geochemistry. . Environmental Science & Technology 49:2606-2624

Wilkinson JJ, Weiss DJ, Mason TFD, Coles BJ (2005) Zinc isotope variation in hydrothermal systems: preliminary evidence from the Irish Midlands ore field. Econ Geol 110:583-590

Williams HM, Archer C (2011) Copper stable isotopes as tracers of metal-sulphide segregation and fractional crystallisation processes on iron meteorite parent bodies. Geochim Cosmochim Acta 75:3166-3178

Yin, N-H, Sivry, Y, Benedetti, MF, Lens, PNL, van Hullebusch, ED (2016) Application of Zn isotopes in environmental impact assessment of Zn-Pb metallurgical industries: a mini review. App Geochem 64: 128-135

Yruela I (2009) Copper in plants: acquisition, transport and interactions. Funct Plant Biol 26:409-430

Zhao Y, Vance D, Abouchami W, de Baar HJW (2014) Biogeochemical cycling of zinc and its isotopes in the Southern Ocean. Geochim Cosmochim Acta 125:653-672, doi:10.1016/j.gca.2013.07.045

Zhu XK, O'Nions RK, Guo Y, Belshaw NS, Rickard D (2000) Determination of Cu-isotope variation by plasma souce mass spectrometry: implications for use as geochemical tracers. Chem Geol 163:139-149

Zhu XK, Guo Y, Williams RJP*, et al.* (2002) Mass fractionation processes of transition metal isotopes. Earth Planet Sci Lett 200:47-62

Zirino A, Yamamoto S (1972) A pH-dependent model for the chemical speciation of copper zinc cadmium, and lead in seawater. Limnol Oceanogr 17:661-671

Figure captions

Figure 1: Temperature dependence of lnβ. The lnβ values of hydrated Cu2+ and Cu(II) chlorides, sulphides, phosphates, carbonates and sulfates (see Table 1) are shown as linear functions of T^2.

Figure 2: Temperature dependence of lnβ. The lnβ values of hydrated Zn2+ and Zn(II) sulphides, phosphates, carbonates and sulfates (see Table 1) are shown as linear functions of T^2.

Figure 3: δ^{65}Cu vs Δ^{17}O for the bulk silicate Earth and the different major groups of chondrites. Meteorite group averages are calculated using data from Luck et al. (2003), Barrat et al (2012) and Savage et al. (2015b). The estimate of the Bulk Silicate Earth is from Savage et al. (2015b). All error bars are 2SD of the mean. The trend implies the presence of at least two, and potentially three, distinct Cu isotope reservoirs which then mixed to create the distinct chondritic bodies, as a result of nebula processing.

Figure 4: A) Box-and-whisker plot of δ^{66}Zn of the different chondrites groups (UOC=Un-equilibrated ordinary chondrites); whiskers denote the maximum and minimum value of the data, box denotes the first and third quartiles and the band denotes the median. Data are taken from Luck et al. (2005), Moynier et al. (2011) and Barrat et al. (2012). Enstatite chondrites, carbonaceous chondrites, and unequilibrated ordinary chondrites have Zn isotopic composition close to the current estimates of BSE. B) Identical plot as 4A but with increased x-axis range. The EL enstatite chondrites of high thermal metamorphic grades (EL6), which are depleted in volatile elements compared to low thermal metamorphic grades (EL3), are highly enriched in the heavier isotopes. This suggests that the origin of the volatile element depletion between EL3 and EL6 chondrites is due to volatilization during the thermal metamorphism.

Figure 5: δ^{66}Zn vs Mg/Zn ratio for different chondrites groups. The negative correlation between δ^{66}Zn and Mg/Zn (refractory element/moderately volatile element) suggests that the origin of the Zn depletion in carbonaceous chondrites is not due to evaporation and is of nebular origin. Data from Luck et al. (2005) and Barrat et al. (2012)

Figure 6: Histogram of the δ^{65}Cu of the various ultramafic and mafic samples analyzed to date (data from Savage et al. 2015b, Liu et al. 2015, Ben Othman et al. 2006 and Ikehata and Hirata 2013). The grey box represents the estimate of the BSE composition from Savage et al. 2015b. Komatiites , fertile orogenic lherzolites as well as a representative selection of both mid-ocean ridge and ocean island basalts have identical Cu isotope compositions suggesting that mantle melting produces a limited Cu isotope fractionation.

Figure 7: δ^{66}Zn and Zn concentration versus degree of differentiation as represented by MgO content for basalts and their differentiates, komatiites and ultramafic samples (data from Herzog et al., 2011, Chen et al. 2013b and Sossi et al. In review). The most evolved samples are enriched in the heavier isotopes. This trend is interpreted as the result of

crystallization of isotopically light olivines or Ti-oxides (Chen et al. 2013b) and led Sossi et al (in review) to propose a BSE δ^{66}Zn composition of 0.15 ± 0.05 ‰. N.B. the abyssal peridotites underwent metasomatism, most likely affecting their Zn isotope composition.

Figure 8: Summary of currently available data for "natural" surface Earth materials. Materials significantly impacted by human activity represent a distinct topic and are treated separately later in this chapter. The range of isotopic compositions found in ore minerals is shown by the black bars at the bottom. Note that Cu isotopes are extremely heterogeneous in Cu-bearing ore minerals, extending well beyond the limits of other Earth surface samples, from δ^{65}Cu -16.5 to +9.98. In the top two panels the thinner lines show the total range of values measured in each type of sample. For the oceanic dissolved pool, the thicker lines show the average and 1SD for all analyses in the homogeneous deep ocean (beneath 600-800m). For the river data the square shows the discharge- and [Cu]- or [Zn]-weighted average for the dissolved flux to the oceans as calculated from the large rivers measured to date. For all the other sample types the thicker line shows the average of all the data ±1SD. In the bottom two panels the red histograms show the range of variability in all igneous rocks, as relative frequencies, including basalts, andesites, dacites, rhyolites, granites, granodiorites, komatiites and peridotites. Clastic sediments (diagonal pattern), including atmospheric aerosols, show close overlap with the igneous samples. In contrast, surface Earth samples whose genesis involves the partitioning of Cu and Zn between solid and aqueous phases (top two panels) exhibit substantial variability. Note the agreement between the values for igneous rocks and clastic sediments with those for the Bulk Silicate Earth in earlier diagrams.

Data from:
Seawater: Bermin et al. (2006), Vance et al. (2008), Boyle et al. (2012), Zhao et al. (2014), Conway and John (2014, 2015), Thomson and Ellwood (2014), Takano et al. (2014). Rivers: Vance et al. (2008), Ilina et al. (2013), Little et al. (2014a), and including two Zn data for the relatively unpolluted Seine system headwaters from Chen et al. (2008). Dust/aerosol: Marechal et al. (2000), Li et al. (2009), Bigalke et al. (2010a), Dong et al. (2013), Little et al. (2014a), and including data for rain (wet deposition?) in Takano et al. (2014). Fe-Mn deposits: Marechal et al. (2000), Little et al. (2014a). Carbonates: Pichat et al. (2003). Siliceous sediments: Andersen et al. (2011), Hendry and Andersen (2013). Organic-rich sediments: Little et al. (2016) Deep, sulphidic Black Sea (dissolved phase):Vance et al. (2016a). Soils and plants: Viers et al. (2007); Bigalke et al. (2010a, 2011), Mathur et al. (2012), Liu et al. (2014), Vance et al. (2016b). Ombrotrophic peat: Weiss et al. (2007, pre-Anthropocene analyses only). Igneous rocks: Marechal et al. (2000), Archer and Vance (2004), Chapman et al. (2006), Cloquet et al. (2006), Bentahila et al. (2008), Toutain et al. (2008), Sonke et al. (2008), Li et al. (2009), Herzog et al. (2008), Chen et al. (2009), Moynier et al. (2010a,b), Bigalke et al. (2010), Weinstein et al. (2011), Moeller et al. (2012), Telus et al. (2012), Chen et al. (2013), Liu et al. (2015), Savage et al. (2015, including data tabulated here from Ben Othman et al., 2006 and Ikehata and Hirata, 2012). Clastic sediments (including dust/aersols in refs above): Marechal et al. (1999, 2000), Asael et al. (2007), Bentahila et al. (2008), Sonke et al. (2008, pre-Anthropocene analyses only), Chen et al. (2009, only relatively unpolluted river sediments from the Seine system, with Zn enrichment factors <2), Bigalke et al. (2010a), Mathur et al. (2012),

Gagnevin et al. (2012), Vance et al. (2016b). Ore minerals: Marechal et al. (1999), Larson et al. (2003), Mason et al. (2005), Wilkinson et al. (2005) Mathur et al. (2005, 2009, 2010), Markl et al. (2006), Asael et al. (2007), Sonke et al. (2008), Gagnevin et al. (2012).

Figure 9: Summary of experimental constraints on the isotopic fractionation of Cu and Zn during important Earth surface processes.

Data from:
Redox (Cu only): Zhu et al. (2002), Ehrlich et al. (2004), Mathur et al. (2005). Organic complexation: Ban et al. (2002), Jouvin et al. (2009), Bigalke et al. (2010b), Ryan et al. (2014). Sorption to oxide, clay and microbial surfaces: Pokrovsky et al. (2005, 2008), Gélabert et al. (2006), Ballistrieri et al. (2008), Juillot et al. (2008), Navarette et al. (2011), Kafantaris and Borrok (2014), Bryan et al. (2014), Coutaud et al. (2014), Guinoiseau et al. (2016). Biological uptake: Zhu et al. (2002), Weiss et al. (2005), John et al. (2007), Pokrovsky et al. (2008), Arnold et al. (2009), Moynier et al. (2009), Weinstein et al. (2011), Caldelas et al. (2011), Navarette et al. (2011), Jouvin et al. (2012), Tang et al. (2012), Ryan et al. (2013), Conway and John (2014).

Figure 10: Cu-Zn isotope and tau data from relatively unpolluted soils in Hawaii (basaltic) and Scotland (granitic) to illustrate important soil processes as discussed in the text (from Vance et al. 2016b). Panels a,b: data from a sequence of soils, all 400kyr in age but having seen different annual rainfall, on the island of Maui (Hawaiian Islands). Grey shading represents mean annual precipitation (MAP) from 2500mm (white), through 3350mm (grey) to 5050mm (black). Horizontal dashed lines show the isotopic composition of the parent basalt. At the 2500mm site Fe is retained in the soil as Fe oxyhydroxides. Cu is depleted with preferential loss of the heavy isotope to aqueous organic complexes and retention of a sorbed isotopically light pool (solid arrow). At higher rainfall these oxyhydroxides are lost by reduction, leading to loss of almost all this residual light Cu and the retention of a very small pool of Cu that is close to the parent material in isotopic composition (dashed arrow). Panel b shows the Zn data, which has a similar pattern though the move towards light isotopic compositions at the low rainfall site is barely analytically resolvable and the move back to heavy isotopic compositions overshoots to values 0.3‰ heavier than the original rock. Panels c,d: data for soils on the island of Hawaii, all having seen 2500mm MAP with colour shading showing different aged soils from 0.3 kyr (white), through 20 kyr (grey), to 150 kyr (black). The solid arrow shows the trajectory for retention of residual light isotopes during chemical weathering in well-drained conditions as in a,b. The dashed arrows in c show the trajectories that would be followed given addition of Asian dust to move the soils away from this trend. In d the dashed arrows are illustrative only because their exact slope depends on how much Cu and Zn the oils has lost when dust is added. Panels e,f: tau data for Zn and phosphate in the upper organic-matter-rich horizons of granitic Scottish soils, as well as Zn isotopic data for parent material (bar at left), plants (bar at right) and soils (open circles), to illustrate correlated behaviour between Zn and a major plant nutrient.

Figure 11: Summary data for soils studied in Viers et al. (2007), Mathur et al. (2012), Liu et al. (2014) and Vance et al. (2016b), in the form of taus and isotopic compositions

integrated over the entire soil profile studied, and in order to assess the overall impact of depletion by chemical weathering on Cu and Zn isotopes. The numbers in brackets in the key, and the intensity of shading, indicate the timescale over which soils have developed, where known. All basaltic soils are shown as diamonds, granitic as circles, and soils developed on black shales as triangles. Preferential loss of the heavy Cu isotope during chemical weathering is clearly significant. The Zn data are plotted on the same scale to illustrate the subtlety of isotope fractionation during weathering by comparison with Cu.

Figure 12: All the Zn isotopic data currently available for the dissolved pool in the oceans (right) with Zn concentrations measured in the same samples as the isotopes (left), plotted versus depth. The middle of the grey bar on the isotope plot marks the average δ^{66}Zn for the deep ocean (beneath 800m) while its width shows a typical analytical uncertainty (±0.06‰). This deep ocean inventory is generally very homogeneous and has an average δ^{66}Zn ~ +0.47‰. In the deep ocean, the data depart from this ratio locally, such as near hydrothermal vent systems at 3-4 km in the Atlantic (Conway and John 2014). In the surface ocean isotope compositions are also very close to this deep ocean average in the Southern Ocean (Zhao et al. 2014), but the upper ocean in the North Atlantic and North Pacific depart significantly from it (Boyle et al. 2012; Conway and John 2014, 2015; Zhao and Vance, unpublished data). Relative to this average deep ocean value, the estimates input is slightly isotopically light, at about +0.33‰ (arrow at top: Little et al. 2014a), while the dominant outputs in the oxic open ocean are much heavier (arrow at bottom: +0.90‰ in Fe-Mn oxides, carbonates and siliceous sediments; Little et al. 2014a).

Figure 13: All the Cu isotopic data currently available for the dissolved pool in the oceans (right) with Cu concentrations measured in the same samples as the isotopes (left), plotted versus depth. Open symbols on this plot are for data in the pioneering work of Bermin et al. (2006) and Vance et al. (2008). These data were obtained pre-GEOTRACES, on samples that had been stored for times on the order of 10 years. Though acidified, they stand out as having significantly heavier isotopic compositions than more recent work on new, cleanly-collected, GEOTRACES samples, including new (as yet unpublished) data from the same group, and in Takano et al. (2014) and Thompson and Ellwood (2014). It seems likely that these early measurements are compromised in some way by the long storage. The middle of the grey bar on the isotope plot marks the average δ^{65}Cu for the deep ocean (beneath 800m, and excluding these older data plotted as open symbols) while its width shows a typical analytical uncertainty (±0.08‰). As with Zn, this deep ocean inventory is generally very homogeneous and has an average δ^{65}Cu ~ +0.66‰. The estimated input is close to this deep ocean average, at about +0.63‰ (arrow at top: Vance et al. 2008; Little et al. 2014a). The only output yet characterised for Cu, though it is probably the most important, is scavenging to Fe-Mn oxide particulates and transfer to sediment (arrow at bottom, +0.31‰: Little et al. 2014a), is significantly lighter than both the input flux and the deep ocean average.

Figure 14: Schematic summary of our current understanding of processes relevant to the overall marine budgets of Cu and Zn isotopes. The inputs are shown as arrows on the left, with the Cu input shown as thick because of the uncertainty over the size of the dust input (Little et al. 2014a; Takano et al. 2014). Within the oceans this input is split into two pools

(schematic isotopic compositions shown as horizontal dashed lines): a dominant ligand-bound pool (ZnL or CuL) and a minor free metal ion pool (Zn^{2+} or Cu^{2+}). In both cases the ligand-bound pool is shown as heavy relative to the free metal ion (Jouvin et al. 2009; Ryan et al. 2014). If the oceans are in steady state the isotopic compositions of the outputs (arrows on right) must balance the input. For Zn the outputs to oxic sediments have $\delta^{66}Zn$ ~ +0.9‰ (Little et al. 2014a), consistent with a positive $\Delta_{sorbed-Zn2+}$ (Bryan et al 2015). This is balanced by a light output to organic-rich sediments (Little et al. 2016) whose isotopic composition is probably controlled by partial sequestration of organic-associated Zn to sulphide in pore waters (Vance et al. 2016a). For Cu the only characterised output is via sorption to Fe-Mn particulates, with $\delta^{65}Cu$ ~ +0.3‰ (Little et al. 2014a), shown as being consistent with a positive $\Delta_{sorbed-Cu2+}$ (e.g. Balistrieri et al. 2008; Pokrovsky et al. 2008). This must balanced by an output that is heavy relative to the input (question marks on right), possibly quantitative removal of seawater Cu in euxinic settings as speculated by Thompson and Ellwood (2014).

Table 1 : $\delta^{66}Zn_{JMC\ Lyon}$ and $\delta^{65}Cu_{SRM\ 976}$ of commonly used geological standards and isotopically certified materials.

	$\delta^{66}Zn_{JMC\ Lyon}$	2se	ref	$\delta^{65}Cu_{SRM\ 976}$	2se	ref
IRMM-3702	0.38	0.10	1			
IRMM-3702	0.25	0.09	1			
IRMM-3702	0.30	0.02	2			
IRMM-3702	0.29	0.05	3			
IRMM-3702						
IRMM-3702 recommended value	**0.30**	**0.01**				
ERM-AE633				-0.01	0.05	3
ERM-AE647				0.21	0.05	3
BHVO-2	0.33	0.04	4	0.10	0.08	5
	0.21	0.09	6	0.10	0.04	3
	0.27	0.06	2	0.10	0.07	4
	0.31	0.03	15	0.15	0.05	9
	0.29	0.09	16	0.13	0.03	8
BHVO-2 recommended value	**0.28**	**0.04**		**0.12**	**0.02**	
BCR-1/2	0.20	0.04		0.19	0.07	5
	0.29	0.12	10	0.14	0.05	3
	0.32	0.13	1	0.07	0.08	11
	0.23	0.08	12	0.19	0.08	12
	0.25	0.01	2	0.22	0.04	8
	0.20	0.09	11	0.21	0.04	8
	0.26	0.05	13			
	0.26	0.09	17			
BCR-1/2 recommended value	**0.25**	**0.03**		**0.17**	**0.05**	
BIR-1	0.31	0.04	4	0.00	0.03	2
	0.26	0.09	7	0.08	0.07	3
	0.20	0.04	2	-0.02	0.10	14
BIR-1 recommended value	**0.26**	**0.06**		**0.02**	**0.06**	
AGV1/2	0.32	0.04	4	-0.01	0.03	5
	0.25	0.09	6	-0.01	0.09	5

	0.29	0.03	15	0.01	0.11	5
	0.28	0.05	15	0.11	0.04	3
				0.1	0.11	3
				0.05	0.04	8
AGV1/2 recommended value	**0.29**	**0.03**		**0.04**	**0.04**	
G2	0.34	0.04	15			
	0.30	0.09	18			
	0.32	0.09	17			
G2 recommended value	**0.32**	**0.02**				

Ref: 1=Cloquet et al. 2006; 2=Sossi et al. 2014, 3=Moeller et al. 2012; 4=Chen et al. 2013; 5=Savage et al. 2015; 6=Moynier et al. 2010; 7=Herzog et al. 2009; 8=Liu et al. 2015; 9=Liu et al. 2014; 10=Chapman et al. 2006; 11=Archer and Vance 2004; 12=Bigalke et al. 2010; 13=Viers et al. 2007; 14=Li et al. 2009 ; 15=S. Chen et al. 2016 ; 16=Telus et al. 2012 ; 17=Paniello et al. 2012a, 18=Paniello et al. 2012b.

Table 2 Logarithm of the reduced partition function, $\ln \beta$, for the pair ^{65}Cu-^{63}Cu. Cu(II) species. Method/Basis set used: B3LYP/TZP for Sherman (2013) and , B3LYP/6-311+G(d,p) for Fujii et al. (2013, 2014).

Species		Coordination number	Temperature (K)							Ref[b]
			273	298	310	323	373	473	573	
Solid	CuO (Tenorite)	-	6.63	5.62	-	4.81	3.65	2.29	1.57	1
Aquo-ion	$Cu(H_2O)_5^{2+}$	5	5.355	4.546	-	3.905	2.968	1.876	1.290	2
			5.36	4.55	-	3.91	2.97	1.88	1.29	1
	$Cu(H_2O)_6^{2+}$	6	5.053	4.288	-	3.682	2.798	1.767	1.215	2
Chloride	$CuCl(H_2O)_4^{+}$	5	4.906	4.161	-	3.572	2.712	1.711	1.176	2
	$CuCl(H_2O)_5^{+}$	6	4.67	3.96	-	3.40	2.58	1.63	1.12	1
	$CuCl_2(H_2O)_3$	5	4.709	3.988	-	3.420	2.592	1.633	1.120	2
	$CuCl_2(H_2O)_4$	6	4.397	3.724	-	3.193	2.421	1.525	1.046	2
	$CuCl_3H_2O^{-}$	4	3.530	2.985	-	2.556	1.933	1.214	0.832	2
Hydroxide	$CuOH(H_2O)_4^{+}$	5	5.307	4.517	-	3.889	2.967	1.883	1.298	2
			5.30	4.52	-	3.89	2.97	1.89	1.30	1
	$Cu(OH)_2(H_2O)_3$	5	5.814	4.966	-	4.288	3.286	2.098	1.451	2
Carbonate	$CuCO_3(H_2O)_2$	4	5.091	4.323	-	3.715	2.825	1.787	1.230	2
	$Cu(CO_3)_2^{2-}$	4	6.176	5.239	-	4.498	3.416	2.158	1.483	2
			6.38	5.41	-	4.65	3.53	2.23	1.53	1
	$CuHCO_3(OH)_2^{-}$	4	5.951	5.075	-	4.376	3.346	2.130	1.471	2
Sulfate	$CuSO_4(H_2O)_4$	5	6.041	5.144	-	4.430	3.381	2.148	1.481	2
Sulfide	$CuHS(H_2O)_4^{+}$	5	4.002	3.386	-	2.900	2.194	1.377	0.942	2
	$Cu(HS)_2(H_2O)_3$	5	3.855	3.264	-	2.797	2.119	1.333	0.914	2
Phosphate	$CuH_2PO_4(H_2O)_4^{+}$	5	5.515	4.684	-	4.026	3.063	1.939	1.334	3
	$CuH_4(PO_4)_2(H_2O)_3$	5	5.553	4.714	-	4.050	3.079	1.947	1.339	3
	$CuH_3(PO_4)_2(H_2O)_3^{-}$	5	5.290	4.492	-	3.861	2.937	1.860	1.280	3
	$CuH_2(PO_4)_2(H_2O)_2^{2-}$	4	6.360	5.403	-	4.645	3.535	2.238	1.540	3
Citrate	$CuH_2(cit)(H_2O)_2^{+}$	5	5.286	4.486	-	3.852	2.927	1.850	1.272	2
	$CuH(cit)(H_2O)_2$	5	5.622	4.772	-	4.099	3.117	1.972	1.357	2
	$Cu(cit)(H_2O)_2^{-}$	5	6.092	5.177	-	4.451	3.389	2.147	1.479	2
	$Cu(cit)_2^{4-}$	4	4.998	4.231	-	3.626	2.748	1.730	1.188	2
Oxalate	$CuC_2O_4(H_2O)_2$	4	6.236	5.302	-	4.561	3.474	2.202	1.516	2
Ascorbate	$CuH(L\text{-ascorbate})(H_2O)_4^{+}$	5	3.924	3.324	-	2.850	2.161	1.362	0.935	2
	$CuH(D\text{-ascorbate})(H_2O)_4^{+}$	5	3.989	3.380	-	2.899	2.199	1.386	0.951	2
Malonate	$Cu(H_2C_3O_4)_2(H_2O)_2^{2-}$	6	7.00	5.94	-	5.10	3.88	2.45	1.68	1
Amino acid complex	$Cu(Glu)(H_2O)_3^{2+}$	5	5.230	4.436	4.117	3.808	2.891	-	-	3
	$Cu(Thr)(H_2O)_4^{2+}$	5	5.220	4.429	4.110	3.803	2.889	-	-	3
	$Cu(His)(H_2O)_3^{2+}$	5	5.274	4.470	4.148	3.836	2.911	-	-	3
	$Cu(His)(H_2O)_4^{2+}$	5	5.299	4.492	4.168	3.855	2.926	-	-	3
	$Cu(Cys)(H_2O)_4^{2+}$	5	3.981	3.369	3.124	2.888	2.187	-	-	3
	$Cu(Met)(H_2O)_4^{2+}$	5	4.632	3.932	3.650	3.378	2.568	-	-	3
	$Cu(GS)H^{0}$	4	4.945	4.194	3.892	3.600	2.734	-	-	3
Lactate	$Cu(L\text{-lact})(H_2O)_3^{+}$	5	5.530	4.695	4.359	4.034	3.068	-	-	3
	$Cu(L\text{-lact})_2$	4	7.110	6.045	5.616	5.199	3.961	-	-	4
	Cu(L-lact)(D-lact) [a]	4	7.125	6.057	5.627	5.210	3.969	-	-	4

[a] Reproduced from Telouk et al. (2015).

[b] 1=Sherman (2013), 2=Fujii et al. (2013), 3=Fujii et al. (2014), 4=This study.

Table 3 Logarithm of the reduced partition function, ln β, for the pair ^{65}Cu-^{63}Cu. Cu(I) species. Method/Basis set used: B3LYP/TZP for Sherman (2013) and , B3LYP/6-311+G(d,p) for Fujii et al. (2013, 2014), Seo et al. (2007) and the present study.

Species		Coordination number	Temperature (K)							Ref[b]
			273	298	310	323	373	473	573	
Solid	Cu_2O (Cuprite)	-	3.99	3.40	-	2.92	2.23	1.41	0.97	1
	$CuFeS_2$ (Chalcopyrite)	-	1.80	1.51	-	1.29	0.97	0.61	0.41	1
Aquo-ion	$Cu(H_2O)_2^+$	2	3.368	2.867	-	2.468	1.882	1.193	0.822	2
Chloride	$CuCl(H_2O)$	2	3.401	2.887	-	2.480	1.885	1.191	0.818	3
			3.40	2.89	-	2.48	1.89	1.19	0.82	4
	$CuCl_2^-$	2	2.775	2.350	-	2.014	1.526	0.960	0.659	3
			2.71	2.29	-	1.97	1.49	0.94	0.64	4
			2.87	2.42	-	2.08	1.57	0.99	0.68	1
	$CuCl_3^{2-}$	3	1.012	0.851	-	0.725	0.545	0.339	0.231	3
			1.02	0.85	-	0.73	0.55	0.34	0.23	4
			1.41	1.19	-	1.02	0.76	0.48	0.33	1
Sulfide	$CuHS(H_2O)$	2	3.208	2.722	-	2.337	1.775	1.121	0.770	3
			2.89	2.45	-	2.10	1.59	1.00	0.69	1
	$Cu(HS)_2^-$	2	2.940	2.489	-	2.133	1.616	1.017	0.697	3
			2.90	2.46	-	2.11	1.60	1.00	0.69	4
			2.69	2.28	-	1.95	1.48	0.93	0.64	1
	$Cu_2S(HS)_2^{2-}$	2	2.648	2.239	-	1.917	1.450	0.911	0.624	3
Lactate	Cu(L-lact) [a]	2	2.195	1.859	1.725	1.595	1.209	-	-	5
	Cu(D-lact) [b]	2	2.202	1.866	1.731	1.600	1.214	-	-	5

[a] Reproduced from Telouk et al. (2015).

[b] 1=Sherman (2013), 2=Fujii et al. (2013), 3=Fujii et al. (2014), 4=Seo et al. (2007), 5=This study.

Table 4 Logarithm of the reduced partition function, ln β, for the pair ^{66}Zn-^{64}Zn. Zn(II) species. Method/Basis set used:, B3LYP/6-311+G(d,p) for Fujii et al. (2013, 2014), Fujii and Albarede (2013), Moynier et al. (2013a), BP86/SVP for Singha Deb et al. (2014), and B3LYP/aug-cc-pVDZ for Black et al. (2012).

	Species	Coordination number	Temperature (K)							Ref[d]
			273	298	310	323	373	473	573	
Aquo-ion	$Zn(H_2O)_4^{2+}$	4	4.539	3.853	3.577	3.310	2.516	-	-	1
			-	5.0	-	-	-	-	-	2
	$Zn(H_2O)_6^{2+}$	6	3.854	3.263	-	2.797	2.119	1.334	0.915	1
			3.61	3.05	-	2.61	1.98	1.25	0.85	3
			-	3.9	-	-	-	-	-	2
	$Zn(H_2O)_{18}^{2+}$	6	-	3.576	-	-	-	-	1.004	4
			3.67	3.11	-	2.66	2.02	1.27	0.87	3
			-	4.3	-	-	-	-	-	2
Chloride	$ZnCl(H_2O)_5^+$	6	3.702	3.136	-	2.689	2.039	1.285	0.882	1
	$ZnCl_2(H_2O)_4$	6	3.486	2.950	-	2.528	1.915	1.205	0.826	1
	$ZnCl_3(H_2O)^-$	4	3.490	2.952	-	2.528	1.913	1.202	0.824	1
	$ZnCl_4^{2-}$	4	2.722	2.293	-	1.957	1.474	0.921	0.629	1
			2.77	2.33	-	1.99	1.50	0.94	0.64	3
Hydroxide	$Zn(OH)_2(H_2O)_4$	6	4.185	3.567	-	3.075	2.350	1.495	1.032	1
Carbonate	$ZnHCO_3(H_2O)_3^+$	5	4.573	3.877	-	3.326	2.525	1.593	1.095	1
	$ZnHCO_3(H_2O)_4^+$ [a]	5	4.579	3.885	-	3.335	2.534	1.602	1.102	5
	$ZnHCO_3(H_2O)_5^+$ [a]	6	4.109	3.482	-	2.988	2.267	1.431	0.983	5
	$ZnCO_3(H_2O)_3$	5	4.940	4.199	-	3.612	2.752	1.745	1.202	1
	$ZnCO_3(H_2O)_4$ [a]	5	4.789	4.076	-	3.509	2.677	1.700	1.172	1
	$ZnCO_3(H_2O)_5$ [a]	6	4.356	3.704	-	3.187	2.429	1.541	1.062	5
Sulfate	$ZnSO_4(H_2O)_6$	5	4.31	3.65		3.13	2.38	1.50	1.03	3
	$ZnSO_4(H_2O)_5$	6	4.154	3.527	-	3.031	2.306	1.460	1.006	5
Sulfide	$Zn(HS)_2(H_2O)_4$	6	3.207[b]	2.717	-	2.330[b]	1.766[b]	1.113[b]	0.764	4
	$Zn(HS)_3(H_2O)_2^{''}$	5	3.580[b]	3.028	-	2.593[b]	1.962[b]	1.233[b]	0.845	4
	$Zn(HS)_4^{`}$	4	2.598[b]	2.190	-	1.871[b]	1.411[b]	0.883[b]	0.604	4
	$ZnS(HS)H_2O^{''}$	5	3.112[b]	2.628	-	2.247[b]	1.697[b]	1.064[b]	0.728	4
Phosphate	$ZnH_2PO_4(H_2O)_5^+$	6	4.092	3.468	-	2.975	2.257	1.424	0.978	6
	$ZnH_4(PO_4)_2(H_2O)_4$	6	4.047	3.428	-	2.940	2.229	1.405	0.965	6
	$ZnH_3(PO_4)_2(H_2O)_4^-$	6	5.027	4.268	-	3.667	2.789	1.764	1.214	6
	$ZnHPO_4(H_2O)_5$	6	4.188	3.559	-	3.060	2.330	1.476	1.017	6
	$Zn_2H_2(PO_4)_2(H_2O)_4$	6	5.156	4.380	-	3.765	2.865	1.814	1.249	6
Citrate	$ZnH(cit)(H_2O)_4$	6	4.033	3.419	-	2.934	2.227	1.406	0.967	6
	$Zn(cit)(H_2O)_3^-$	6	4.154	3.523	-	3.024	2.297	1.452	0.999	6
			4.39	3.72	-	3.20	2.43	1.54	1.06	3
	$Zn(cit)_2^{4-}$	6	2.889	2.437	-	2.083	1.572	0.986	0.675	6
	$Zn_2H_{-2}(cit)_2(H_2O)_4^{4-}$	4	5.330	4.523	-	3.884	2.953	1.867	1.284	6
Malate	$ZnH_2(mal)(H_2O)_4^{2+}$	6	3.842	3.250	-	2.784	2.107	1.325	0.909	6
	$ZnH(mal)(H_2O)_4^+$	6	3.984	3.376	-	2.896	2.197	1.386	0.952	6
	$Zn(mal)(H_2O)_4$	6	4.103	3.479	-	2.987	2.268	1.433	0.986	6
	$Zn(mal)_2(H_2O)_2^{2-}$	6	3.274	2.771	-	2.376	1.801	1.135	0.780	6
Oxalate	$ZnC_2O_4(H_2O)_2$	4	5.500	4.678	-	4.025	3.068	1.946	1.341	5
	$Zn(C_2O_4)_2^{2-}$	4	5.215	4.421	-	3.794	2.880	1.818	1.250	5
Amino acid complex	$Zn(Glu\text{-}H_{-1})^+$ [c]	2	1.923	1.633	1.517	1.404	1.070	-	-	7
	$Zn(Glu)(H_2O)_2^{2+}$	4	4.473	3.796	3.524	3.260	2.478	-	-	1
	$Zn(Glu)(H_2O)_4^{2+}$	6	3.888	3.292	3.053	2.822	2.139	-	-	1
	$Zn(Thr)(H_2O)_3^{2+}$	4	4.774	4.056	3.767	3.487	2.654	-	-	1
	$Zn(Thr)(H_2O)_5^{2+}$	6	3.916	3.315	3.075	2.842	2.154	-	-	1
	$Zn(His\text{-}H_{-1})+$ [c]	2	4.381	3.728	3.465	3.210	2.448	-	-	7
	$Zn(His)^2+$ [c]	2	4.223	3.591	3.336	3.090	2.355	-	-	7
	$Zn(His)(H_2O)_2^{2+}$	4	4.670	3.959	3.673	3.397	2.578	-	-	1
	$Zn(His)(H_2O)_4^{2+}$	6	3.541	2.996	2.777	2.566	1.943	-	-	1
	$Zn(His)(H_2O)_3^{2+}$	4	4.635	3.930	3.647	3.373	2.561	-	-	1
	$Zn(His)(H_2O)_5^{2+}$	6	3.724	3.150	2.921	2.699	2.043	-	-	1
	$Zn(Cys\text{-}H_{-1})^+$ [c]	1	1.417	1.196	1.108	1.023	0.771	-	-	7
	$Zn(Cys)^{2+}$ [c]	1	1.545	1.307	1.211	1.119	0.847	-	-	7
	$Zn(Cys)(H_2O)_3^{2+}$	4	3.912	3.313	3.072	2.840	2.152	-	-	1

$Zn(Cys)(H_2O)_5^{2+}$	6	3.196	2.702	2.504	2.313	1.750	-	-	1
$Zn(Met)(H_2O)_3^{2+}$	4	4.397	3.733	3.466	3.207	2.438	-	-	1
$Zn(Met)(H_2O)_5^{2+}$	6	3.478	2.947	2.734	2.528	1.918	-	-	1
$Zn(GS)^-$	4	4.311	3.655	3.392	3.137	2.381	-	-	1

[a] HCO_3^- and CO_3^{2-} were treated as monovalent ligands.

[b] Reproduced from Fujii et al. (2011).

[c] Hydration water molecules were not arranged (anhydrous).

[d] 1=Fujii et al. (2014), 2=Singha Deb et al. (2014), 3=Black et al. (2011), 4=Fujii et al. (2011), 5=This Study, 6=Fujii and Albarède (2012), 7=Moynier et al. (2013a).

Moynier et al. RIMG Cu-Zn Figure 1

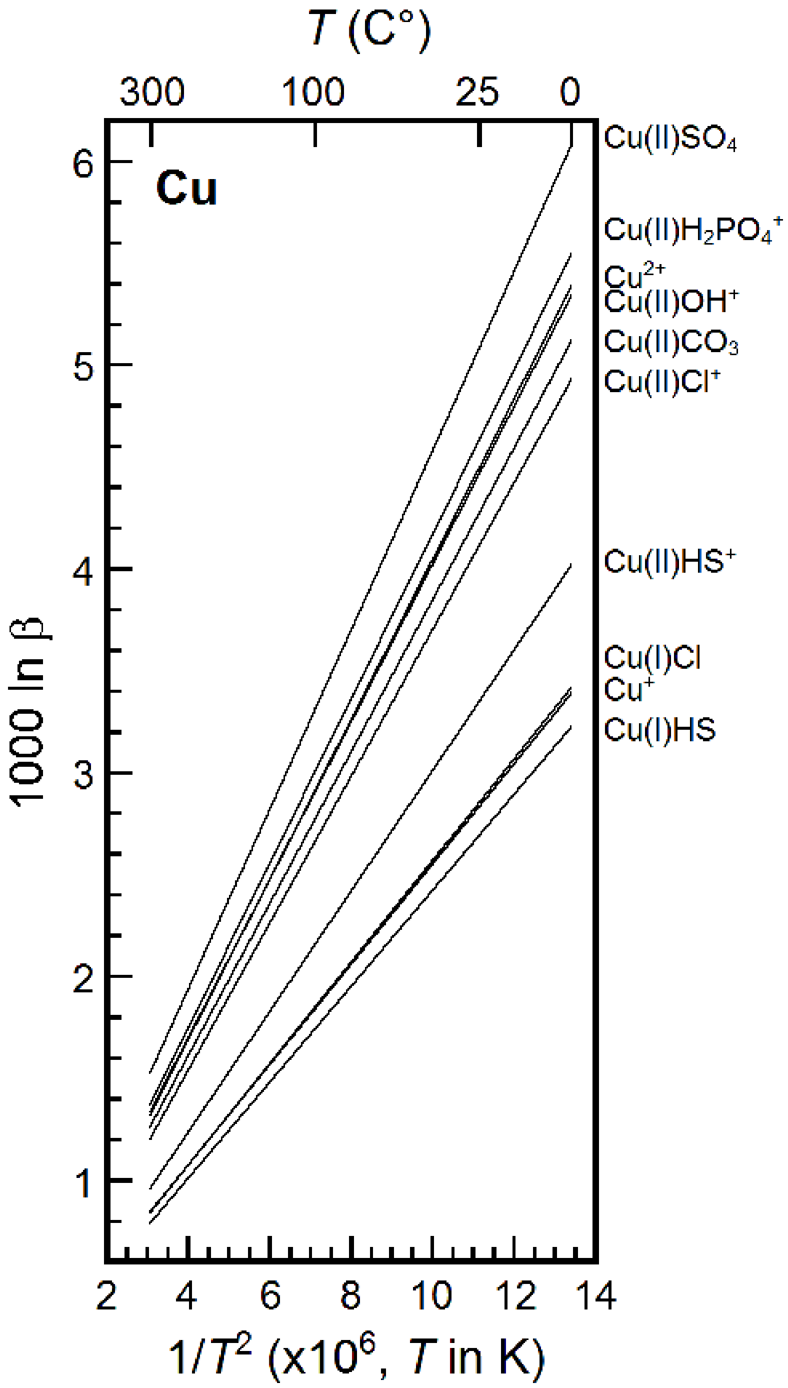

Moynier et al. RIMG Cu-Zn Figure 2

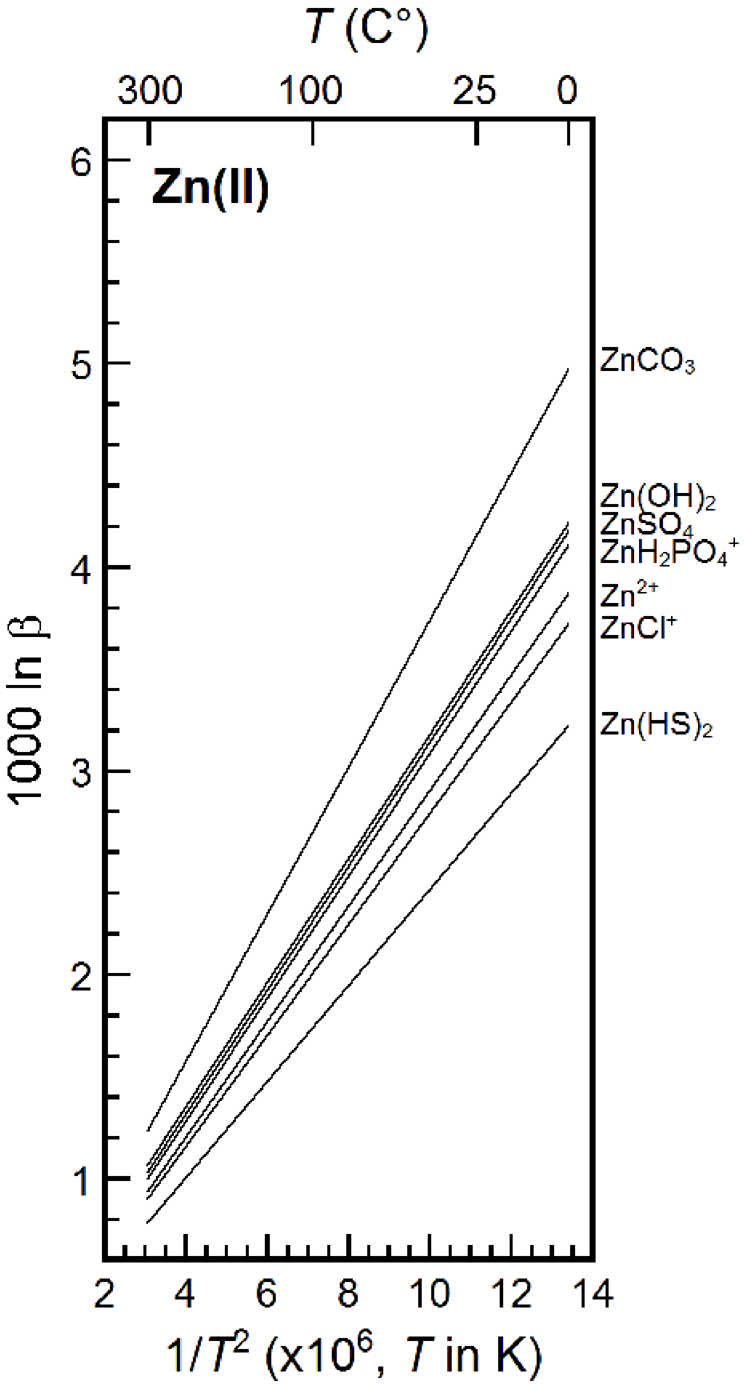

Moynier et al. RIMG Cu-Zn Figure 3

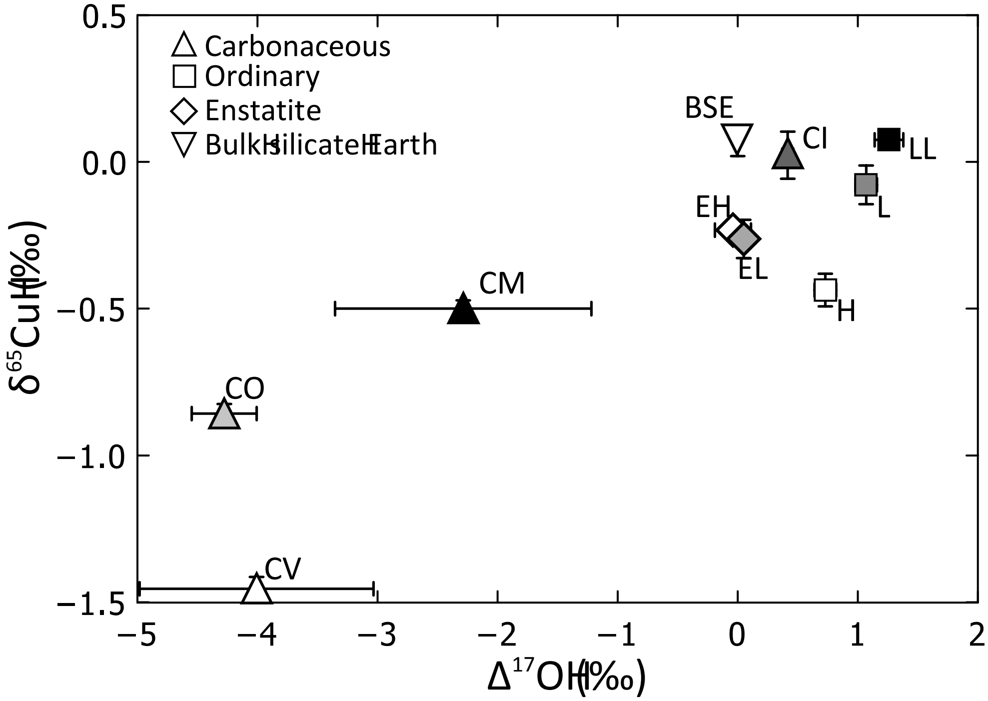

Moynier et al. RIMG Cu-Zn Figure 4

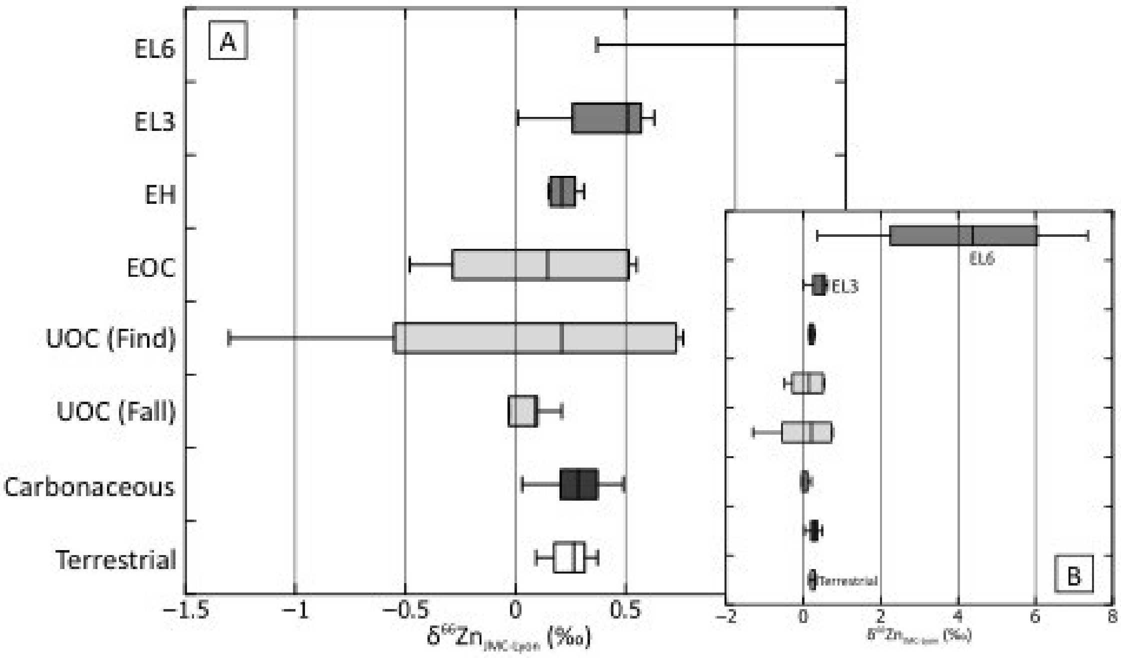

Moynier et al. RIMG Cu-Zn Figure 5

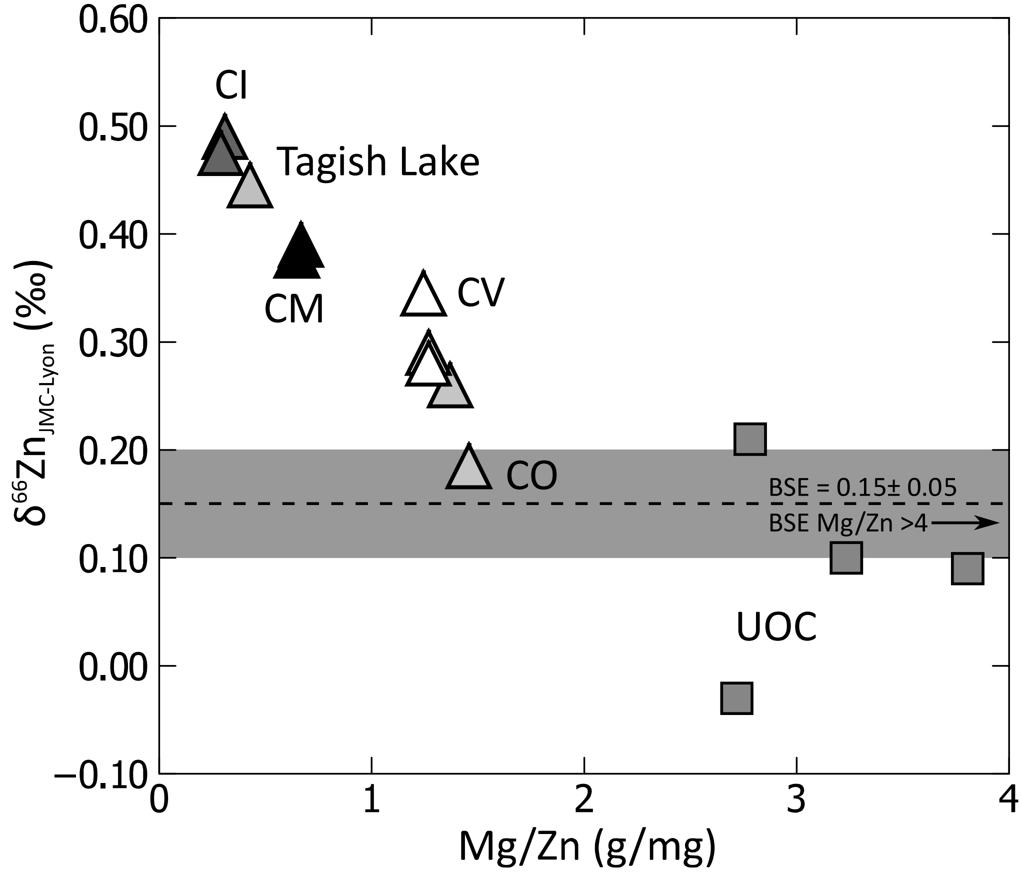

Moynier et al. RIMG Cu-Zn Figure 6

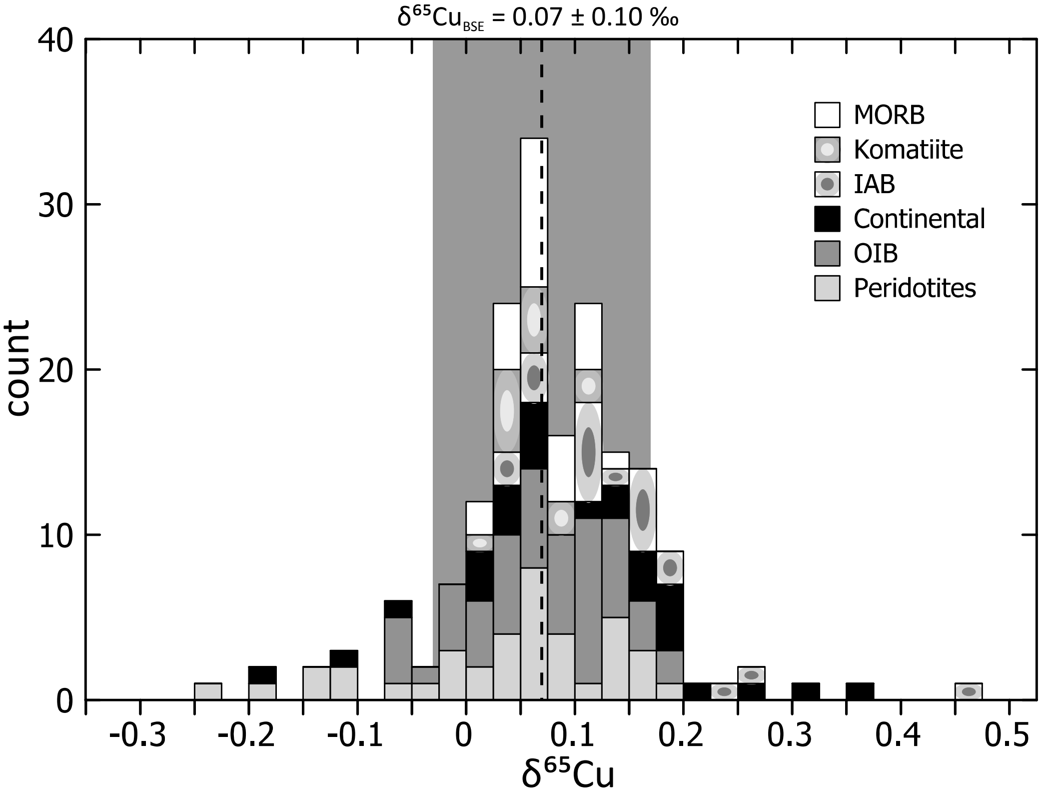

Moynier et al. RIMG Cu-Zn Figure 7

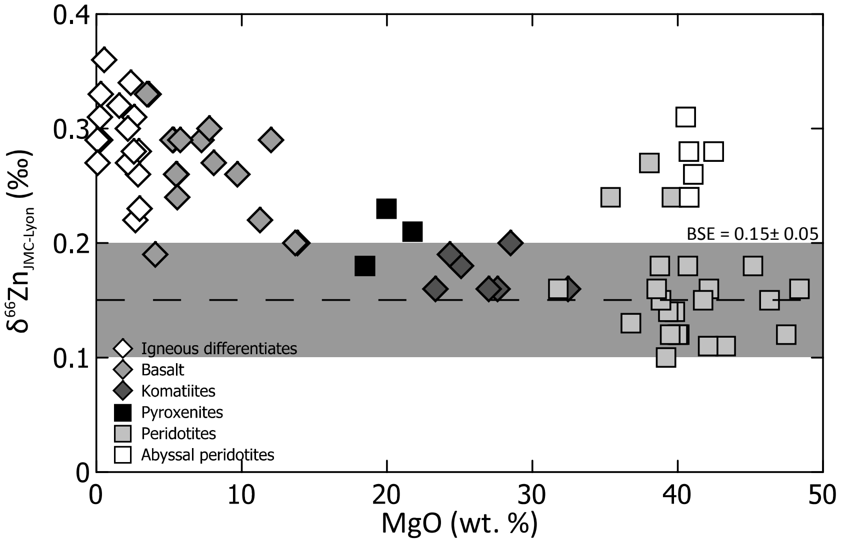

Moynier et al. RIMG Cu-Zn Figure 8

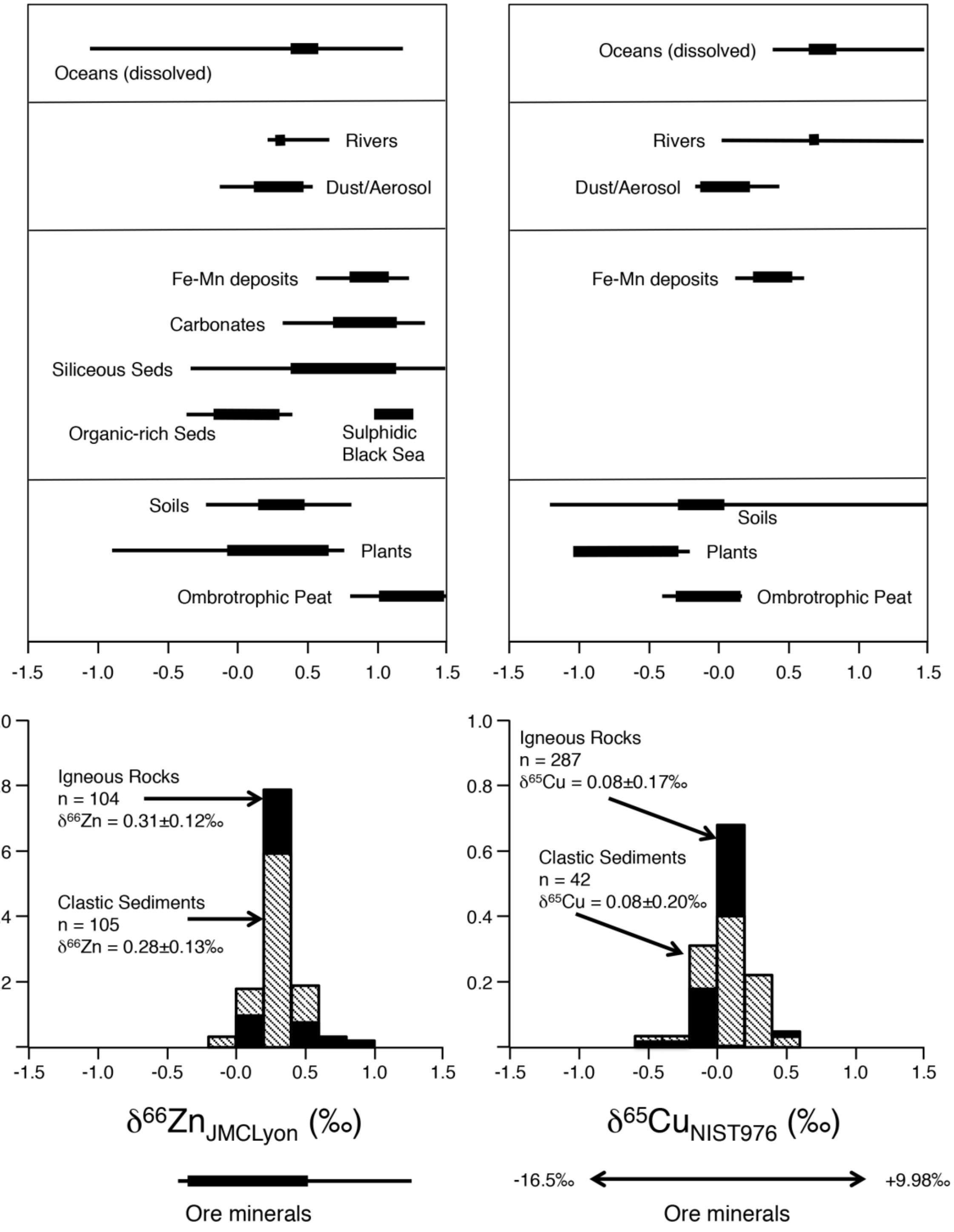

Moynier et al. RIMG Cu-Zn Figure 9

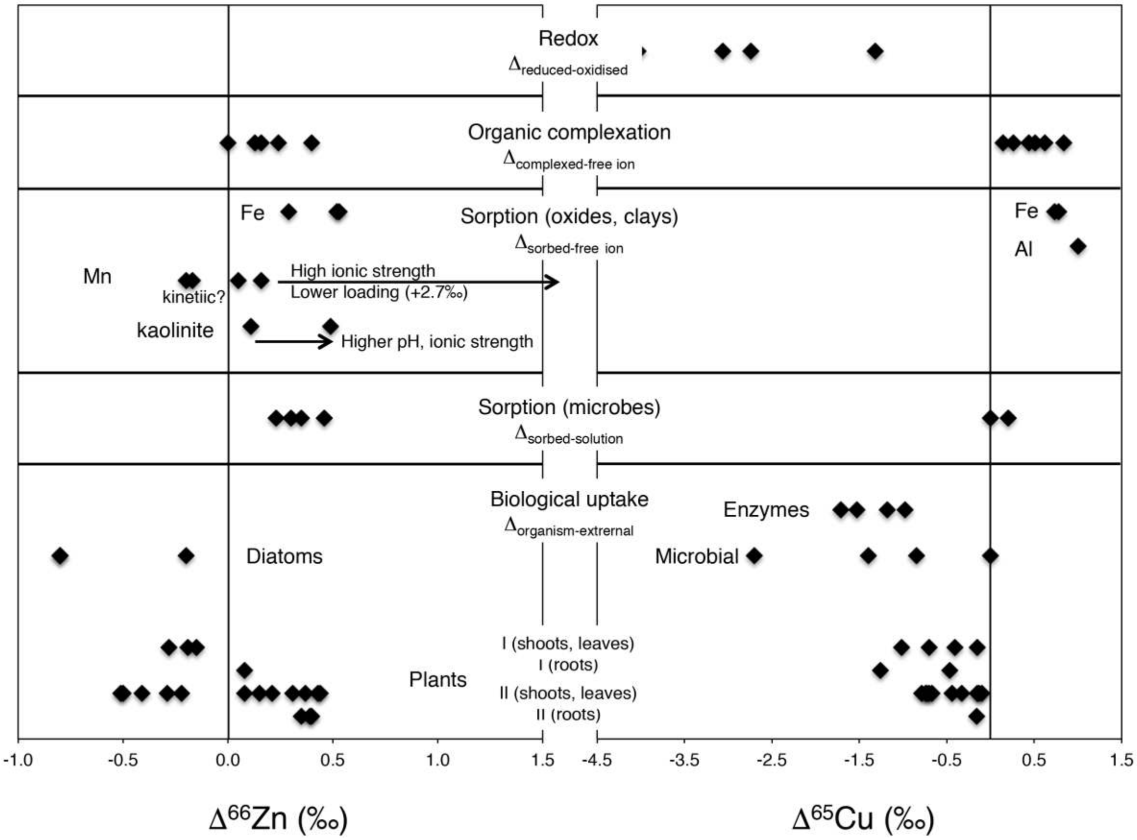

Moynier et al. RIMG Cu-Zn Figure 10

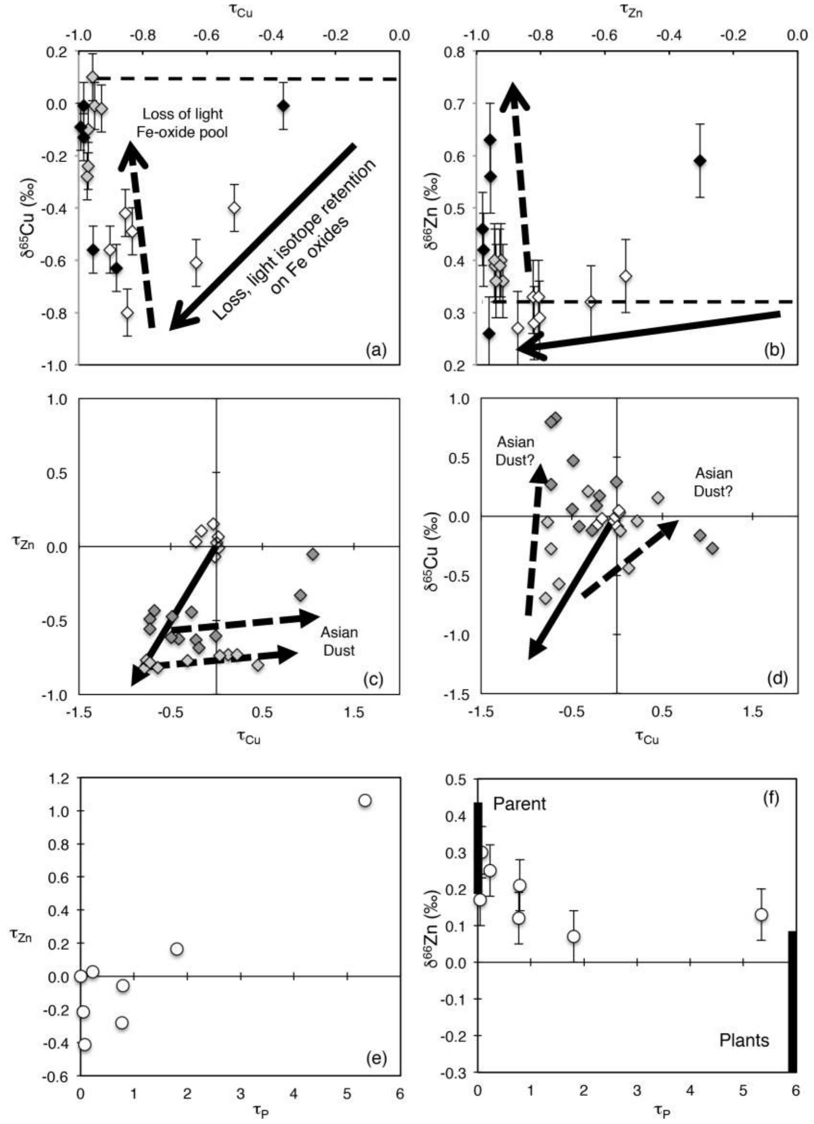

Moynier et al. RIMG Cu-Zn Figure 11

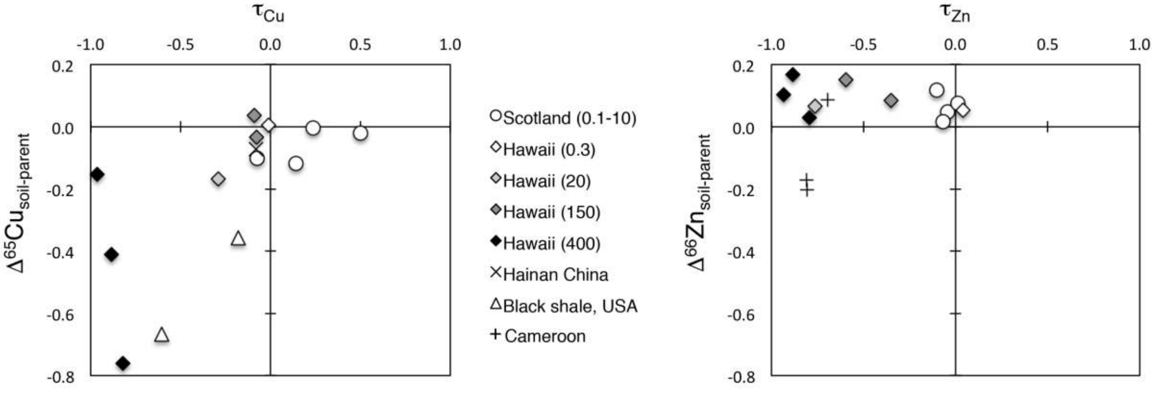

Moynier et al. RIMG Cu-Zn Figure 12

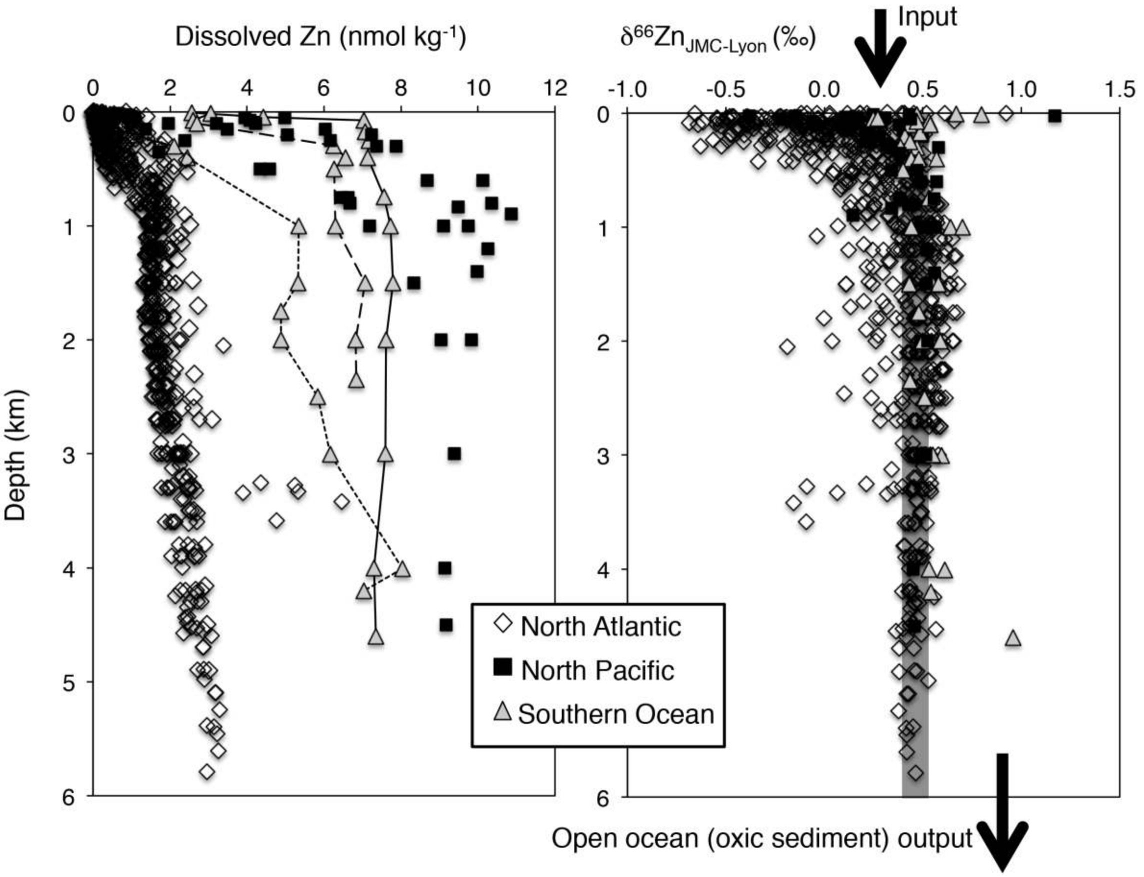

Moynier et al. RIMG Cu-Zn Figure 13

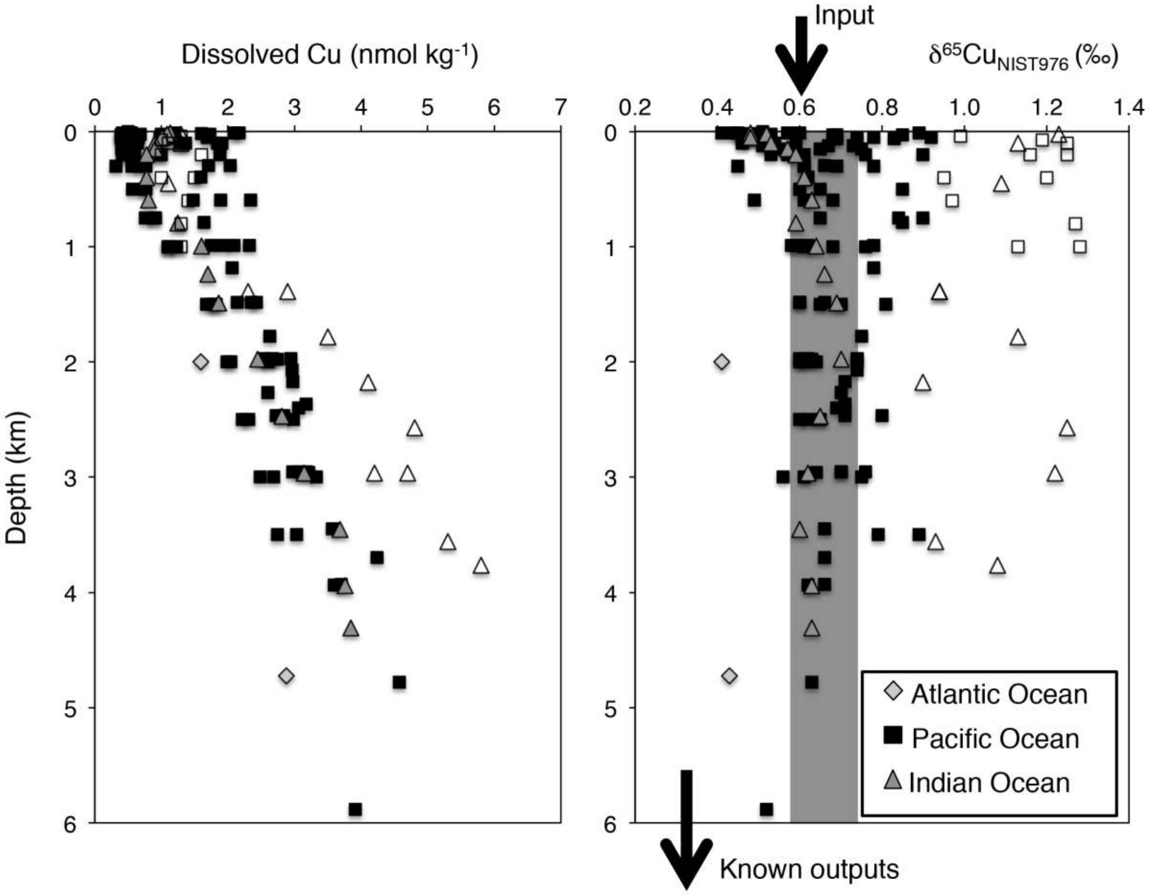

Moynier et al. RIMG Cu-Zn Figure 14